
# Epileptic Seizure Detection and Source Localization Based on Stockwell Transform

**By:**

**Tewodros Sewnet Tefera**

A thesis submitted in partial fulfillment of the requirements for the Degree of Master

Science in Biomedical Engineering

(Biomedical Imaging & Instrumentation)

**Center of Biomedical Engineering**

**Addis Ababa Institute of Technology**

**Addis Ababa University**

**Advisor: Dawit Assefa Haile (PhD)**

**Addis Ababa, Ethiopia, February 2020**

# DECLARATION

I declare that this thesis is my work and that all sources of materials used for this thesis have been properly acknowledged. This thesis has been submitted in partial fulfillment of the requirements for the MSc degree in Biomedical Engineering at Addis Ababa University.

I earnestly declare that this thesis is not submitted to any other institution anywhere for the award of any academic degree, diploma, or certificate.

Name: Tewodros Sewnet Tefera

Signature: _____

Place: Addis Ababa, Ethiopia

Date of Submission: _____

This thesis has been submitted for my approval as a university advisor.

Name: Dr. Dawit Assefa Haile

Signature: _____

Place: Addis Ababa, Ethiopia

Date: _____


# Epileptic Seizure Detection and Source Localization Based on Stockwell Transform

**By:**

**Tewodros Sewnet Tefera**

**Center of Biomedical Engineering**

**Addis Ababa Institute of Technology**

**Addis Ababa University**

APPROVED BY BOARD OF EXAMINERS

| | |
|---|---|
| _____ | _____ |
| Chairman, Department or Graduate Committee | Signature |
| Dr. Dawit Assefa Haile _____ | _____ |
| Name of Advisor | Signature |
| _____ | _____ |
| Name of External Examiner | Signature |
| _____ | _____ |
| Name of Internal Examiner | Signature |

# ABSTRACT

Neurologists often have to scan long term electroencephalogram (EEG) recordings in order to diagnose epilepsy. Detection of seizures from recorded EEG signal is crucial for diagnosis of epilepsy. Localization of the seizure origin is also important for treatment and surgery of focal epilepsy cases. Visual scanning of EEG is time consuming and suffers from issues of subjectivity due to imprecise definition of abnormal seizure EEG patterns. EEG recordings between seizures or inter-ictal EEG findings also offer evidence of epilepsy though not decisive as observed epileptic seizures. Although the main task is detecting seizures, the accuracy of a seizure detection scheme is based on clear characterization of inter-ictal, seizure and normal EEG's. The challenge here is that abnormal patterns of EEG signals from epilepsy patients are case specific, especially for inter-ictal EEG. Additionally, EEG signals are composed of multiple frequencies and hence non-stationary. This thesis majorly considers temporal lobe epilepsy. An automated EEG signal classification scheme has been proposed for use in efficient detection and source localization of epileptic seizures based on the Stockwell (S) transform. Important features were extracted from the S-transform plane of EEG segments to categorize them into seizure, inter-ictal and normal signals. Classification of the features was done using support vector machine. For classification problem between seizure and normal EEG (recorded with closed eyes and/or open eyes), 100% sensitivity, 100% specificity and 100% accuracy were obtained. For classification between seizure and inter-ictal EEGs recorded from the epileptogenic zone, the proposed scheme achieved 99 % sensitivity, 99% specificity and 99 % accuracy. For seizure and inter-ictal signals recorded from non-epileptogenic zone, the classification scheme resulted in 99% sensitivity, 98% specificity and 98.5% accuracy. Empirical mode decomposition was also employed to improve the performance of the classification between seizure and non-seizure dataset. The methodology used for seizure detection was also employed to automated epileptic focus localization. The features extracted for source localization were intended to characterize focal and non-focal signals. A scatter plot was generated using the features and simple thresholding was able to classify focal and non-focal EEGs with 84% sensitivity, 90.21% specificity and 88% accuracy. The proposed method uses fewer number of features resulting in smaller feature space which in turn makes it simple and robust compared to other schemes proposed in the literature.



**Keywords:** Epileptic Seizure, Focus Localization, Stockwell Transform, Empirical Mode Decomposition, Vector Support Machine.

## Acknowledgements

I would first like to thank the almighty GOD, his words gave me strength and patience to complete this thesis. Then, I would like to give my gratitude and acknowledgement to my senior advisor, Dr. Dawit Assefa Haile (PhD) for his guidance, expertise, patience and time commitment throughout this entire work. Without his guidance to keep me on track, regular meeting and feedbacks, help in writing up and editing the literature, this work would not have been completed.

My thanks also goes to Dr. Masreshaw Demelash, PG coordinator, for his guidance and valuable advice. I would like to say thanks to all staff members of the Center of Biomedical Engineering at the Addis Ababa Institute of Technology. I would also like to thank my friends for their suggestions and help related to my work, especially Muliye Kibabew and Habtamu Abraham.

Finally, I would like to thank my brother, Zelalem Sewnet and my sister Friwet Sewnet for their continuous support and faith in me, and be with me in the long journey of completing this thesis.

## Table of Contents

**Abstract** ..... **i**

**Acknowledgements** ..... **ii**

**Table of Contents** ..... **iii**

**List of Figures** ..... **v**

**List of Tables** ..... **vi**

**Acronyms** ..... **vii**

**CHAPTER ONE** ..... **1**

**1. INTRODUCTION** ..... **1**

1.1 Background ..... 1

1.2 Statement of the Problem ..... 4

1.3 Significance of the Thesis ..... 5

1.4 Objective of the Study ..... 6

1.5 Organization of the Thesis ..... 6

**CHAPTER TWO** ..... **9**

**2.THE HUMAN BRAIN AND ELECTROENCEPHALOGRAM** ..... **9**

2.1 The Nervous System ..... 9

2.1.1 Neurons ..... 10

2.1.2 The Human Brain ..... 11

2.1.2.1 Cerebral Cortex ..... 12

2.1.2.2 Functional Brain Systems ..... 14

2.2 Electroencephalograph (EEG) ..... 14

2.2.1 EEG Rhythms and Waveforms ..... 17

2.2.2 Applications of EEG ..... 19

2.3 Epilepsy ..... 20

2.3.1 Role of EEG in Epilepsy Diagnosis and Treatment ..... 23

**CHAPTER THREE.....27**

**3.SIGNAL ANALYSIS FOR AUTOMATED EEG SEIZURE DETECTION AND SOURCE LOCALIZATION.....27**

3.1 Classical Approaches for EEG Analysis.....28

3.2 Time-Frequency Analysis of EEGs .....30

3.2.1 Short –Time Fourier Transform (STFT).....30

3.2.2 Wigner-Ville Distribution .....33

3.2.3 Continuous Wavelet Transform.....35

3.2.4 Discrete Wavelet Transform (DWT).....36

3.2.5 Stockwell Transform……...39

3.3 Empirical Mode Decomposition (EMD) and Singular Value Decomposition(SVD) for Seizure Detection and Source Localization.....41

3.3.1 Singular Value Decomposition (SVD) .....43

3.4 Nonlinear Dynamics and Chaos Theory for Seizure Detection and Source Localization ....44

3.5 Limitations of Previous Works…….....46

**CHAPTER FOUR.....52**

**4.PROPOSED EPILEPTIC SEIZURE DETECTION AND LOCALIZATION BASED ON STOCKWELLTRANSFORM……...52**

4.1 Overview of the Proposed Scheme.....52

4.2 Preprocessing of EEG Segments.....53

4.3 Stockwell Transform.....54

4.3.1 Definition and Relation of the S-transform with STFT and CWT.....54

4.3.2 Comparison of the S-transform, CWT, and Cohen's Class Quadratic Time-Frequency Distributions……...57

4.3.3 Comparison of Time-Frequency Distributions Through Simulated Signal.....58

4.4 Empirical Mode Decomposition(EMD)..... 59

4.5 Feature Extraction.....60

4.6 Classification Using SVM.....64

4.7 Performance Evaluation.....65

**CHAPTER FIVE.....67**

**5.RESULTS AND DISCUSSION.....67**

5.1 Dataset.....67

5.2 Result of Seizure Detection.....69

5.3 Result of Seizure Detection Using EMD.....75

5.4 Comparative Study on the Performance of the Proposed Seizure Detection Scheme and Other Methods Proposed Previously……76

5.5 Results of Focus Localization.....78

**CHAPTER SIX.....82**

**6.CONCLUSION AND FUTURE WORKS.....82**

6.1Recommendations and Future Works.....83

Appendix .....84

## List of Figures

Figure 2.1 (a) A typical neuron (b) three inter connected neurons ……..……11

Figure 2.2 (a) Adult brain structure (b) Lobes and sulci of the cerebrum …….....13

Figure 2.3 (a) Longitudinal bipolar montage (b) Ipsilateral ear referential montage……16

Figure 3.1 (a) times series the synthetic signal (b) DFT of the synthetic signal (c) Short time – Fourier transform of the synthetic signal…….....31

Figure.3.2 Wavelet decomposition of a signal (Third level) ……37

Figure 4.1 Overview of the proposed seizure detection and localization scheme…….....53

Figure 4.2 Performance of different time –frequency distribution under noisy signal……..…59

Figure 4.3 (a) The way the S-transform plane is used to extract features…….....62

Figure 4.3 (b) Average distribution of PSD over time axis for the three class of EEG……63

Figure 5.1 Segments of EEG data for seizure detection (a) Normal, (b) Inter-ictal (c) Ictal…....68

Figure 5.2 PSD of S-transform plane and average distribution PSD over frequency……...70

Figure 5.3 (a) Scatter plot of S, N and O dataset……...72

Figure 5.3 (b) Scatter plot of S, F and Z data sets…….....72

Figure 5.4 (a) Scatter plot of S, N and O dataset of sub-plane of delta and theta rhythm…….73

Figure 5.4 (b) Scatter plot of S, F and Z data sets using sub-plane of delta and theta rhythm.....73

Figure 5.5 (a) Scatter plot of feature 1 versus feature 2 ……...80

Figure 5.5 (b) Scatter plot of feature 2 versus feature 3……...….80

## List of Tables

Table 5.1 Canberra distance between seizure and non-seizure data set……74

Table 5.2 Performance of proposed seizure detection scheme……..75

Table 5.3 The range (mean ± standard deviation) of the features extracted from different IMFs of different data sets……...76

Table 5.4 Comparative Study on the Performance of the Proposed scheme seizure detection….77

## Acronyms

| | |
|---|---|
| AED | Administration of Antiepileptic Drugs |
| ANN | Artificial Neural Networks |
| CWT | Continuous Wavelet Transform |
| DFT | Discrete Fourier Transform |
| DWT | Discrete Wavelet Transform |
| FFT | Fast Fourier Transform |
| EEG | Electroencephalograph |
| EMD | Empirical Mode Decomposition |
| IMFs | Intrinsic Mode Functions |
| IEDs | Inter-ictal Epileptiform Discharges |
| MRI | Magnetic Resonance Imaging |
| PCA | Principal Component Analysis |
| PSD | Power Spectral Density |
| SVD | Singular Value Decomposition |
| STFT | Short –Time Fourier Transform |
| SSWs | Spikes and Sharp Waves |
| SVM | Support Vector Machine |
| TIPDA | Temporal Intermittent Polymorphic Delta Activity |
| WVD | Wigner-Ville distribution |

# CHAPTER ONE

# 1. INTRODUCTION

## 1.1 Background

The brain is complex and sophisticated organ in charge of the nervous system, a controlling and communicating system of our body. Sensing the environment, coordination of muscles for movement, communication between different organs, controlling physiological process are few tasks performed by the nervous system. Brain is a central computing and information processing part of the nervous system. Various neurological disorders and diseases affect the brain. One of the major neurological disorders is epilepsy. Epilepsy is neurological disorder with manifestations of sudden and recurrent bursts of electrical discharges in the brain [1]. This abnormal burst of electrical discharges in the brain is called epileptic seizure. During seizure, the patient may experience altered perception of the environment, loss of muscle control and even loss of consciousness. Epileptic seizures may cause negative physical, psychological and social consequences, injuries and sudden death.

According to an estimate by the World Health Organization (WHO), about 1-2% of world population is affected by epilepsy [2][3]. Approximately one in every 100 persons will experience a seizure at some time in their life [2]. The population prevalence of epilepsy varies across countries from 0.5 to 5% where higher levels tend to be seen in developing countries [3]. The prevalence of epilepsy in Ethiopia was reported as 5.2/1000 population [4]. The annual incidence was 64/100,000 population as reported in a community-based study conducted in Mescal and Marko districts of rural central Ethiopia [5].

Generally, epileptic seizures are classified as partial or focal, generalized and unknown seizures based on their clinical manifestations [1]. Focal epileptic seizures occur only on part of the brain. Focal seizures could be single focal, multifocal and seizures involving one hemisphere. The symptoms could range from simple change of emotion or the way the environment is perceived to loss of consciousness. Generalized epileptic seizures involve the entire brain and produce bilateral motor symptoms usually with loss of consciousness. If the onset of a seizure is not known, the seizure would be categorized under unknown. Through time, the beginning of a seizure becomes clear then the seizure type could be categorized into focal and generalized.

Unknown onset seizure type is common in infancy and is characterized by tonic flexion of the head, neck and trunk, with circumflexion of the upper extremities. It is usually seen in infants with extensive brain abnormalities and gross structural lesions.

Epilepsy is treated by continuous administration of antiepileptic drugs (AED). Most epilepsy cases are drug administered and curable but it takes a long time to completely control seizure. Beside that, the antiepileptic drugs should be taken strictly. To make things worse, not all cases have solution this way. About one third of epileptic cases are drug resistant [6]. Only surgery, removing the nervous cells that are origins of the epileptic seizures, works for those subgroups of patients.

Epilepsy might result from a variety of causes. It is not a singular disease entity. Head injury, a brain infection (such as meningitis) or a stroke can be the causes of epilepsy. Some inherited conditions, genetics, passed from parents to child, diseases such as meningitis, HIV, tuberous sclerosis, can also be cause of epilepsy [7][8]. However, for most people there are no clear reasons why they have epilepsy. Therefore, the diagnosis of epilepsy is lengthy and it should be conducted by neurologists or trained technicians.

There are a number of tests that have to carried out before concluding whether a seizure happened due to epilepsy or not. The first step is to gather information from the patient or someone related about what happened before, during and after the seizures. Some types of faints can look like epileptic seizures, and often before fainting a person feels cold, clammy and her/his vision goes blurry. But epileptic seizures happen very suddenly and a person may have no warning that a seizure is about to happen. General health tests such as blood sugar level test and electrocardiogram (ECG) should be carried out to check whether the seizure is due to low sugar level or other heart conditions [7]. Medical history should also be considered as part of the diagnosis. If the results of those tests make the person suspicious to epilepsy, electroencephalograph (EEG) test and magnetic resonance imaging (MRI) scan could be conducted further.

EEG is a recording about the change in electrical activity of the brain via electrodes placed on the scalp or brain cerebral cortex surface (intracranial EEG). Accordingly, long term EEG is the basic information source for diagnosing epilepsy. EEG recording from epilepsy patients show characteristic EEG alterations during an epileptic seizure (ictal recordings) and between seizures

(inter-ictal recording). From abnormal patterns of EEG, inter-ictal epileptiform discharges (IEDs) composed of occasional transient waveforms such as isolated spikes, sharp waves and spikes with sharp wave complexes have high interconnection with epilepsy. Generally, information provided by EEG investigation can be used to identify the type of seizures, distinction between focal and generalized seizure disorders, recognition of photosensitivity, selection of proper type of AED and assessing risk of recurrence after an unprovoked seizure [9].

Usually EEG recording for epilepsy diagnosis is done in dark and quiet room for half an hour with open and closed eye of the patient [10]. But using this clinical routine, the possibility of capturing seizure (ictal) events is low. The EEG might be done for prolonged time (long term EEG) to capture seizure. Long term recordings are often done while video filming the patient, allowing the neurologist to correlate EEG findings to visual findings in order to improve seizure assessment. Such recording is referred as long term video EEG and is usually done in hospitals over a period of several days. In addition to that, seizure activations such as hyperventilation and photic stimulation might be used. Hyperventilation is EEG recording after the patient is instructed to breath rapidly and deeply. Photic stimulation is hitting the patient face using a strobe of flashing light at a rate of 1-25 hertz [10].

### 1.2 Statement of the Problem

The clinical routine for the detection of epilepsy is visual scanning of EEG recordings by experienced neurologist or by trained clinical technician to find signatures of ictal or inter-ictal activities. Though, diagnosis of epilepsy is usually based on observed epileptic seizures, inter-ictal findings also offer evidence of epilepsy. From different abnormal EEG patterns, inter-ictal epileptiform discharge (IED) is associated with epilepsy to be used sufficiently for clinical use [8]. Focal slowing of inter-ictal activities are indications of epilepsy especially in temporal lobe epilepsy. Focal slowing of EEGs can also be due to epilepsy caused by tumor and regional lesion [11]. Usually, recordings of 20-minutes EEG might be examined to gather enough information for diagnosis [12]. However, the probability of capturing a seizure is less and thus to get sufficient information, EEG recordings of several hours might be required. Besides, EEG recording done for several hours is assisted by video to get how the patient behaves during seizure which is referred as long-term video recording. In addition to detecting seizures,

questions like what type of seizure and weather the seizure is focal or generalized can be answered based on long term video EEG recordings.

Visual scanning of EEG data to detect epilepsy has serious drawbacks. First of all, it is time consuming and inefficient. Secondly, it is highly subjective due to disagreement among neurophysiologists on the variety of inter-ictal spikes morphology. Moreover, the EEG patterns that characterize an epileptic seizure are similar to waves that are part of the background noise and artifacts (especially in scalp recordings) such as eye blinks and other eye movements, muscle activity, electrocardiogram, electrode and electrical interferences [12]. Hence, developing automated seizure detection system is vital and can be used as a tool to make the life of neurophysiologists easier.

Some of the epilepsy cases are drug resistant or develop tendency of drug resistance during the course of AEDs. About one third of the total patients diagnosed for epilepsy treatment become resistant to drug therapy and from that population about 20% is generalized and 60% is focal epilepsy [6]. If seizure onset site is localized to a well-defined area of the brain that doesn't interfere with vital functions such as speech, language, motor function, vision or hearing then clinical resection of the affected brain area by surgery could be a solution. But the patient should meet certain criteria to be candidate for refractory surgery. Some of the criteria include diagnosis of epilepsy is secure, failure of at least two AEDs in controlling seizure, benefits/risks and complications due to surgery should be understood fully [7] [13].

The mandatory requirement before refractory surgery is correct localization of the brain area affected by epilepsy. Physicians gather information in this pre-surgical stage using imaging instruments such as magnetic resonance imaging (MRI) and sometimes even functional magnetic resonance imaging (fMRI). EEG also plays a great role in locating the epileptogenic focus and the assessment of functional properties and activities of the epileptogenic focus. The imaging devices have superior spatial resolution compared to EEG. But EEG has still place in localization procedures since it is simple to use and has greater temporal resolution. EEG helps in initial distinction between a focal and generalized seizure cases to select surgery candidates. Further inquiry can be done using MRI or other imaging instruments. Intracranial EEG again can be used to localize seizure onset zones (targets of surgical resection) and to follow the surgery process. Here the work is traditionally done by visual scan of EEG segments by experienced neurologist.

Signal processing techniques are used to automate the localization process and make the delineation of the epileptogenic focus useful and robust. An automated scheme which can classify EEG signals from epileptogenic areas as focal and EEGs from healthy regions as non-focal is core for a system that delineates the epileptogenic focus area graphically.

Refractory surgery is more effective in some epilepsy cases. One such kind of cases is temporal lobe epilepsy (TLE), where seizures originate in the medial or lateral temporal region of the brain. Many of these patients develop tendency of resistance to medical treatment. Temporal lobe is just one specific area of the brain (the detail is found in the next chapter). Majority of TLE patients have had excellent results after surgery and this often relies on the EEG and MRI data during pre-surgical evaluation [11] [14]. The current thesis specifically deals with temporal lobe epilepsy.

### 1.3 Significance of the Thesis

Diagnosis of epilepsy through visual scanning of long term EEGs has been practiced for long time and it is still in use. The visual scanning is done based on facts accumulated by neurologist about abnormal EEG patterns that have association with epilepsy. Even though there is disagreement among the neurophysiologists on EEG patterns that characterize an epileptic seizure, it is still a ground truth in the diagnosis process. Visual scanning of EEG is often a time consuming task and prone to observer variability issues. In this regard different techniques have been suggested in the literature to automate the process and develop tools for seizure detection as well as focus localization. These methods usually excluded facts accumulated by neurologist about abnormal EEG patterns during features extraction process from EEG waveforms. This lead to extraction of complex features and big feature space. Feature complexity adversely affects robustness of the features for both seizure detection as well as focus localization scheme on real time signal, or on online EEG data. Accumulated knowledge of neurologists has been used as a basis to develop the automated EEG signal analysis tool in this thesis. The fact that EEG signature ictal segments are full of high amplitude polymorphic waveforms while inter-ictal ones are occasional transient waveforms and the association of temporal epilepsy with focal slow EEG activity from temporal region in intermittent, localized fashion (temporal intermittent rhythmic delta activity - TIRDA) has been utilized majorly to extract simple and accurate features. For instant, temporal intermittent rhythmic delta activity is utilized to extract a feature

that classify healthy and inter-ictal EEG segments effectively. After power spectral density is obtained on the S-transform plan, energy of each of the five EEG rhythms is obtained. A ratio of energy in delta sub-bands to sum of energy in alpha and beta sub-bands could classify normal and inter-ictal EEG segments easily. The value of this ratio for inter-ictal segments is higher than normal ones since most of the EEG activity is concentrated in delta sub-band. The feature extraction way that utilize background facts of neurologist results simpler and accurate features that can be used to characterize healthy, ictal (seizure) and inter-ictal EEG segments effectively in a comprehensive fashion. This characterization enables to approach seizure focus location problem with the same scheme used in detection problem, taking non-focal signal as healthy segment and non-focal segments as epileptic one.

## 1.4 Objectives of the Study

### General Objective:

The general objective of the study is to develop sensitive, efficient and accurate epilepsy seizure detection and focus localization scheme.

### Specific Objectives:

- Develop robust and efficient seizure detection and focus localization scheme, especially for temporal lobe epilepsy cases, that uses few medically sound full features based on Stockwell -transform instead of numerous and complex features;
- Characterization of seizure, inter-ictal and healthy EEG segments from temporal epilepsy cases;
- To carry out qualitative and quantitative assessments of the proposed algorithm with respect to gold standards provided by experts and show directions of their clinical implications.

## 1.5 Organization of the Thesis

The rest of the thesis has been organized into five chapters. Chapter 2 discusses the background, definitions and scientific literatures related to the human brain, EEG and epilepsy. The goal of this section is to give the reader a brief idea about the human brain and different parts of it, EEG, epilepsy and the role of EEG on diagnosis, treatment and management of epilepsy. Chapter 3 reviews important signal processing literatures on epilepsy seizure detection and focus localization. Major literatures are categorized and reviewed well. The chapter also shows the

prospects of the topics and the research gap to be fulfilled. Chapter 4 presents the proposed algorithm and methodology used in this thesis. Chapter 5 present results obtained from the proposed methodology and useful discussions on the results while Chapter 6 includes conclusions and possible future directions.

**References**


1. Commission on Classification and Terminology of the International League Against Epilepsy. Proposal for revised clinical and electroencephalographic classification of epileptic seizures. *Epilepsia*, Vol. 22, PP. 489–501,1981.

2. B. Saraceno, G. Avanzini and P. Lee, Atlas: Epilepsy care in the world, WHO, Geneva, 2005. Available online: http://www.who.int/mental health/neurology/epilepsy atlas r1.pdf

3. World Health Organization (WHO), Initiative of Support to People with Epilepsy, Division of Mental Health, Geneva, Switzerland, 1990.

4. R. Tekle-Haimanot, M. Abebe, A. Gebre-Mariam et al., "Community-based study of neurological disorders in rural central Ethiopia," *Neuroepidemiology*, Vol. 9, No. 5, pp. 263–277, 1990.

5. R. Tekle-Haimanot, L. Forsgren, and J. Ekstedt, "Incidence of epilepsy in rural central Ethiopia," *Epilepsia*, vol. 38, no. 5, pp. 541–546, 1997.

6. S. Pati, A.V. Alexopoulos ''Pharmacoresistant epilepsy: From pathogenesis to current and emerging therapies,'' *Clevel. Clin. J. Med.*, Vol. 77, pp. 457–467, 2010.

7. Mayo Clinic Staff, Symptoms and causes - Epilepsy - Mayo Clinic, Mayoclinic.org, 2018. [Online]. Available at http://www.mayoclinic.org /diseases-conditions/epilepsy/symptoms causes/dxc-20117207. [Accessed: 08/3/2018].

8. I. E. Scheffer, S. Berkovic, G. Capovilla et al. "ILAE classification of the epilepsies: Position paper of the ILAE Commission for Classification and Terminology'' Epilepsia, Vol. 58, No. 4, pp. 512–521, 2017 .

9. S. J. M. Smith, "EEG in the diagnosis, classification, and management of patients with epilepsy,'' *J Neurol Neurosurg Psychiatry*, Vol. 76 (Suppl II): ii2–ii7, 2005. doi: 10.1136/jnnp.2005.069245.

10. L. Sornmo and P. Laguna, Bioelectrical signal processing in cardiac and neurological application (First Edition), Elsevier academic press, 2005.

11. S. Wiebe, W. T. Blume, J. P. Girvin, and M. Eliasziw, “A randomized, controlled trial of surgery for temporal-lobe epilepsy,” *The New England Journal of Medicine*, Vol. 345, No. 5, pp. 311–318, 2001.

12. A. T. Tzallas, M. G. Tsipouras, D. G. Tsalikakis et al. “Automated epileptic seizure detection methods: A review study,” *Epilepsy - Histological, Electroencephalographic and Psychological Aspects*, *ed. by Dr. Dejan Stevanovic*, 2012. Available online:

http://www.intechopen.com/books/epilepsy-histological-electroencephalographic-and-psychological aspects / automated-non-invasive-identification-and-localization-of-focal-epileptic-activity-by-exploiting inf

13. J. de Tisi, G. S. Bell, J. L. Peacock et al. “The long-term outcome of adult epilepsy surgery, patterns of seizure remission, and relapse: a cohort study,” *The Lancet*, Vol. 378, No. 9800, pp. 1388–1395, 2011.

14. M. Javidan, ''Electroencephalography in Mesial Temporal Lobe Epilepsy: A Review,'' Epilepsy Research and Treatment, Vol. 2012 (20120), Article ID 637430, pp.17.

# CHAPTER TWO

# 2. THE HUMAN BRAIN AND ELECTROENCEPHALOGRAM

The subject of epilepsy seizure detection and focus localization is multidisciplinary, it requires good understanding of neurology and signal processing. Since EEG comprises electrical signals taken from the brain by electrodes which are placed on the scalp, understanding of the basic brain anatomy makes the processing of EEG signals easier.

## 2.1 The Nervous System

The master controlling and communicating system of our body is the nervous system. Every physiological process, movement, thought and emotion of our body is under the control of the nervous system. Nervous system can be divided into the central nervous system (CNS), (which consists of the brain and the spinal cord) and the peripheral nervous system (PNS). The PNS consists of the nerves fibers which communicate the central nervous system to the other parts of the body. Sensory organs gather information about the changes occurring both inside and outside the body. Sensory or afferent nerve fibers convey nerve impulses from the sensory organs to the brain and spinal cord. Processing, interpreting the gathered information and finally commanding muscles and glands to respond accordingly is the job of the CNS. The responses of the CNS are sent through efferent or motor nerve tracts to our body. The two systems work closely in integrated fashion. The CNS command specific parts of the body based on reflexes, current conditions, and past experiences. Accordingly, the peripheral has two functional subdivisions. The nerves transmitting signals to the CNS are called afferent or, alternatively, sensory nerves. The nerves transmitting signals from the CNS are called efferent or, alternatively, motor nerves.

The nervous system can be classified as somatic and autonomic nervous system. The somatic (soma means body) nervous system is under the voluntary or conscious control of the CNS. The sensory or motor nerves of somatic nervous system called somatic nerve fiber, convey impulses to and from the skin skeletal muscles and joints. The autonomic nervous system (ANS) consists

of visceral motor nerve fibers that regulate the activity of smooth muscles, cardiac muscles, and glands. The ANS, also called the involuntary nervous system, control involuntary actions such as the pumping of our heart or the movement of food through our digestive tract**.**

### 2.1.1 Neurons

Neurons are nerve cells, basic units of the nervous system. Neurons are highly specialized cells that conduct messages in the form of nerve impulse. Nerve cells are collectively referred as neurons and have different sizes, shapes and functions. As illustrated in Fig 2.1, a typical neuron has a cell body, also called Soma, from which two types of structures originates: the dendrites and the axons. Dendrites are hairy structures with many branches, where with each branch, impulse signals are received from other neurons. The effect of these impulses may be excitatory or inhibitory. The axon is usually a single branch which transmits the signal from the cell body to another neuron or a muscle cell. The length of an axon ranges from less than 1 mm to more than 1m; the longer axons are those which run from the spinal cord to the feet. Dendrites are rarely longer than 2 mm [1]. Any long axon is called a nerve fiber. The axon may be covered with an insulating layer called the myelin sheath. The junction between an axon terminal of one neuron (the pre-synaptic terminal) and the next neuron (post-synaptic terminal) is called the synapse. Information transmission from a neuron to another neuron or muscle cell takes place at this junction. The communication is unidirectional and electrical up to pre-synaptic neuron (part of the synapse that is on the side of the axon). It will be converted to chemical signal in the pre-synaptic neuron using neurotransmitter chemical that diffuse across the synaptic gap and it will be converted back to electrical signal by post synaptic neuron. Between these pre and post synaptic terminals, there is a gap called the synaptic cleft, a fluid filled space that is approximately 30 to 50 nanometer wide [2]. Based on their function neurons are classified into three: sensory neurons (connected to the sensory receptors), motor neurons (connected to muscles), and interneurons (connected to other neurons).

The electrical potential difference between the inner and the outer surface of a neuron membrane is called transmembrane potential. If a nerve cell is stimulated, the transmembrane voltage necessarily changes. But without any stimulants, the transmembrane voltage record varies from 40 mV to 90 mV in different types of neurons and it is called resting membrane potential [2]. Two factors generate the resting membrane potential: differences in the ionic composition of the

intracellular and extracellular fluids, and differences in the permeability of the plasma membrane to those ions. Excitatory stimulus (depolarizing) causes a decrease in membrane potential. Inhibitory stimulus(hyperpolarizing) causes an increase in membrane potential. If the membrane stimulus is insufficient to cause the transmembrane potential to reach the threshold, then the membrane will not activate. The response of the membrane to this kind of stimulus is essentially passive. If the excitatory stimulus is strong enough, the transmembrane potential reaches the threshold and the membrane produces a characteristic electric impulse, the nerve impulse. The electric recording of the nerve impulse is called the action potential. The principal way neurons send signals over long distances is by generating and propagating actions potentials. Only cells with excitable membranes (neurons and muscle cells) can generate action potentials.

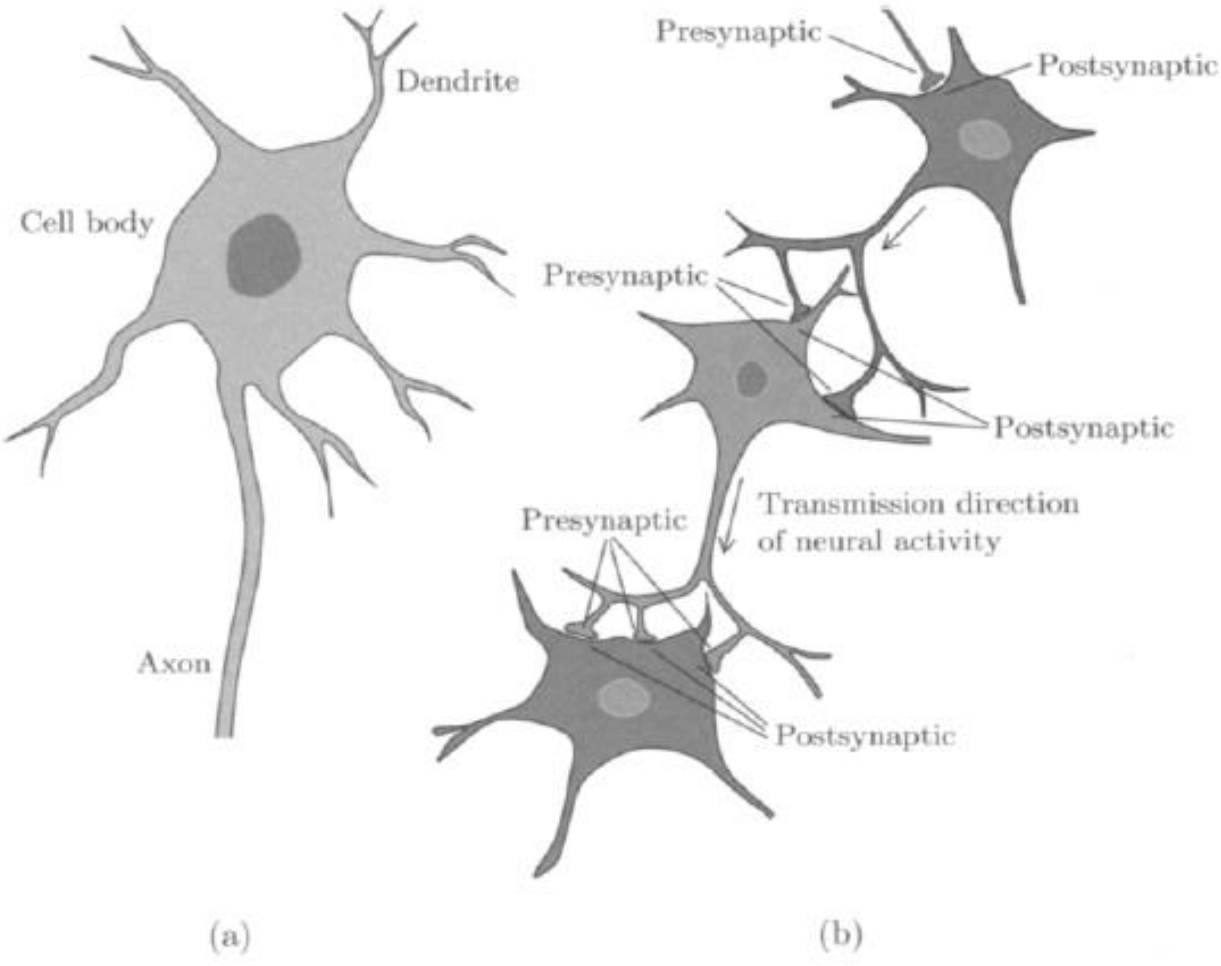


*Figure 2.1 (a) A typical neuron, (b) three inter connected neurons [1]*

### 2.1.2 The Human Brain

The human brain is the central computing and information processing part of the CNS. Adult human brain weighs about 1500g [2]. As seen in Fig. 2.2, adult human brain can be divided into four regions: cerebral hemispheres, diencephalon, brain stem (composed of mid brain, pons and medulla oblongata) and cerebellum. Since most epilepsy case related to cerebral hemisphere, it will be discussed in detail. Cerebral hemisphere is the superior and the conscious part of the brain with a folded look. It accounts about 83% of the total brain mass [2]. Each cerebral hemisphere has three basic regions. The first layer is cerebral cortex of gray matter, which looks gray in fresh brain tissue, bellow that we will find internal white matter and finally we will find islands of gray matter situated deep within the white matter called basal nuclei. Cerebral cortex is the conscious part of our brain in the cerebral hemisphere and the other two layers are supporting layer for the cerebral cortex. The function of white matter is to create communication between the two cerebral hemispheres, between different cerebral areas and between the cortex and the lower central nervous system. A deep longitudinal fissure (deep grove) separates the cerebral hemisphere into two hemispheres. Each hemisphere is again divided by shallow groves called sulcus into four lobes-frontal, parietal, temporal and occipital. The central sulcus separates the frontal lobe from the parietal lobe. The deep lateral sulcus outlines the temporal lobe and separates it from the parietal and frontal lobes. In some literatures, a fifth lobe insula is also mentioned. It is buried deep and covered by portions of the temporal and frontal lobes.

#### 2.1.2.1 Cerebral Cortex

The cerebral cortex is composed of billions of neurons arranged in six layers. It has 2–4 mm thickness. Its many convolutions effectively triple its surface area and the total area is as large as 2.5 $m^2$ [1]. Many studies show that specific motor and sensory functions are localized in discrete cortical areas called domains or primary areas since these neurons are specialized for a particular purpose. The functional areas of the cerebral cortex or domain are three: motor areas, sensory areas and association areas. Motor domains send neural pulses and control our body functions e.g. movement of skeletal muscles. Sensory areas are concerned with receiving information from sensory areas and processing it. Association areas are involved with a task of linking sensory and motor areas. The primary areas are relatively small in size, but are supplemented with larger, surrounding neurons which are essential for higher mental tasks (see also Fig.2.2).

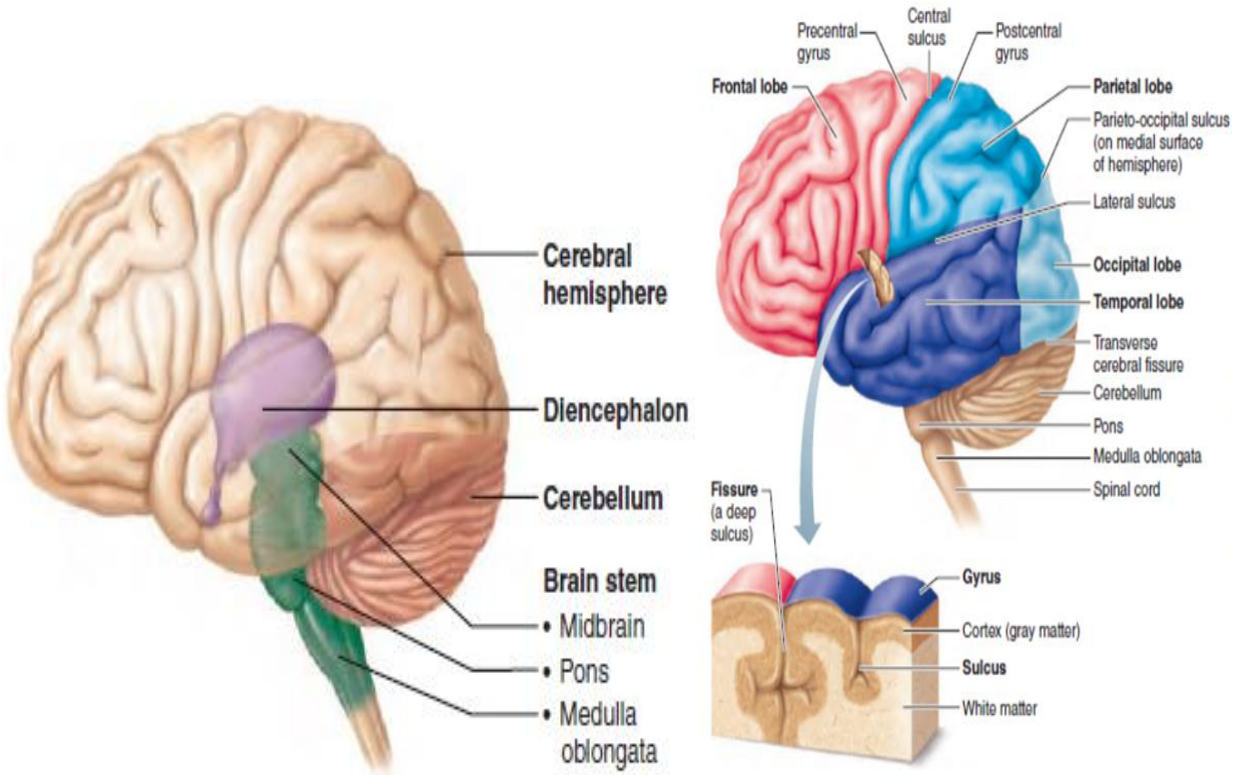


*Figure 2.2 (a) Adult brain structure (b) Lobes and sulci of the cerebrum [2].*

Voluntary movement is primarily controlled by the motor cortex, located in the frontal lobe. The motor cortex also allows us to plan and sequence basic movements into more complex tasks. But tasks requiring considerable muscle control, e.g., speech, certain facial expressions, and finger movements, are associated with the largest subarea of the motor cortex. Sensory information is processed in various parts of the lobes: the auditory cortex is located in the superior part of the temporal lobe, the visual cortex is located at the posterior part of the occipital lobes, and the somatic (touch, pressure and pain) sensory cortex is located just posterior to the central sulcus of the parietal lobe. However higher mental tasks such as memory and language are controlled by different domains and supporting areas in different areas of the cortex working together in overlap fashion. For instant visual information processing with respect to shape, color, and size of an object requires more lobes of the brain, not only the visual cortex, in associated way. Association neurons facilitate the association between different areas of the brain. Most of the frontal lobe part is dedicated to multimodal association area. It receives inputs from the impulse sensory cortex and give meaning to the information, store it in memory tie it to previous experiences and knowledge, and decides what action to take. Those decisions are relayed to the

motor cortex. Multimodal association cortex is the area where sensations, thoughts, and emotions become conscious.

#### 2.1.2.2 Functional Brain Systems

Functional brain systems are networks of neurons and a group of brain structures that work together but are not located in anatomically distinct structures or located in different part of the brain. The limbic system is an excellent example. The limbic system is a group of structures located on the medial aspect of each cerebral hemisphere and diencephalon. The limbic system includes various parts but the most important ones are the amygdaloid body and the C-shaped hippocampus. The limbic system plays roles in our emotion, feeling, in arrangement of information from short-term memory to long-term memory and spatial navigation. Hippocampal tissue damage is often observed in temporal lobe epilepsy [3].

## 2.2 Electroencephalograph (EEG)

Electroencephalograph (EEG) is a recording about the electrical activity of the cerebral cortex via electrodes placed on the scalp or brain cerebral cortex surface. EEG shows dynamics of the cerebral function with good temporal resolution – approximately 2 to 4 milliseconds in conventional digital EEG machines [4]. The electrical activity of single neuron is difficult to be measured due to attenuation effects of thick layers of tissue (fluids, bones and skin). But, the summation of the synchronous activity of millions of cortical neurons with similar spatial orientation, produces an electrical field which is sufficiently strong to be measured on the scalp or brain cortex surface. Generally, EEG measure reflects the total sum of the inhibitory or excitatory postsynaptic potential created by millions of neighboring neurons, primarily generated by groups of pyramidal neurons. Approximately $6cm^2$ synchronous cortical activity can be picked up by single scalp electrode [5].

Researchers before Richard Caton believed that brain has electrical activities and it can be recorded. But it was Richard Caton who demonstrated for the first time in 1875 that electrical signals in the microvolt range can be recorded from exposed brain or the cerebral cortex of rabbits and dogs using sensitive galvanometer [6]. In 1924 Hans Berger recorded weak electrical voltages (in micro volt range) generated in the brain for the first time without opening the skull

by attaching electrodes to the human scalp and depicted graphically on a strip of paper [4]. He observed that the signal changes in many ways according to the location of the scalp the signal is recorded from and the functional status of the brain, such as in sleep, anesthesia, lack of oxygen and whether eyes are opened or closed during recording. Hans Berger used the word electroencephalogram as the first for describing brain electric potentials in humans [6]. After EEG discovery of Berger, it only took a few years time to become very basic instrument for diagnosing neurological pathologies and mentoring of brain health. The first clinical EEG laboratories were established in the United States in the 1930s and 40s. In 1947, the American EEG Society, later the American Clinical Neurophysiology Society, was founded [5]. Now-a-days with the help of computer aided signal processing software, even communication between human brain and machines is possible using EEG signals only.

EEG is referred as intracranial EEG if the recording is done by placing electrodes directly on brain cortex. Intracranial recording is usually done during surgery. It is invasive procedure but it gives fine resolution EEG signal with less noise. When the recording of EEG is done using non-invasive electrodes placed on the scalp, is referred to as a scalp EEG. Signals recorded from the scalp in general have amplitudes ranging from a few micro volts to approximately 100μV [1]. The acquired EEG signals would be amplified before the signals are sampled. Usually for clinical purpose, placement of electrodes on the scalp follow the international 10/20 system, which is a standardized system of the International Federation of Societies for Electroencephalography and Clinical Neurophysiology (IFSECN) [7]. This particular electrode configuration employs 21 electrodes. The numbers 10 and 20 indicate the distance between adjacent electrodes. It is either 10% or 20% of a specified distance measured that depends on each person skull, the total distance between the front and back or between left and right of the head. Electrode placements are labelled according to adjacent brain areas: F (frontal), C (central), T (temporal), P (posterior), and O (occipital). The letter Z is used for the line of electrodes sited on the midline of the head. The letters are accompanied by odd numbers at the left side of the head and with even numbers on the right side. When the total number of electrodes used increases the spatial resolution of the EEG system will be improved. Certain application such as brain mapping uses 64 or more number of electrodes. Brain mapping constitutes a spatial analysis technique in which the EEG activity is represented as a topographic map projected onto the scalp [8].

EEG montage is a standardized arrangement, selection of channel pairs and chains for display and review. EEG recording can be done in either a bipolar or a referential montage. In bipolar system adjacent electrodes are paired, either anterior to posterior (longitudinal bipolar) or side to side (transverse bipolar), which is a good way to try to localize EEG potentials. In referential system each electrode is connected to a differential amplifier and compared with a common electrode (usually placed at the earlobe). Common referential choices include the vertex ($C_z$ electrode), the mastoid process (either individual ears, or a mathematical derivation of both sites), or a common average reference.

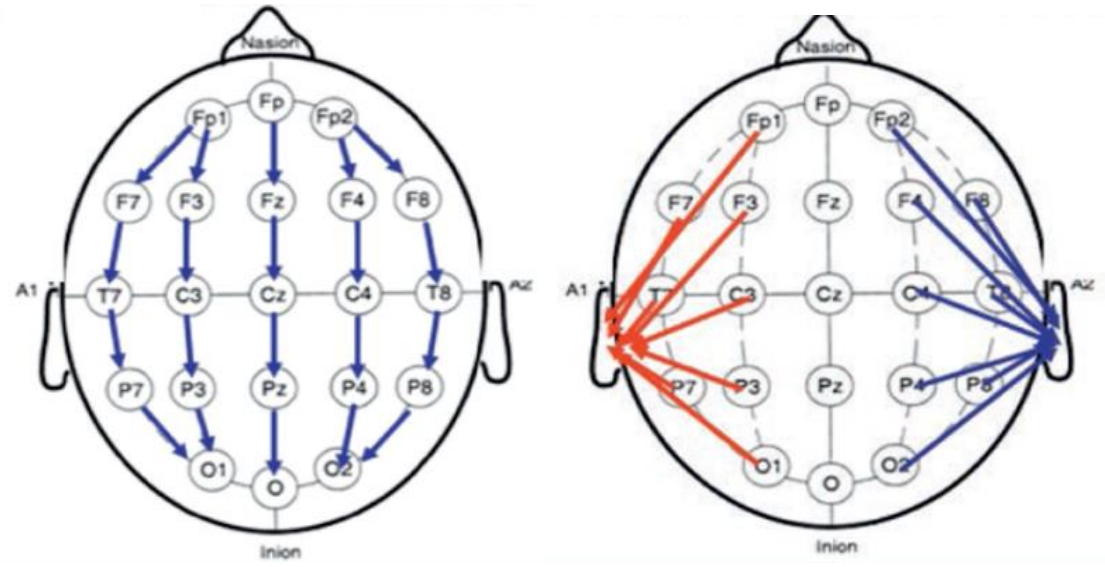


(a) (b)

*Figure 2.3(a) Longitudinal bipolar montage (b). Ipsilateral ear referential montage*

**(Copyright. Mayo Foundation for Medical Education and Research, 2013).**

More recent and advanced montage is the Laplacian or source derivation montage. The Laplacian montage uses tree electrodes in concentric manner or the Tri-polar Concentric Ring Electrode (TCRE). The Laplacian EEG is a mathematical weighted average of the active recording of each surrounding electrodes. The Laplacian montage provides improvement in the signal-to-noise ratio, improvement in spatial resolution and attenuation of common mode artifacts [9].

### 2.2.1 EEG Rhythms and Waveforms

The prominent signal from background EEG with oscillatory, repetitive behavior is referred as EEG rhythm or sometimes EEG wave. EEG rhythms are dependent on the general mental state of the subject, whether the subject was in a state of attention, relaxation, or sleep. EEG rhythms also show different look for healthy subject and subjects with certain neurological pathologies. Majorly, EEG rhythms show different frequency, amplitude, morphology and spatial distribution depending on the subject brain conditions. The amplitude of the EEG rhythm is related to how a group of neurons found in specific brain area or the same brain network fire at the same time or synchronously. Synchronous excitation of a group of neurons produces a large-amplitude signal on the scalp because the signals originating from individual neurons will add up in a time-coherent fashion. On the other hand, asynchronous excitation of the neurons results in an irregular looking EEG with low amplitude waveforms. The frequency of an EEG rhythm is partially sustained by input activity from the thalamus**.** This part of the brain consists of neurons which possess pacemaker properties, i.e., it has the intrinsic ability to generate a self-sustained, rhythmic firing pattern. Another reason to the rhythmic behavior is coordinated interactions arising between cortical neurons themselves in a specific region of the cortex. In the latter case, no pacemaker function is involved, but the rhythms are rather an expression of a feedback mechanism that may occur in a neuronal circuit [10].

EEG rhythms are conventionally classified into five different frequency bands. The interpretation of these bands in terms of "normal" or "abnormal" is relative and depends on the age and mental state of the subject. For example, the EEG of a newborn is drastically different from that of an adult and has, in general, a considerably higher frequency content. The frequency bands indicated below are somewhat coarse, but nevertheless provide a clinically useful categorization of different rhythms. The five rhythms are presented below starting from slow frequency wave, delta rhythm. The frequency division of each rhythm and much of the following discussions are derived from a previous literature [1] [11].

**Delta** rhythm also known as slow-wave, occurs between 0.5 and 4 hertz with large amplitude. It is usually associated with deep sleep and help in characterizing the depth of sleep. If delta rhythm is observed in awake, normal adult, it may be an indication of cerebral damage or brain

disease (encephalopathy). Brain tumor, temporal lobe epilepsy and lesion are some of brain disorders that are cause of delta rhythm in awake, adult subjects.

**Theta** rhythms have frequency band of oscillation between 4 and 7 hertz. The theta rhythm occurs during drowsiness, deep meditation and in certain stages of sleep. Theta activity is observed when our senses are withdrawn from the external world and focused on signals originating from within.

The **alpha** rhythm oscillation is between 8 and 16 hertz and is most prominent in normal adult subjects over the more posterior aspects of the head, the occipital lobe, during wakeful relaxation with closed eyes. Alpha rhythm is reduced with open eyes, mental activity such drowsiness, concentrating and sleep. For healthy adults, alpha rhythms are common with a bell-shaped frequency distribution curve, centering around 10.0 hertz [11]. The frequency distribution is significantly affected by cerebral blood flow.

**Beta** rhythm is a fast rhythm with low amplitude, associated with an activated cortex in between 16 and 30 hertz. Beta rhythms are common when someone is alert or have taken high dose of certain medicines such as benzodiazepines. It can also be observed during certain sleep stages. The beta rhythm is mainly observed in the frontal and central regions of the scalp. Alpha and beta rhythm are described for the first time by Hans Berger in 1929. Berger described alpha rhythm as EEG with larger amplitude, slower frequency (relative to beta rhythm) that appeared over the posterior scalp when adult person eye is closed and in relaxed condition. The smaller amplitude, faster frequency rhythm that replaced alpha rhythm when the person opened his or her eyes were then termed as beta rhythm according to Berger's explanation [12].

**Gamma** rhythm is neural oscillation greater than 30 hertz. The gamma rhythm is related to a state of active information processing of the cortex. Gamma rhythms are traditionally termed as cognitive rhythms.

Most of the above rhythms may persist up to several minutes, while others occur only for a few seconds, such as the gamma rhythm. Most of the time EEGs have irregular look, which is background EEG. Sometimes one rhythm dominates and stands out from the background EEG form. Generally, normal EEG for adult in awake and resting condition is dominated by alpha rhythm. Depending on eye condition, beta rhythms may appear. Sleep condition is mostly

dominated by theta and delta rhythms; especially deep sleep stage is delta rhythm. The gamma rhythm is cognitive or thinking rhythm. There are also other less familiar rhythms such as mu rhythm, Phi rhythm, Sigma and others introduced by researchers [11]. Their connection with epilepsy is not so much.

### 2.2.2 Applications of EEG

In previous times, the output of EEG was only accessible on paper or analog cathode ray tube. That made the uses of EEG difficult. But after computerized digital recording techniques, storage and transmission of EEG signal came into reality, the clinical roles of EEG in diagnosis and monitoring of brain related cases increased dramatically. EEG is suitable for bedside use in intensive care unit (ICU) to monitor, provide timely and therapeutically important information regarding cerebral function. Doctors can access EEG of their patient on computers while setting in their office. Generally, the EEG is suitable for continuous monitoring of cerebral functions with reasonable spatial resolution and excellent temporal resolution (2-4 milliseconds in conventional digital EEG machines) [13]. The spatial resolution is due to EEG signal from electrodes on different regions of the brain. Therefore, activities in different brain regions can be accessed simultaneously with those electrodes. Compared to other brain imaging instruments such Magnetic Resonance Imaging (MRI), functional Magnetic Resonance Imaging (fMRI) and Computed Tomography (CT), EEG has its own advantages and disadvantages. EEG provides less spatial resolution compared to MRI and fMRI and that is one of the major disadvantages of EEG. Electrical activity of deep Cortical, particularly in basal and mesial areas of the hemispheres, may not be registered by EEG electrodes [13]. The advantages are easy to use along bed side, has excellent temporal resolution, high scope of use and cost effective compared to MRI or CT. The most frequent clinical applications of EEG are monitoring of alertness, coma and brain death, controlling anaesthesia depth, locating areas of damage following head injury, stroke, tumor, diagnosis of epilepsy and monitoring the progenies of medication of epilepsy as well as, classification and staging of sleep disorder [14**]**.

There are still ongoing efforts by different researchers to make EEG important diagnostic instrument. Brain-computer interface(BCI) is one such hot research area [15]. The main idea of BCI is to make machines and human brain communication possible using EEG signals only. When the results of such kinds of researches come to reality, many people with disability will be

beneficiary. For example, robotic arm can make communication with tip of neurons in disabled person's arm and can be commanded by the disabled person's brain without any interference. That way, robotic arms could replace functions of a normal arm. EEG based researches on advanced systems on early detection of brain dementia, detection and prediction of epileptic seizures are also hot research areas. In the next section application of EEG on diagnosis and treatment of epilepsy will be explored in detail.

### 2.3 Epilepsy

Epilepsy is a disease of neurological disorder with main manifestations of abnormal bursts of electrical discharges, epileptic seizure, from a group of neuron. Epileptic seizure is usually sudden and recurrent. Seizures may involve convulsion, loss of consciousness, untoned movement or sensations in parts of the body, experience abnormal behavior and emotional disturbances. The expression of seizures varies from patient to patient depending on the type epilepsy. Some patients simply experience different look of the environment and on severe cases, the patient may fall stiffly to the ground, wracked by uncontrollable jerking. Seizures are typically recurrent events at a highly variable rate, ranging from a few seizures during a lifetime to a few dozen during a single day. The duration of each seizure ranges from a few seconds to a few minutes [17].

There is no known cause for epilepsy. But there are some conditions believed to be important causes of epilepsy. Those conditions include brain injury due to stroke, brain tumor, infectious diseases such as meningitis, AIDS, Cysticercosis especially in the developing world and genetic factors [17] [18]. About half of the epileptic seizures have an unknown cause and are called idiopathic [19]. The imbalance of excitatory and inhibitory neurotransmitter chemicals at synapse is also considered as a cause of seizures [1]. If the excitatory neurotransmitters are too active or the inhibitory ones are not active enough, there is likelihood for bursts of uncontrolled electrical activity, seizure, to occur. But the imbalance of signaling chemicals may be due to epilepsy or other cases. Recently developed antiepileptic drugs are aimed at changing this impaired balance of the neurotransmitters by either decreasing the excitatory activity or increasing the inhibitory activity.

Epilepsy is manageable disease by continuous administration of antiepileptic drugs (AEDs). Even though, most epilepsy cases are drug administered and curable, it takes a long time to completely cure the patient. Besides, the AEDs should be taken strictly. To make things worse, not all cases can be solved this way. About one third of epileptic patients are drug resistant [20]. Such types of cases are called refractory epilepsy. The major treatment option for such cases is refractory epilepsy surgery if the seizure causing cells are located in specific location. There are also other therapies used to reduce the effects of seizure. Vagus nerve stimulation and the ketogenic diet are the common forms of such kinds of therapies. Vagus nerve stimulation is basically the act of stimulating the vagus nerve and brain by sending energy from battery powered implanted devices under the skin chest like peacemaker. It's not clear how this inhibits seizures, but the device can usually reduce seizures incidence. Some children with epilepsy have been able to reduce their seizures by following a strict diet that is high in fats and low in carbohydrates. In this diet program, called a ketogenic diet, the body breaks down fats instead of carbohydrates for energy. After a few years, some children may be able to stop the ketogenic diet and remain seizure-free [17].

Epilepsy can be classified based on seizure type, specific location of brain where epileptic cells are found, and brain networks that are responsible for seizure. Temporal, frontal, parietal, occipital and diencephalic epilepsy are common terms related to epileptic cell location based classification system. Limbic, thalamo-cortical and brain stem epilepsy are good examples for brain network epilepsy. But more structured system for classification of epilepsies is based on seizure type. The International League Against Epilepsy (ILAE) established a standardized classification and terminology for epileptic seizures in 1981 and get updated at least every four years [21]. The following discussion is based on the1981 classification scheme. The widely accepted classification scheme of seizures is based on the location of the brain where the seizure starts and part of the brain the seizure involve. Accordingly, the two main group of seizures are partial (focal) seizures and generalized seizures. There are also seizure types categorized under unknown type seizure. If the onset of a seizure is not known, the seizure would be categorized under unknown. Partial seizures start only from a restricted area of the brain and thought to arise within an area confined to one hemisphere. Focal seizures could be single focal, multifocal and seizures involving one hemisphere. Generalized seizure is conceptualized as originating within,

and rapidly engaging neuronal networks in both hemispheres (though not necessarily the entire cortex).

Partial seizures are further classified based on patient experience during seizure. Simple partial seizures do not cause loss of consciousness but might alter emotions or change the way things look, smell, feel, taste or sound. Simple partial seizures may also result in involuntary jerking of a body part, such as an arm or leg, and subjective sensory experience and unusual sensations called auras that precede the onset of a seizure. Auras may include unpleasant odors or tastes, the sensation of unfamiliar surroundings and visual or auditory hallucinations that last from a fraction of a second to a few seconds. Complex partial seizures involve partial loss of consciousness or awareness. During a complex partial seizure, the patient may stare into space and not respond normally to the environment or perform repetitive movements, such as hand rubbing, chewing, swallowing or walking in circles.

Generalized seizures involve the whole brain and their symptom are strong compared to partial seizures. Based on their symptoms we can classify generalized seizures into 6 groups. *Absence (Petit mal)* seizure is most common in children with the main symptom of consciousness disturbance for 5 to 10 seconds, staring into space or subtle body movements such as eye blinking or lip smacking. *Tonic* seizures cause sudden loss of healthy muscle contraction or loss of postural tone. Tonic seizure causes stiffening of muscles. It usually affects muscles in the back, arms and legs and may cause one to fall to the ground. *Atonic (Drop)* seizures cause a loss of muscle control and may cause sudden collapse or fall down. *Clonic* seizures are associated with repeated or rhythmic, jerking muscle movements. Clonic seizures usually affect the neck, face and arms. *Myoclonic* seizures involve sudden brief jerks or twitching of any limb or axial musculature, usually with preserved consciousness. *Tonic-clonic (grand mal)* seizures can be assumed as combinations of tonic and clonic seizures. It causes an abrupt loss of consciousness, body stiffening and jerking of body. After the fall, the body stiffens because of generalized tonic contraction of the muscles; the lower limbs are usually extended and the upper limbs flexed. Following the tonic stage, clonic (jerking) movements occur in the arms and legs. The tongue may be bitten during involuntary contraction of the jaw muscles, and loss of bladder control may occur. Usually, the entire generalized tonic-clonic seizure is over in less than five minutes.

Immediately afterward, the individual is usually confused and sleepy and may have a headache but will not remember the seizure**.**

### 2.3.1 Role of EEG in Epilepsy Diagnosis and Treatment

Long term EEG recordings are the basic information source to diagnose epilepsy along with other tests like MRI, fMRI, intracarotid sodium amobarbital (WADA) test and blood sugar test if a seizure is caused by diabetes. During EEG recordings, video filming the patient will be done to help neurologists correlate EEG findings to visual finding in order to improve seizure assessment. The EEG recordings of patients suffering from epilepsy show abnormal activities. Abnormal EEG signals recorded between epileptic seizures are termed as inter-ictal. It is composed of occasional transient waveforms such as isolated spikes, sharp waves and spikes with sharp wave complexes. Ictal is EEG activity recording during an epileptic seizure. Ictal recording is composed of polymorphic waveforms of variable amplitude and frequency, spike and sharp wave complexes. The EEG recording just before the seizure is a pre-ictal signal. As ictal recordings are rarely obtained, neurologists usually rely on inter-ictal findings to perform EEG analysis of epileptic patients.

Even though recent imaging modalities such as MRI and fMRI take share of EEG in diagnosis of epilepsy, EEG still got many uses in diagnosis and management of epilepsy. EEG can be used to differentiate between a focal and generalized seizure disorder, recognition of photosensitivity of epilepsy, likelihood of seizure relapse if medication is withdrawn and identification of epileptogenic region in epilepsy surgery candidates. One of the difficulties in diagnosis of epilepsy with EEG is correlation between different EEG patterns and variation of epilepsy depending on the type of epilepsy. Epileptiform EEG abnormalities are abnormal EEG patterns that have association epilepsy. Inter-ictal wave forms, called inter-ictal epileptiform discharges (IED), have sufficiently close relation with most epilepsy cases to be used clinically. Focal slow EEG activities, especially during inter-ictal recordings, are the second common epileptiform EEG abnormalities. Focal slow activities from temporal regions in intermittent, localized fashion called temporal intermittent polymorphic delta activity (TIPDA) have close association with temporal epilepsy and extra temporal epilepsy [22]. Focal slow activity also indicates tumor and lesion related epilepsies.

Spikes and sharp waves (SSWs) are transient waveforms that stand out from the background EEG with an irregular, unpredictable temporal pattern (paroxysmal activity) as EEG rhythms. Spikes or sharp waves are major constituents of IEDs. Epileptic inter-ictal EEG are events that occur between ictal events, i.e., epileptic seizures. The distinction between these two patterns has no etiologic or prognostic significance. In clinical discussions, the terms are often used interchangeably; both types of waveforms are generally characterized by a steep initial upstroke. By convention, a spike is differentiated from a sharp wave by its duration: a spike has a duration in the range 20-70 milliseconds, while a sharp wave is 70-200 milliseconds long [13]. The presence of IEDs in a routine EEG has high predictive value to whether a paroxysmal event represented an epileptic seizure. Spikes and sharp waves occur rarely in the general population the incidence being about 1% in healthy adults and 3% in healthy children [15].

Spike-wave complex is isolated spike followed by slow wave and Polyspike-wave complex is same as spike-wave complex but with two or more spikes associated with one or more slow waves. The spike may occur at repetition rates which range from less than 3 to 6 Hertzs [14]. The repetition rate may correlate with different clinical interpretations. But care should be taken to be not confused by artifacts. For example, cardiac activity may interfere with the EEG to such a degree that a heartbeat (particularly the waves of the QRS complex) masquerades as a spike.

Neurologists have to scan, examine long term EEG visually and should associate abnormal EEG pattern findings with patient symptoms and information from imaging modalities. Some of the purposes of visual scanning of long term EEGs include seizure detection, locating seizure onset zone for refractory seizure epilepsies and identifying type of seizure whether focal or generalized seizure disorder. Visual scanning of vast amount of EEG data has serious drawbacks. First it is time consuming and it is highly subjective. Moreover, the EEG patterns that characterize an epileptic seizure are similar to waves that are part of the background noise and to artifacts (especially in extra cranial recordings) such as eye blinks and other eye movements, muscle activity, electrocardiogram, electrode and electrical interference. So, developing automated system is vital and can be used as a tool to make the life of neurophysiologist easier. The major concern of the current thesis work is developing automated EEG classification system for seizure detection and localization, especially for the case of temporal lobe epilepsies.

**References**

1. L. Sornmo and P. Laguna, Bioelectrical signal processing in cardiac and neurological application (First Edition), Elsevier academic press, 2005.

2. H. Katja and N. Marieb Elaine, Human anatomy and physiology (Ninth Edition), Pearson Education, 2013.

3. M. Javidan, “Electroencephalography in Mesial Temporal Lobe Epilepsy: A Review,’’ Epilepsy Res. Treat., Vol. 2012, pp. 1–17, 2012.

4. M. L. Scheuer “Continuous EEG Monitoring in the Intensive Care Unit,’’ Epilepsia, Blackwell Publishing, International League Against Epilepsy, Vol43 (Suppl. 3), PP.114–127, 2002.

5. L. C. Frey, Erik K. St. Louis et al. Electroencephalography (EEG): An Introductory Text and Atlas of Normal and Abnormal Findings in Adults, Children, and Infants, Chicago, IL: American Epilepsy Society, 2016.

6. J. D. Bronzino, “Principles of Electroencephalography,’’ The Biomedical Engineering Handbook, CRC Press, pp. 201-212, Ed. In: J.D. Bronzino,1995.

7. H. H. Jasper, “The ten-twenty electrode system of the International Federation,’’ EEG and Clinical Neurophysiology, PP. 371-375, 1958.

8. A. S. Gevins and S. L. Bressler, "Functional topography of the human brain," in Functional Brain Mapping, pp. 99-116, Toronto: Hans Huber Publishers, 1988.

9. K. Koka and W. G. Besio, “Improvement of spatial selectivity and decrease of mutual information of tri-polar concentric ring electrodes,” Journal of Neuroscience Methods, Vol. 165, pp. 216–222, 2007.

10. M. F. Bear, B. W. Connors, and M. A. Paradiso, “Exploring the Brain,’’ Neuroscience Baltimore: Williams & Wilkins, 1996.

11. D. L. Schomer, The Clinical Neurophysiology Primer, The normal EEG in an adult, Chapter7, Humana Press Inc., 2007.

12. G. Buzsaki , Rhythms of the Brain(first edition), New York: Oxford University Press, Chapter 3,2011.

13. E. Niedermayer and F. Lopes da Silva, "Abnormal EEG patterns: Epileptic and paroxysmal," in Electroencephalography. Basic Principles, Clinical Applications and Related Fields Chapter 13, pp. 235-260, Baltimore: Williams & Wilkins, 1999.

14. A. J. E. Geerts, Detection of interictal epileptiform discharges in EEG, master thesis in applied mathematics, University of Utwente, Faculty of Electrical Engineering, Mathematics and Computer Science, 2012.

15. S. J. M Smith, “EEG in the diagnosis, classification, and management of patients with epilepsy,’’ J Neurol Neurosurg Psychiatry, Vol. 76 (Suppl II):ii2–ii7, 2005.

16. M. Teplan, “Fundamentals of EEG measurement,’’ Institute of Measurement Science, Slovak Academy of Sciences, Measurement science review, Vol. 2, Section 2, 2002.

17. Mayo Clinic Staff, ''Symptoms and causes - Epilepsy - Mayo Clinic,’’ Mayoclinic.org, 2018. Available online: http://www.mayoclinic.org/diseases-conditions/epilepsy/symptomscauses/xc-20117207. [Accessed: 08/3/2018].

18. I. E. Scheffer, S. Berkovic, G. Capovilla et al. “ILAE classification of the epilepsies:Position paper of the ILAE Commission for Classification and Terminology’’ Epilepsia, Vol.58,No.4,pp.512–521, 2017

19. M. J. England, C. T. Liverman, A. M. Schultz, and L. M. Strawbridge, “Epilepsy across the spectrum: Promoting health and understanding. A summary of the Institute of Medicine report,” Epilepsy Behav., Vol. 25, No. 2, pp. 266–276, 2012.

20. S. Pati, A. V. Alexopoulos, "Pharmacoresistant epilepsy: From pathogenesis to current and emerging therapies " Clevel. Clin. J. Med. 2010, Vol. 77, pp. 457–467.

21. Commission on Classification, International League Against Epilepsy proposed provisions of Clinical and electroencephalographical classification of epileptic seizures. Epilepsia, Vol. 22, pp. 489-501, 1981.

22. M. Javidan, ''Electroencephalography in Mesial Temporal Lobe Epilepsy: A Review ,’’Epilepsy Research and Treatment, Vol. 2012 (20120, Article ID 637430, 17 pages.

# CHAPTER THREE

# 3. SIGNAL ANALYSIS FOR AUTOMATED EEG SEIZURE DETECTION AND SOURCE LOCALIZATION

Studies in automated analysis of EEG recordings for detection of seizures and localization of the epileptic focus showed many developments in the last four decades. Although, various works have been done previously, epilepsy detection and localization studies have common flows. Extracting relevant descriptors (features) contained in EEGs signals through some mathematical formulation and classifying those features for specific purpose are common procedures almost in all studies. The features extracted should be relevant enough to the problem raised in the research. Specifically, the question in seizure detection studies is to discriminate epileptic EEGs from normal. As a result, features that describe polymorphic seizure signals or interictal spikes morphology are used in detection works. Accordingly, seizure detection studies can be classified as spike detection and seizure analysis [1]. Whereas the aim of epilepsy source localization is to classify EEGs from epilepsy affected areas and normal regions for delineation of epileptogenic focus. In effect localization works use features that can characterize EEGs from channels of epilepsy affected areas.

Some of the features have connections to the physiological phenomena of epileptic seizures. For instance, during a seizure many epileptic neurons fire synchronously in abnormal manner. Due to synchronous firing, EEGs from channels containing seizure are expected to be high in amplitude and energetic. Based on the fact that seizure EEGs have high energy, power spectral density has been used as a feature in previous literatures [2][3][4]. Phase synchrony between EEG channels is another example of physiological features used for both detection and localization studies. To get a measure of “synchronicity”, different features have been used such as the autocorrelation function [5], the synchronization likelihood [6] and the nearest neighbor phase synchronization [7]. Seizure is uncontrolled, chaotic and nondeterministic state of the brain. Inter-ictal state is less random state compared to seizures. But still it is a random state compared to normal state of the brain. One would expect, EEGs from different state of the brain to have different complexity level. Different entropy features have been used to quantify the complexity level of EEGs. Approximate, phase, and Shannon entropy are some of them [8] [9]. There are also mathematical features used that are not connected directly with the physiological processes of seizures. Larger

singular values and Lyapunov exponent are representative examples from features that are not directly connected with the physiological processes of seizures.

Different transforms and signal decomposition technique have been applied in seizure detection and localization studies. The signal processing techniques used for feature extraction matter a lot on understanding of the information contained in the signal. For instance, approximate entropy as feature has been extracted from raw EEGs, intrinsic mode functions of the EEGs after empirical mode decomposition and from wavelet sub bands of EEG signals [8] [10]. The effort of those researchers was to improve the performance of the approximate entropy feature using different signal processing techniques.

This chapter focuses on reviewing those signal processing techniques used previously to extract meaningful features. The chapter starts with time and frequency domain EEG analysis techniques and move on to methods that make use of joint time-frequency signal information including the short time Fourier transform, Cohen's class transforms as well as wavelets. It also includes a sections devoted discussing methods that make use of empirical mode decomposition (EMD) and singular value decomposition (SVD) followed by those that rely on non-linear dynamics and chaos theory at last.

### 3.1 Classical Approaches for EEG Analysis

Time domain and frequency domain analysis of EEGs are classical approaches used in seizure detection and localization researches. The time domain approach is based on analyzing the time variation of the raw EEG voltage reading. As stated in the previous chapter, inter-ictal EEGs have occasional waveforms, such as isolated spikes, spike trains, sharp waves or spike-wave complexes. Early seizure detection works concentrate on characterizing inter-ictal spikes, traditionally referred as spike detection. In a previous research, Gotman et al. developed an algorithm that first breaks down the EEG signal into half-waves traveling in opposite directions [11] [12]. Then morphological characteristics of these half-waves, such as amplitude and duration, were used to determine the existence of epileptic seizures. Another approach used to detect seizures emphasized on characterizing seizure EEGs. Embedding entropies such as approximate kolmoogrov-sinai entropies can be directly calculated from the EEG time series to discriminate seizure and non-seizure signals [13]. Approximate entropy quantifies the regularity

of a time series. The value of approximate entropy drops during seizures due to the synchronous discharge of large groups of neurons during an epileptic activity [14]. In another study, the authors in [15] developed seizure detecting algorithm using group of statistical features including the mean, variance, zero-crossing rate, entropy, and autocorrelation. Many statistical features such as the histogram, different entropy measures, mean, variance, zero-crossing rate and autocorrelation are also used in time -domain analysis [16].

In frequency domain analysis, the information about the frequency content of the signal can be extracted and analyzed. The approach can be broadly divided into two: classical methods which are based on the Fourier transform and modern methods such as those based on the estimation of model parameters and nonparametric methods [17]. Fast Fourier transform is common algorithm used in determining the discrete Fourier transform of digitized signals. Both the magnitude and phase information of the Fourier transform are exploited in different researches. In one of the previous studies, epileptiform discharges of seizure EEGs is quantified by power spectral density using fast Fourier transform based on Welch spectral analysis [18]. In the common approach, power spectral density is calculated by averaging the magnitude of square of the Fourier transform of the waveform. Averaging improves the statistical properties of the result and is commonly referred as periodogram. In the Welch approach, a signal is divided into window of overlapping segments, the power spectrum in each segment is calculated and then average of the power spectra is found. The authors divided each EEG data in segments of 256 data points with 50% overlap and using triangular window. Decision tree classifier was used to group the data into seizure and non-seizure EEG and the classification accuracy obtained was 98.72%. The EEG data used was publicly available database of Bonn University [19]. The data base consists of five sets of EEG segments (denoted as Z, O, N, F and S), each containing 100 single –channel segments of 23.6s duration with a sampling rate of 173.6 HZ. Sets Z and O consisted of segments taken from surface EEG recordings from five healthy volunteers in relaxed and awake state with eyes open (Z) and eyes closed (O), respectively. Sets N and F consisted segments from five patients in the epileptogenic zone (F) and from the hippocampal formation of the opposite hemisphere of the brain (N) measured during seizure-free intervals, i.e. inter-ictal period. Set S contained seizure activity, selected from all recording sites exhibiting ictal activity. Set N, F and S are recorded from intracranial electrodes. Most of the works reviewed in this chapter made use of the Bonn University database to develop and test their EEG processing algorithms.

### 3.2 Time-Frequency Analysis of EEGs

Many biological signals are not stationery in that they change their spectral content over time, and have multiple signal components [17]. The spectral content of EEGs for example changes considerably depending on various internal states of the subject. Frequency domain analysis of a signal shows the frequency contents of the signal. When the frequency content changes temporally, such as in the case of non-stationary signals, one would also want to see what type of frequencies exist in time and a simple frequency analysis is not adequate to do so [20]. The need to describe how the spectral content of a signal changes with time yields a number of time-frequency analysis methods. The time-frequency techniques analyze signals in both time and frequency domain simultaneously. Using a joint time-frequency technique, the way how the frequency component of a signal changes with respect to time can be shown. This could give information about the temporal localization of the spectral components of a signal, especially for multicomponent bio-signals [20]. Therefore, time–frequency techniques are more suitable to extract local features and to handle signals with highly localized events such as bursts, spikes, and discontinuities, which typically occur in EEG signals during seizures [21].

To illustrate the advantages of joint time-frequency methods in handling multicomponent and non-stationary signals, a synthetic signal consisting of a low frequency signal for the first half, a middle frequency signal for the second half, and a short lived high frequency burst is used [22]. Figure 3.1 presents the synthetic discrete time series, the amplitude of its discrete Fourier transform and the amplitude spectrum computed using one of the joint time-frequency analysis techniques, the short time Fourier transform (discussed in the next section). Clearly the traditional Fourier transform offered inadequate information about the signal while the short time Fourier transform showed all three signal components resolved both in time and frequency.

#### 3.2.1 Short –Time Fourier Transform (STFT)

As the name indicates the approach of the short-time Fourier transform is based on dividing the signal under consideration into series of small pieces and perform standard Fourier transform on each segment. The result is a joint time-frequency information. The STFT assumes the signal as quasi-stationery, i.e. stationery over the time duration where a segment has been taken.

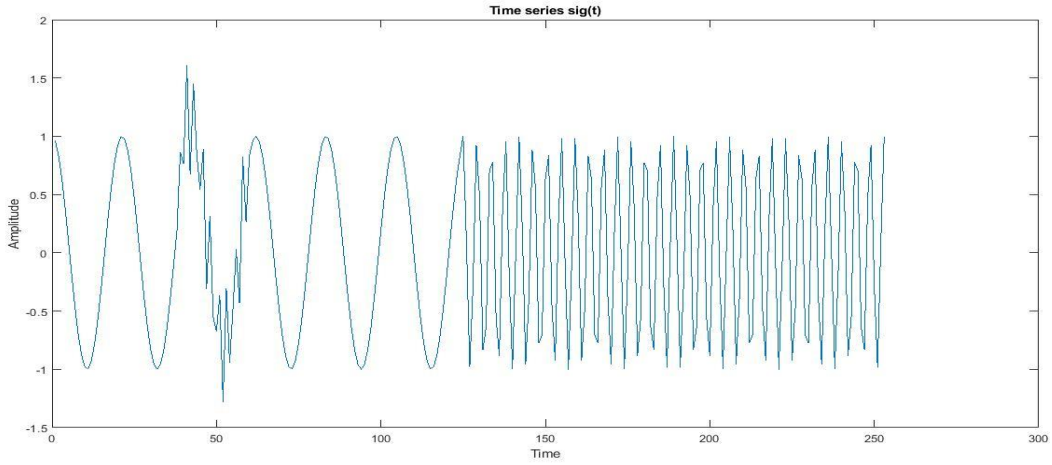


*Fig 3.1 (a) times series the synthetic signal.*

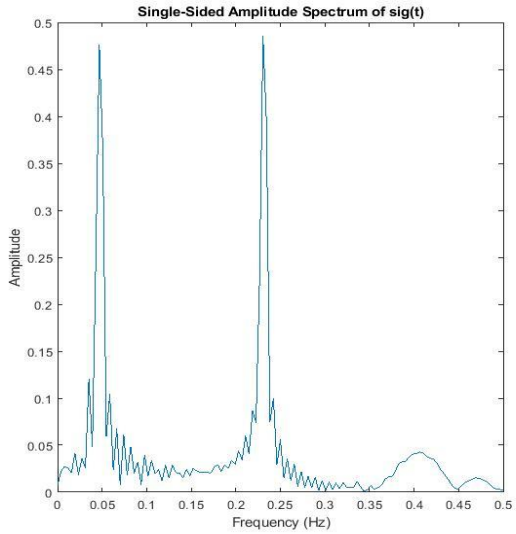


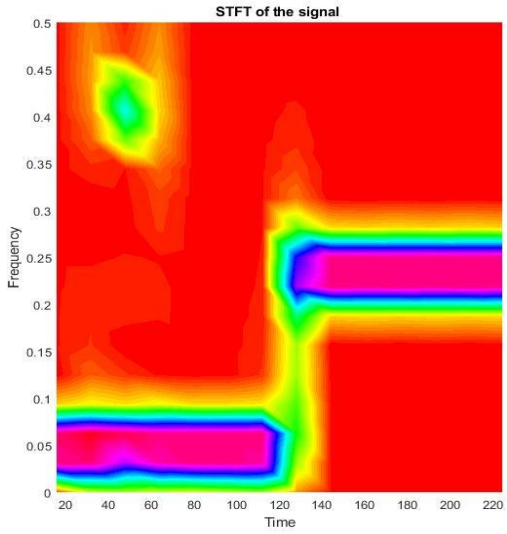


*Figure 3.1 (b) DFT of the synthetic signal.* *(c) Short time –Fourier transform of the synthetic signal.*

The intent behind localizing the Fourier transform is to get insight on how the frequency contents changes with time. Different localizing windowing techniques are applied to isolate the segments from the overall waveform effectively. Selecting the most appropriate window length is critical issue to get good resolution. The formula to compute the STFT of a continuous signal is shown in Eqn.3.1 below. The picture of the square coefficient of the STFT is known as spectrogram. Spectrogram shows the energy distribution of the signal in time and frequency. The major limitation of the STFT is trade-off between the choices of time versus frequency resolution.

Shortening the data segment improves the time resolution of the STFT but could also result in the loss of low frequencies that are no longer fully included in the short data segment. Hence, if the window is made smaller to improve the time resolution, then the frequency resolution is degraded and vice versa. Uncertainty principle dictates that the product of frequency resolution (expressed as bandwidth, B) and time, T, must be greater than some minimum value, specifically $BT \geq 1/4\pi$ [ 17]. It was proven that a Gaussian window is the only window that meets the lower bound of the uncertainty principle; the Gabor transform is similar to the STFT computed using a Gaussian window [23].

$$\mathbf{X(t,f)} = \int_{-\infty}^{\infty} \mathbf{x(t)w} * (\boldsymbol{\tau} - \mathbf{t})\mathbf{e}^{-\mathbf{j2\pi\tau f}}\, \mathbf{d\tau} \tag{3.1}$$

In Eqn. (3.1), w(τ-t) is the window function, * is the complex conjugate of w, and τ is the variable that slides the window across the waveform, x(t). One strength of the STFT is that it is a simple solution that rests on a well understood classical theory of the Fourier transform and is easy to interpret. Despite the limitations of having trade-off between resolution of time and frequency simultaneously, STFT has been used successfully in a wide variety of problems, particularly those where only high frequency components are of interest and frequency resolution is not critical. For example, the area of speech processing has benefitted considerably from the application of the STFT [17].

STFT is not much utilized for EEG analysis, but it worth to mention the epileptic seizure detection work by Sengur et al. [24]. The main idea of this scheme was to use the time-frequency plane of the STFT of a given EEG signal as grayscale image to extract features that can describe the epileptic EEG signal. The STFT time-frequency plane of heathy and epileptic EEG signals is converted into 8-bit grayscale image and divided into five sub-images corresponding to the frequency bands of the EEG rhythms to localize significant structures. The EEG rhythms on frequency ranges were delta (0-4 Hz), theta (4-8hz), alpha (8-12Hz), beta (12-30Hz) and gamma (30-50Hz). Texture descriptors such as gray-level co-occurrence matrix (GLCM), texture feature coding method (TFCM), and local binary pattern (LBP) are computed for each sub-image. Features such as histogram, contrast, correlation, energy, and homogeneity were finally computed. Using support vector machine(SVM) as a classifier, the authors were able to secure an overall accuracy of 92.5%, sensitivity of 95% and specificity of 90% in detecting seizures.

### 3.2.2 Wigner-Ville Distribution

Unlike the STFT, Wigner-Ville distribution(WVD) shows how the signal energy distribution is in time and frequency at once, not the signal amplitude. The development of the WVD was inspired by the classical way of calculating the power spectrum of a signal from the Fourier transform of the autocorrelation function. The autocorrelation function is constructed by comparing the signal with itself for all possible relative shifts or lags. Given a signal *x(t)*, its autocorrelation is computed using Eqn. (3.2).

$$r_{xx}(\tau)=\int_{-\infty}^{\infty} x(t)x(t+\tau)dt \qquad (3.2)$$

In the standard autocorrelation function, the autocorrelation, $r_{xx}(\tau)$ is only a function of the lag, or shift, $\tau$. If instead of integrating over time, if the comparison is done for all possible values of time, then the resulting equation is called instantaneous autocorrelation. The equation for the instantaneous autocorrelation function is shown in Eqn. (3.3):

$$R_{xx}(t,\tau)= x\left(t+\frac{\tau}{2}\right) x*(t-\frac{\tau}{2}) \qquad (3.3)$$

In Eqn. (3.3), τ represents time lags and * represents the complex conjugate of the signal. The instantaneous autocorrelation is a two dimensional function of lags and time. Interesting fact about the instantaneous autocorrelation function is cross products between signal components, which are resulted from the nature of the cross multiplication. The Wigner-Ville distribution repeats the classical way of calculating power spectrum by taking the Fourier transform of the instantaneous autocorrelation function, but only along the τ (i.e., lag) dimension. The result is a function of both frequency and time as shown in Eqn. (3.4).

$$W(t,f) = \int_{-\infty}^{\infty} x(t+\frac{\tau}{2})x*\left(t-\frac{\tau}{2}\right)e^{-j2\pi f\tau}\,d\tau \qquad (3.4)$$

The primary problem of this approach is cross-terms inherited form instantaneous autocorrelation**.** Despite the problem of the cross-terms, WVD provides a high resolution representation in time and in frequency. Especially, for mono-component non-stationary signals such as chirp, the WVD provides good outcomes. The WVD has many interesting properties. The WVD is invariant to shifts in time and frequency. It also has a property of finite support in time and frequency. The details about those properties of WVD can be found in [25]. But the

WVD representations of multicomponent signals, like EEG, often are misleading due to the cross terms. The WVD has also poor noise properties and negative regions that have no meaning. Different smoothing kernel functions, g, are designed to reduce the effect of cross-terms from the instantaneous autocorrelation function before taking the Fourier transform. The WVD is member of the Cohen's class time–frequency distribution and the primary differences between each type of Cohen distribution is simply the type of kernel function that is used to reduce cross terms and windowing function. The general equation of the Cohen class is:

$$\boldsymbol{W(t,f) = \iiint g(v,\tau) e^{j2\pi v(u-t)}\ x\left(u+\frac{\tau}{2}\right) x*\left(u-\frac{\tau}{2}\right) e^{-j2\pi f\tau} dudvdt} \qquad (3.5)$$

In Eqn. (3.5), $g\ (v, \tau)$ serves as windowing and smoothing of the instantaneous autocorrelation kernel function. It is this smoothing and windowing kernel that differentiates between the various distributions in Cohen's class. For the WVD distribution, the kernel is simply 1 (i.e. $g\ (v, \tau) = 1$). One popular example from Cohen's class is the Choi-Williams which assumes an exponential-type kernel. Specifically, the kernel is $g\ (v\ ,\tau) = e^{-v^2\tau^2/\sigma}$. The other famous example is the smoothed -pseudo-Wigner-Ville distribution (SPWVD).

In a previous study, Tzallas et al. used 12 different quadratic Cohen's class distributions (QCCD) for epileptic seizure detection. Margenau-Hill (MH), Wigner-Ville (WV), Rihaczek (RIH), Reduced interference (RI), Pseudo Margenau-Hill (PMH), and Pseudo Wigner-Ville (PWV) were some of the distributions employed in the research [2]. In this work, the time -frequency distribution plane of each EEG signal was first partitioned into 15 windows. Accordingly, the time axis is divided into 3 equal intervals and the frequency axis is divided into 5 sub bands using pervious medical knowledge. The distribution is integrated over the time and frequency axis to get fractional energy in each window. Including the energy of the whole time-frequency plane,16 features were then extracted for each signal. Principal component analysis (PCA) was used to reduce the dimension of the feature set. Finally, the classification of the feature space was done using artificial neural networks (ANN). The algorithm was tested on Bonn University EEG database by formulating 3 classification problems. In the first problem, two classes were examined, normal (Z-set) and seizure (S-set). The second classification problem includes three classes: normal (Z-set), seizure free (F-set) and seizure (S-set). In the third problem, five classes are used by including all EEG segments from the described dataset (thus 500 EEG segments).

Results showed that Reduced interference (RI) distribution performed better compared to the other distribution. For the first and second classification problems, RI distribution scored 100 percent of classification accuracy. For the third problem, the classification accuracy dropped due to the fact that both Z and O are normal expect that the two signals are recorded with two eyes open and closed respectively as well as and sets F and N are recorded during inter-ictal phase from different regions. Similar work was done by authors in [26]. The only difference here is that the feature extraction was based on modules of the time frequency plane instead of the whole time-frequency plane. The reduced interference (RI) distribution time-frequency plane was modularized into uniform 32*32 modules. Energy and entropy features were extracted as features from each module to classify normal and seizure EEG segments. Using Bonn University database and ANN as classifier, average selectivity, sensitivity and accuracy as high as 97.3% were achieved.

### 3.2.3 Continuous Wavelet Transform

The continuous wavelet transform was developed to overcome the resolution problem of the STFT due to fixed window width. The continuous wavelet transform (CWT) of a signal *x(t)*, is defined as the integral of the signal multiplied by scaled and shifted versions of an analyzing function called wavelet, $\psi$, [ 27] [ 28].

$$\boldsymbol{CWT(a,b) = \int_{-\infty}^{\infty} x(t) \frac{1}{\sqrt{|a|}} \psi * (\frac{t-b}{a}) dt} \quad (3.6)$$

In the above equation, the analyzing function, wavelet $\psi(t)$, is enlarged or compressed by the variable *a*. For $a>1$, the wavelet is stretched along the time axis and for $a<1$ the wavelet is contracted in time. It is called scaling parameter since it varies the size of the wavelet. Negative values of *a* simply flip the analyzing function on the time axis. Basically the wavelet has oscillatory form, hence the term "wavelet" is used. The * indicates complex conjugation, and the normalizing factor $1/\sqrt{|a|}$ ensures that the energy is the same for all values of *a* . The parameter *b* is called shifting parameter and translate the wavelet function across the time axis. The wavelet coefficients *CWT (a, b)* then describe the correlation between the signal and the wavelet at various translations*(b)* and scales*(a)* and the coefficients must be added together to reconstruct the original signal. For decreasing values of the scaling parameter, *a*, the wavelet will get compressed, thus CWT provides better time resolution but reduced frequency resolution. On the

other hand, for increasing value of *a*, the wavelet will get dilated and the CWT provides better frequency resolution but poor time resolution. Therefore, there is a tradeoff between time and frequency resolution just as in STFT. The other difficulty of the CWT is calculation of coefficients for continuous value of the scaling parameter, *a*, which is computationally expensive. The scaling and translation parameters should be discretized and that is the topic of the next section.

### 3.2.4 Discrete Wavelet Transform (DWT)

The CWT is highly redundant and provides an oversampling of the input signal by generating more coefficients than is necessary to distinctively characterize the signal. This is due to the fact that calculating wavelet coefficients at every possible scale is computationally very expensive. Computationally efficient DWT can be achieved by restricting the variation in translation and scale parameters, usually to powers of 2. That is sometimes termed as the dyadic wavelet transform [27]. Even this is not enough, the wavelet family (scales) should be selected in a way that leads to an orthogonal basis. To produce DWT of orthogonal scales, a special function called scaling or smoothing function is defined. The wavelet function sometimes can be defined from the scaling function. The DWT analyzes signals in multiresolution fashion, from finest to coarse resolution. In DWT, the signal is expanded into coefficients approximation, $a_j(k)$ and detail coefficients, $d_j(k)$. Equation (3.7) shows how to find coefficients from the scaling and wavelet function. Using orthogonal DWT, we can achieve bilateral, non-redundant transform to analyze and reconstruct the original signal effectively. Details about DWT and scaling function can found in [ 29].

$$\boldsymbol{aj}(\boldsymbol{k}) = \int_{-\infty}^{+\infty} \mathbf{2}^{\boldsymbol{j}}\ \boldsymbol{x}(\boldsymbol{t})\boldsymbol{\varphi}\left(\mathbf{2}^{\boldsymbol{j}}\,\boldsymbol{t} - \boldsymbol{k}\right)\boldsymbol{dt} \quad \text{and } \boldsymbol{dj}(\boldsymbol{k}) = \int_{-\infty}^{+\infty} \mathbf{2}^{\boldsymbol{j}}\ \boldsymbol{x}(\boldsymbol{t})\,\boldsymbol{\psi}\left(\mathbf{2}^{\boldsymbol{j}}\,\boldsymbol{t} - \boldsymbol{k}\right)\boldsymbol{dt} \tag{3.7}$$

In Equ. (3.7), the functions $\varphi(t)$ and $\psi(t)$ are the basic scaling and mother wavelet respectively, $j$ is the scale index, and $k$ is the translation parameter. Usually the DWT is implemented by passing the signal through a series of low-pass (LP) and high-pass (HP) filter pairs known as filter banks. The procedure of decomposing the signal into frequency bands is also known as subband coding. The process is illustrated in Fig.3.2.

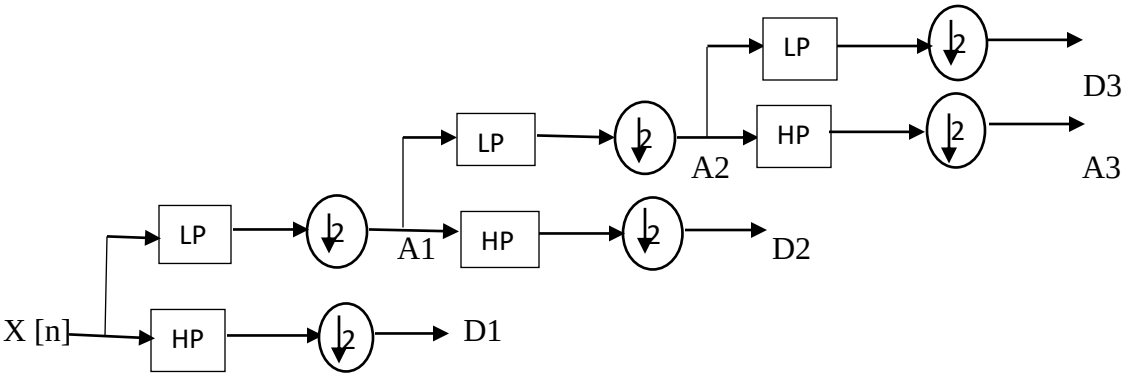


*Figure.3.2 Wavelet decomposition of a signal (Third level).*

As shown in Fig.3.2, for a signal with sampling frequency, fs, the outputs from the high and low pass filters of the first stage have the frequency content 0–fs/4 and fs/4–fs/2. Before passing into the second stage, half of the samples can be eliminated without loss of generality. Simply discarding every other sample will subsample the signal by two, and the signal will then have half the number of points. This operation is known as down sampling and in this case the signal is down sampled by half. The operation is illustrated schematically by the symbol ↓2. During each decomposition, referred as level, the filtering and subsampling will result in half the number of samples (and hence half the time resolution) and half the frequency band spanned (and hence double the frequency resolution). The high-pass filter is analogous to the application of the wavelet to the original signal, having coarse resolution. While the low-pass filter is analogous to the application of the scaling or smoothing function. The output from the low and high pass filters are referred to as approximation (A) and detail (D) coefficients of each level respectively. It can be repeated for further decomposition. Two decomposition schemes exist: dyadic decomposition and complete (balanced) decomposition. In balanced decomposition scheme, both high pass and lowpass sub bands are further decomposed into high pass and low pass sub bands up till the terminal signals. The scaling functions and wavelets associated with such general tree structures are known as wavelet packets. While in dyadic decomposition structure only the low pass filter is decomposed further. The set of filters that decompose the original signal into sub bands are termed analyzing filters while the set of filters that reconstruct the close approximation of the original signal from the decomposed sub signal are termed synthesizing filters. The criterion placed on the filter to cancel aliasing effect, the requirement placed on the filters to be able to recover the original waveform from the subband waveforms and the criterion for the high pass filter output to be orthogonal to that of the lowpass output are stated briefly in [29].

The DWT has been widely utilized in fields of EEG signal analysis for detection of seizures and localization of seizure onset regions for refractory focal epilepsy surgery. The common method is extraction of features after decomposition of the EEG signal into five sub-bands or EEG rhythms. Sometimes using the inverse wavelet transform, time domain signal is reconstructed from the wavelet coefficients derived for each sub-bands. After the reconstruction, time-domain features in different sub-bands can be extracted to characterize EEG segments. The selection of an appropriate wavelet and the number of decomposition levels is also very important in any analysis of EEG signals using the wavelet transform.

**S**imple features like energy, standard deviation and entropy have been used in many published papers. The major differences in those papers are the way the decomposition is done, the decomposition level and the classifier used. Panda et al. for example proposed SVM classifier based seizure detection system using DWT [30]. The authors used EEG segments from Bonn University data base. Each EEG segment is decomposed into five levels using DWT filters (after fifth levels of decomposition, the components obtained were 0-2.7 Hz, 2.7-5.4 Hz, 5.4-10.81Hz, 10.81-2l.62 Hz, and 2l.62--43.25 Hz. The extracted features for signal classification were energy, standard deviation, and entropy. The classifier was tested on healthy subjects with open eyes, healthy subjects with closed eyes, and seizure signals. The simulation results revealed an accuracy of 91.2% in seizure activity detection. Ocak et al. also proposed a similar system for seizure detection using DWT with three levels of decomposition and approximate entropy (ApEn) as feature [10]. The EEG segments were again taken from Bonn University data base. Sets Z, O, and F were taken as normal class and set S as ictal class. The 400 EEG segments were decomposed into sub-bands using DWT. The frequency ranges for these detail and approximate coefficients were A1 (0–43.4 Hz), A2 (0–21.7 Hz), A3 (0–10.85 Hz), D1(43.4–86.8 Hz), D2 (21.7–43.4 Hz) and D3 (10.85–21.7 Hz). ApEn values of the approximation and detail coefficients at each level of the wavelet decomposition were computed. Seizure detection was based on applying a threshold to the ApEn values, ictal class have ApEn values less than the threshold. D1 (43.4–86.8 Hz) outperformed all the other sub-bands for classification. Using D1, 96% of the EEG segments from the ictal class were correctly classified and 93.7 % of the EEG segment from the normal class were correctly classified.

Authors in [31] proposed seizure detection scheme based on wavelet features and statistical pattern recognition. First, the frequency content of the EEG signal segments was restricted to 0-64 Hz using low-pass finite impulse response (FIR) filter. The filtered EEG segments were then decomposed into 4 levels using 4th order Daubechies wavelet**.** The computed features were mean, standard deviation and entropy of the wavelet coefficients in each sub-band and relative wavelet energy (ratio of energy in delta sub-band to total sum of energy of the signal). Applying the inverse wavelet transform, signals were reconstructed using computed coefficients in the previous stage. After the signals were reconstructed in each sub band, time domain features including standard deviation were computed. In total, 25 features were extracted from all 300 EEG segments,100 healthy surface EEG and 200 intracranial EEG segments taken from epilepsy patients. From the 200 EEG segments,100 of them exhibited interictal activity and 100 segments exhibited ictal activity. The dimension of the resulting 25 by 300 feature matrix was reduced using scatter matrices-based dimension reduction concept. Two quadratic classifiers were designed which are able to distinguish all three groups of the EEG signals of interest from each other. The authors showed the performance of the system using scatter plot. The proposed classification algorithm offered an overall classification accuracy of 99%.

Discrete wavelet transform (DWT) has been also used for seizure source localization [32]. The authors in this study tried to find trade-off between decomposition level and EEG signal classification accuracy. According to the authors, best results could be found using sym6 as mother wavelet and decomposition level 7. Features such as the maximum coefficient, the minimum coefficient, the mean of coefficients, the standard deviation of coefficients, the skewness of coefficients, the kurtosis of coefficients, and the squared sum of all coefficients (Energy) were extracted for wavelet coefficients in each band. The research was experimented on publicly available Bern-Barcelona EEG database. Finally, the EEG segments were classified into focal and non-focal EEG segments using SVM with RBF-kernel. The best classification accuracy achieved in this work was 83.07%.

### 3.2.5 Stockwell Transform

The Stockwell (S) transform was first proposed by R. G. Stockwell et al. in 1996 [33]. The Stockwell-transform suitably combines the strengths of the STFT and wavelet transforms. In short, the S-transform can be viewed as either as a variable sliding window STFT or as a phase-

corrected Continuous Wavelet Transform (CWT). Since the factor that controls the width of the Gaussian localizing window of the S-transform is defended as the reciprocal of the absolute value of frequency, it gives frequency dependent resolution while maintaining a direct relationship with the natural Fourier transform. As a result, the S-transform provides good localization in the frequency domain for low frequencies while providing good localization in time domain for higher frequencies. S-transform produces a time-frequency representation that retains absolutely referenced phase information compared to CWT. Detail about the S-transform is stated in the next chapter.

The S-transform has been used in different literatures to deal with epileptic seizure analysis. Some of the previous works have been summarized below.

In one of the previous studies, A. Yan et al. proposed an automatic seizure detection scheme using the S-transform and boosting algorithm for long-term EEG [34]. The S-transform was implemented to obtain joint time–frequency representation of each EEG segments. Then the time axis was divided into 3 parts and the frequency axis into 4 parts based on the δ wave (0.4–4 Hz), θ wave (4–8 Hz), α wave (8–12 Hz), and β wave (12–30 Hz). As a result, the S-transform plane is divided into 12 sub planes. The power spectral density and then energy of the EEG segments was calculated in each sub-plane by squaring the coefficient and by summing the square of the coefficients. After that, a classifier based on gradient boosting algorithm was used to make the classification. Finally, a post processing was utilized on the outputs of the classifier to obtain more stable and accurate detection results, which includes Kalman filter, threshold judgment, and collar technique. The long-term intracranial EEG (IEEE) database used in this study came from the Epilepsy Center of the University Hospital of Freiburg, Germany. The EEG dataset was collected from 21 patients, with eleven patients whose epileptic foci located on neocortical brain structures, eight patients with a focus in the hippocampus, and the remaining two patients with seizures arising from both areas. The datasets were classified into ictal and inter-ictal (non-seizure) with average accuracy of 98.38 %, average sensitivity of 94.26%, specificity of 96.34% and seizures were detected with very short delay time of 0.56s by this algorithm.

A similar work on epileptic seizure detection based on the S-transform was proposed by S. Chatterjee et al. [35]. The scheme employed generalized S-transform to obtain the time–frequency representation of the EEG signals and then standard deviation and energy as

classifying features were evaluated from the S-transform plane. The EEG dataset used in the research was from publicly available database of Bonn University. Three dataset each containing 100 single segments were used, seizure, inter-ictal and healthy. In this work, two different class classification problems were considered, namely (i) seizure and healthy (ii) seizure and inter-ictal. In each classification problem, three cases were considered again. In the first case, the whole signal containing 4096 data points was used. Two features were extracted from each EEG segment and 100 feature vectors were generated separately for each class. In the second case, 4096 data points of each set were further subdivided into four subsets, resulting in a total of 400 subsets, with each set having 1024 samples. The third case, the whole signal (4096 data points) is dived into eight subsets, each subset containing 512 samples, yielding a total of 800 subsets of EEG signals. 400 and 800 feature vectors were created for the second case and third case, respectively. From the three cases investigated in the study, the highest overall classification accuracy of 98.44% was achieved using SVM classifier for the first case where as 100% accuracy was obtained using k-nearest neighbor (KNN) classifier again for the first case.

### 3.3 Empirical Mode Decomposition (EMD) and Singular Value Decomposition (SVD) for Seizure Detection and Source Localization

Empirical mode decomposition is an adaptive, data-dependent decomposition method and suitable for the analysis of nonlinear and non-stationary signals, such as EEG [36]. EMD decomposes a signal into a finite set of oscillatory components, known as intrinsic mode functions (IMFs). Thus, using EMD a signal can be represented as the sum of IMFs. Each IMF should satisfy the following two conditions. The first condition is the number of extrema and the number of zero-crossings should be either equal or differ at most by one, in the whole dataset. The second one is the mean value of two envelopes, one defined by connecting local maxima and the other defined by connecting local minima, at any point is zero. For a given signal $x(t)$, IMFs can be derived using an iterative process, known as the sifting process. The starting point of the sifting process is identification of all local maxima and minima. The second step involves defining two envelopes: $e_{max}(t)$ calculated by connecting all of the maxima and $e_{min}(t)$ obtained by connecting all of the minima using interpolation method. Usually the interpolation methods are cubic splines or piecewise cubic Hermite interpolating polynomials. Then, the third step is computing the average of $e_{max}(t)$ and $e_{min}(t)$ as: $m(t)=$ (absolute value of $(e_{max}(t) + e_{min}(t))) /2$

and is subtracted from the signal. If the difference, $h(t) = x(t) - m(t)$, do satisfy the two basic conditions of IMF, then it will be taken as the first IMF. If not, the above steps will be repeated taking h*(t) as x(t),* until it satisfies the conditions of IMF. When *h(t)* satisfies the conditions of IMF, *h(t)* is defined as *h(t)= IMF1*. Once *IMF1* is derived, the remaining IMFs can be obtained by repeating the previous steps on the residual signal $r1(t) = x(t) - IMF1(t)$, treating it as a new signal. The whole procedure is terminated when the residue is either a constant, a monotonic slope, or a function with only one extremum. Finally, the original signal *x(t)* can be expressed as the sum of the IMFs and the final residual.

$$\boldsymbol{x(t) = \sum_{i=1}^{k} IMFi(t) + R(t)} \tag{3.8}$$

where *k* is the number of extracted IMFs and *R(t)* is the final residual. The process stops when a Cauchy stop criterion is fulfilled. The details of the procedure can be found in [37]. The next paragraphs revise seizure and source localization works based on EMD as main part the methodology.

In one of the previous studies, EMD and Hilbert transform were used as main part of the methodology to classify normal and seizure EEGs [38]. The EEG signals were windowed using sliding window of different lengths. Then, EMD was implemented on windowed EEG segment to obtain IMFs. The lengths of the window have impact on IMFs extracted and the optimal one selected after many tries. Best result was obtained with 1500 samples of sliding window with 50% overlap. The authors used EEG datasets of five patients selected from the Epilepsy Center of the University Hospital of Freiburg database. Hilbert transform was applied on the first eight IMFs. The authors believed that Hilbert transform of IMFs are physically meaningful. The absolute value of the Hilbert transform of each IMF was computed and the mean of this result was considered as a feature. ANN as classification method and self-organizing map(SOM) as clustering method were used on the computed features. Using this method best accuracy of 91.2% was achieved.

EMD was also utilized in epilepsy affected source localization in another study [39]. After the IMF of the EEG signal is computed, different entropy measures of IMF were used as features to classify focal and non-focal signals. Shannon entropy, average Renyi's entropy, average approximate entropy, average phase entropies and average sample entropy were computed from

the first eight IMFs of focal and non-focal EEG signals. Least squares support vector machine (LS-SVM) was used as a classifier. The purposed method to differentiate focal and non-focal EEG signals was experimented on publicly available Bern-Barcelona EEG database and achieved an average classification accuracy of 87%.

### 3.3.1 Singular Value Decomposition (SVD)

The singular value decomposition (SVD) is a very powerful technique for recognizing and ordering the dimensions along which data points display the most variation [40]. The SVD technique decomposes a matrix X into three matrices $U$, $\sum$ and $V$ such that:

$$\boldsymbol{X=U_{mm}\sum_{m\,n}V^{T}_{n\,n}} \tag{3.9}$$

where, $U_{mm}$ and $V_{n\,n}$ are orthogonal matrices, and $\Sigma_{mn} = diag\,(\sigma_i)$ is a diagonal matrix containing singular values of $X$ in descending order of magnitude ($\sigma_{i\,j} = 0$ *if* $i \neq j$ *and* $\sigma_{11} \geq \sigma_{22} \geq \cdots \geq 0$). The columns of the two matrices $U_{mm}$ and $V_{n\,n}$ are called the left and right singular vectors, respectively.

An interesting property of the vectors is that they are mutually orthogonal. Larger singular values correspond to higher model correlation with the original data. For that reason, the SVD allows the extraction of dominant components from a given data by keeping the largest singular values. The singular values ($\sigma_{ii}$) represent the importance of individual SVs in the composition of the matrix. In other words, SVs corresponding to the larger singular values have more information about the structure of patterns embedded in the matrix than the other SVs and have high correlation to the original data.

A.Shahid et al. in their study presented an algorithm based on SVD for the detection of seizures [41]. In this work, a matrix of size 18-rows from the 18-channels of the EEG electrodes was formed. The EEG data was further divided into small windows of one second each with 256 data points. SVD was then applied on the resulting 18 by 256 matrix. The obtained diagonal matrix of singular values was converted to a column vector and the 2nd norm of singular value column vector is calculated. The above step is repeated for the next one second 18×256 window and a plot of the second norms of the singular values verses time is generated. The authors observed that the second norms of the singular values deviated notably upwards at the start of epileptic

seizures from the graphs. EEG recordings of four pediatric patients with 20 seizures obtained from publicly available Physio Net online EEG database were used to validate the algorithm. Even though, the performance of the algorithm is not stated in numbers, the authors stated that the result of the algorithm on the tested EEG segments was promising.

The SVD technique was also used in time-frequency based seizure detection scheme in [42]. The authors used B-distribution which is customized quadratic class distribution with new smoothing function to reduce cross terms. The EEG data is segmented into 30 second epochs. Then SVD is applied after B-distribution of 30 second EEG segment is obtained. Vectors from the right and left matrix corresponding to the largest singular values were used to extract features. The reason was that the authors believed the right and left SVs contain the time and frequency domain information of the signal respectively. The performance of the develop algorithm was accessed on self-recorded EEG data of eight newborns. The recorded EEG signal were segmented into 30-second epochs associated with seizure and non-seizure activities. Totally, 300 seizure and 800 non-seizure EEG segments were included for the experiment. To train the neural network classifier, 200 seizures and 200 non-seizures were randomly selected and applied to the classifier. The proposed scheme detected 90% of seizures from the total seizure segments with 5.7% false detection rate.

### 3.4 Nonlinear Dynamics and Chaos Theory for Seizure Detection and Source Localization

Most researchers believe that brain is a chaotic system and its state changes in unpredictable manner. As a result, outputs of the brain EEG signals are generally chaotic and their amplitude changes randomly with respect to time. Linear analysis such as frequency analysis (e.g. Fourier and Wavelet Transforms) only provides a limited amount of information about the electrical activity of the brain because the method ignores the underlying nonlinear dynamic nature of the EEG. Different features from nonlinear dynamics and chaos theory have been used in EEG epilepsy analysis [43]. Measures of complexity (e.g., the correlation dimension) and stability (e.g., the Lyapunov exponent and embendding entropy) have been used to quantify chaotic nature of the brain dynamics. Before reviewing articles from nonlinear analysis, let us start from the basic concepts.

The state of a certain dynamical process can be given by a set of values of all variables that describe the system at a particular time. The dynamics of such system can be modeled as a system of ordinary differential equations. A dynamical system is linear if all the corresponding equations of its dynamics are linear. Otherwise, it is nonlinear. Considering that a system is defined by n-variables, its state in a particular moment in time can be represented by a point in an n-dimensional space. This space is usually known as state space or phase space. The sequence of consecutive states over time defines a curve in the phase space which is called trajectory. For some systems, the trajectory tends to converge to a bounded subspace of the phase space if the evolution of the system is studied for sufficiently long time. This kind of dynamical system is known as dissipative. This bounded subspace is referred to as an attractor, because it attracts trajectories from all initial conditions. Attractors are classified according to the geometrical shape of the attractor. It can be fixed point for attractors that evolve towards a point whatever the initial conditions of the system are. Closed one dimensional attractors are also common systems with a periodic motion. Attractors with a toroidal surface (in an integer dimension) are commonly referred as limited torus. They represent a quasiperiodic motion with an integer number of incommensurable frequencies. Finally, for a system that exhibits complex behaviors (chaos), its attractor is also a complex object. In this case, points that are initially close in the phase space may become exponentially separated after time. The dynamics corresponding to a strange attractor is deterministic chaos: same initial conditions converge to same final state; but the final state is very different for small changes to initial conditions.

The common approach in using nonlinear dynamical analysis for applied research involves two steps. The first step is representing a state space of a dynamic system from a time series which is called state space reconstruction, or embedding of the time series. The second step is to use different measures to characterize attractors. Dimension of the attractor is one of the measures. It is the spatial distribution of the corresponding geometrical object, i.e., its ‘complexity’. There are several techniques for estimating the dimension of the attractor, the correlation dimension is the most popular approach. Lyapunov exponents and entropy are also common measures used to characterize attractors. Embendding entropy give information about the ‘stability’ of the attractor, i.e., quantify the chaos of the attractor. Correlation dimension and largest Lyapunov are the most common non-linear dynamics measures in EEG signal analysis.

The Lyapunov exponents measure the average rate of expansion and folding of the chaotic attractor in a state space. It is the measure of the average exponential rate of divergence or convergence of the nearby orbits in the phase space. Any system containing at least one positive Lyapunov exponent is defined to be chaotic. The magnitude of the exponent reflects the time scale on which the system dynamics become unpredictable A negative exponent entails that the trajectories tend to a common fixed point; and a zero exponent means that the trajectories maintain their positions: they are on a stable attractor. Largest Lyapunov exponents for short segments of EEG is used for the characterization of the epileptic activities by authors in [44]. EEG segments for interictal, normal and ictal phase of epilepsy are characterized using largest Lyapunov exponents. Accordingly, the seizure onset corresponds to the maximum drop in the Lyapunov exponent value determined for seizure containing electrodes. Similar methodology is presented with slight modifications by Adeli et al. [45]. In this study, five wavelet sub-bands of EEG segments were used to calculate largest Lyapunov exponents and correlation dimension. Finally, the authors concluded that in the higher frequency beta and gamma sub-bands, the correlation dimension helps for differentiating healthy, ictal and inter-ictal EEG segments whereas in the lower frequency alpha subband, the largest Lyapunov exponent helps to differentiates between the three groups.

### 3.5 Limitations in the Previous Works

Background facts of clinical electroencephalographers about abnormal EEG patterns are not taken into account by existing automated signal processing schemes for seizure detection and focus localization. This point becomes clear, when one considers that most of the previous works tried to study more than one type of epilepsy cases with one automated scheme. Even when the research is on a single type of epilepsy, the way features are extracted exclude background facts of neurophysiologists.

Numerous and complex features are used in previous researches to obtain results that can be achieved by few features. Existing researches divot much effort on developing, modifying, selecting and applying effective signal processing techniques. But those signal processing techniques should be utilized in a way that reveal background facts of neurophysiologists. If the signal processing techniques utilizes years of accumulated facts of neurologists, few, simple and effective features could be extracted.

Beside the performance of the classification scheme, previous works did not go much further on characterization of EEG segments, seizure, inter-ictal and healthy. A system can achieve higher accuracy for recorded EEG data by combining numerous features but it should be simple, accurate and revel descriptive aspects of the signal so that it can be robustly be used in arbitrary EEG data. Most of the previous works were done on recorded EEG data and promised the system would be tested on real time signal, or on online EEG data. If the ultimate goal of a system is to be tested on real time signal, it should be simple, robust and accurate.

**References**

1. A. T. Tzallas, M. G.Tsalikakis, D. G. Karvounis et al. ''Automated Epileptic Seizure Detection Methods: A Review Study,'' *Epilepsy-Histological, Electroencephalographic and Psychological Aspects*, Dr. Dejan Stevanovic (Ed.), ISBN: 978-953-51-0082-9, In Tech, 2012.

2. A. T. Tzallas , M. G. Tsipouras, D. I. Fotiadis, ''Epileptic seizure detection in EEGs using time-frequency analysis,'' In Proceedings of the Twentieth IEEE International Symposium on Computer-Based Medical Systems, pp. 135–140,IEEE Computer Society Washington, DC, USA, 2007.

3. L. Guo, D. Rivero, J. A. Seoane et al. ''Classification of EEG Signals Using Relative Wavelet Energy and Artificial Neural Networks,'' Department of Information Technologies and Communications, Campus de Elvina, University of A Coruna, A Coruna, 15071, Spain, 2009.

4. I. Omerhodzic , S. Avdakovic, A. Nuhanovic et al. ''Energy Distribution of EEG Signals: EEG Signal Wavelet-Neural Network Classifier,'' World Academy of Science, Engineering & Technology, Vol. 4, 2010.

5. H. S. Liu, T. Z. Hang, F. S. Yang, ''A multistage, multimethod approach for automatic detection and classification of epileptiform EEG, '' IEEE Trans Biomed Eng., Vol. 49 (12 Pt 2), pp. 1557-1566, 2002.

6. J. Altenburg, R. J. Vermeulen, R. L. Strijers et al. ''Seizure detection in the neonatal EEG with synchronization likelihood'', Clin Neurophysiol, Vol. 114, No. 1, pp. 50-55, 2003.

7. M. J. V. Putten, ''Nearest ne ghbor phase synchronization as a measure to detect seizure activity from scalp EEG recordings,'' Journal of clinical neurophysiology, Vol. 20, pp. 320-325, 2003.

8. R. Sharma, R. B. Pachori, and U. R. Acharya, ''Application of Entropy Measures on Intrinsic Mode Functions for the Automated Identification of Focal Electroencephalogram Signals,'' Entropy, Vol. 17, pp. 669-691, 2015. doi:10.3390/e17020669

9. V. Srinivasan, ''Approximate Entropy-Based Epileptic EEG Detection Using Artificial Neural Networks, '' IEEE transactions on information technology in biomedicine, Vol. 11, No. 3, May 2003.

10. H. Ocak, ''Automatic detection of epileptic seizures in EEG using discrete wavelet transform and approximate entropy,'' Expert Systems with Applications, Science Direct, Vol. 36, pp. 2027–2036, 2009.

11. J. Gotman, ''Automatic recognition of epileptic seizures in the EEG,'' Electroencephalogram Clin Neurophysiol, Vol. 54, No. 5, pp. 530-540, 1982.

12. J. Gotman, ''Automatic detection of seizures and spikes.'' J Clin Neurophysiol, Vol. 16, No. 2, pp. 130-140, 1999.

13. N. Kannathala, M. L. Choob , U. R. Acharyab, P. K. Sadasivana, "Entropies for detection of epilepsy in EEG," Computer Methods and Programs in Biomedicine, Vol. 80, No. 3, pp. 187-194, Dec. 2005.

14. A. Feltane, "Time-Frequency Based Methods for Non-Stationary Signal Analysis with Application To EEG Signals," Open Access Dissertations. Paper 445, 2016.

15. A. Dalton, S. Patel, A. R. Chowdhury et al. ''Development of a body sensor network to detect motor patterns of epileptic seizures,'' IEEE Trans. Biomed. Eng., Vol. 59, No. 11, pp. 3204–3211, 2012.

16. T. P. Runarsson, S. Sigurdsson, ''On-line detection of patient specific neonatal seizures using support vector machines and half-wave attribute histograms,'' International Conference on Computational Intelligence for Modelling, Control and Automation, Web Technologies and Internet Commerce (CIMCA-IAWTIC) (Vienna), pp. 673–677, 28–30 Nov 2005.

17. J. L. Semmlow, Bio-signal and Medical Image Processing. MatLab based application, CRC Press, pp. 303-370, 2004.

18. K. Polat, S. Gunes, ''Classification of epileptiform EEG using a hybrid system based on decision tree classifier and fast Fourier transform, '' Applied Mathematics and Computation, Science Direct, Vol. 187, pp. 1017–1026, 2007.

19. R. G. Andrzejak, K. Lehnertz, F. Mormann et al. ''Indications of nonlinear deterministic and finite dimensional structures in time series of brain electrical activity: dependence on recording region and brain state,'' Physical Review E, Vol. 64, No. 6, 61907, 2001.

20. S. Qian and D. Chen, Joint time-frequency analysis: methods and applications, Prentice-Hall Inc., New York, USA, 1996.

21. B. Boashash, M. Mesbah, and P. Golditz, Time-Frequency detection of EEG abnormalities, Elsevier, Article 15.5 in Chapter 15, pp. 663-9, 2003.

22. R. G. Stockwell, L. Mansinha, and R. P. Lowe, ''Localization of the Complex Spectrum: The S Transform,'' IEEE transactions on signal processing, Vol. 44, No. 4, April 1996.

23. F. Hlawatsch and G. F. Boudreaux-Bartels, ''Linear and Quadratic Time-Frequency Signal Representations,'' IEEE Signal Processing Magazine, pp. 21-67, 1992.

24. A. Sengur, Y. Guo and Y. Akbulut, ''Time–frequency texture descriptors of EEG signals for efficient detection of epileptic seizure,'' Brain Informatics, Vol. 3, pp. 101–108, 2016.

25. L. Cohen, Time-frequency analysis, Prentice-Hall Signal Processing, New York, USA, 1995.

26. P. P. Acharjee, C. Shahnaz, '' Multiclass Epileptic Seizure Classification Using Time-Frequency Analysis of EEG Signals,'' 2012 7th International Conference on Electrical and Computer Engineering 20-22 December, 2012, Dhaka, Bangladesh.

27. L. Chun-Lin, A Tutorial of the Wavelet Transform, February 23, 2010.

28. C. S. Burrus, R. A. Gopinath, H. Guo, Introduction to wavelets and wavelet transforms, A primer, Prentice-Hall, Upper Saddle River, NJ, 1998.

29. G. Strang, T. Nguyen, Wavelet and filter banks (2nd Ed), Wellesley-Cambridge Press, Chapter-7, 1997.

30. J. R. Panda, P. S. Khobragade, P. D. Jambhule et al. ''Classification of EEG Signal Using Wavelet Transform and Support Vector Machine for Epileptic Seizure Diction'', Proceedings of 2010 International Conference on Systems in Medicine and Biology16-18 December 2010, liT Kharagpur, India.

31. D. Gajic, Z. Djurovic, S. Di Gennaro et al., ''Classification of EEG signals for detection of epileptic seizures based on wavelets and statistical pattern recognition'', World Scientific Publishing, Biomedical Engineering: Applications, Basis and Communications, Vol. 26, No. 2, 2014.

32. D. Chen, S. Wan, F. S. Bao, ''Epileptic focus localization using EEG based on discrete wavelet transform through full-level decomposition'', IEEE international workshop on machine learning for signal processing, Sept. 17–20, 2015, Boston, USA.

33. R. G. Stockwell, L. Mansinha and R. P. Lowe, ''Localization of the complex spectrum: The S-transform, '' IEEE Transactions on Signal Processing, Vol. 44, No. 4, 1996.

34. A. Yan, W. Zhou, Q. Yuan, ''Automatic seizure detection using Stockwell transform and boosting algorithm for long-term EEG," Epilepsy & Behavior Vol. 45, PP. 8–14, 2015.

35. S. Chatterjee, N. R. Choudhury and R. Bose, ''Detection of epileptic seizure and seizure-free EEG signals employing generalized S-transform, '' IET Science, Measurement & Technology, Vol. 11, Iss. 7, pp. 847-855,2017.

36. N. E. Huang, Z. Shen, S. R. Long et al. "The empirical mode decomposition and Hilbert spectrum for nonlinear and nonstationary time series analysis," Proc. R. Soc. London, Vol. 454, pp. 903-995, 1998.

37. G. Rilling, P. Patrick, P. Gonçalves, "On empirical mode decomposition and its algorithms," IEEE-EURASIP workshop on nonlinear signal and image processing, Italy, 2003.

38. A. K. Tafreshi, A. M. Nasrabadi and A. H. Omidvarnia, ''Epileptic Seizure Detection Using Empirical Mode Decomposition,'' IEEE Shahed University Press, Iran, 2009.

39. R. Sharma, R. B. Pachori, U.R. Acharya, ''Application of Entropy Measures on Intrinsic Mode Functions for the Automated Identification of Focal Electroencephalogram Signals'', Entropy, Vol. 17, pp. 669-691, 2015. doi:10.3390/e17020669

40. D. Kalman, “A singularly valuable decomposition: the SVD of a matrix, '' College Math Journal, Vol. 27, pp. 2–23, 1996.

41. A. Shahid, N. Kamel, M. A. Jatoi and et al., ''Epileptic Seizure Detection using the Singular Values of EEG Signals'', Proceedings of 2013 ICME International Conference on Complex Medical Engineering, May 25 - 28, Beijing, China.

42. H. Hassanpour, M. Mesbah, B. Boashash, ''Time-frequency feature extraction of newborn EEG seizure using SVD-based techniques, '' EURASIP Journal on Applied Signal Processing, Vol. 16, pp. 2544–2554, 2004.

43. G. R. Bermudez and P. J. G. Laencina, '' Analysis of EEG Signals using Nonlinear Dynamics and Chaos: A review'', Appl. Math. Inf. Sci., Vol. 9, No. 5, pp.2309-2321, 2015.

44. B. Swiderski, S. Osowski and A. Rysz, ''Lyapunov Exponent of EEG Signal for Epileptic Seizure Characterization, '' Proceedings of the European Conference on Circuit Theory and Design, Vol. 2, 2005.

45. H. Adeli, S. G. Dastidar and N. Dadmehr, ''A Wavelet-Chaos Methodology for Analysis of EEGs and EEG Sub bands to Detect Seizure and Epilepsy, '' IEEE Transactions on Biomedical Engineering, Vol. 54, No. 2, February 2007.

# CHAPTER FOUR

# 4. PROPOSED EPILEPTIC SEIZURE DETECTION AND LOCALIZATION BASED ON STOCKWELL TRANSFORM

## 4.1 Overview of the Proposed Scheme

The proposed method uses Stockwell transform (S-transform) and empirical mode decomposition mainly for two related problems, epileptic seizure detection and focus localization of epilepsy affected brain area. Checking whether an EEG segment contains a seizure or not is the central idea of the epileptic seizure detection problem. In addition to that, characterization of normal, interictal and seizure EEG segment is also addressed. After S-transform is implemented on preprocessed EEG segments, features are extracted from power spectral density (PSD) of the S- transform time-frequency sub-planes. Classification of features into normal, interictal and seizure is done by vector support machine (SVM). Apart from traditional classification using SVM, two best features are chosen and scatter plot of the features is used to show the efficacy of the detection scheme. Canberra distance between the clusters quantify the classification performance. The detection algorithm is also implemented after intrinsic mode function of EEG segments is obtained using empirical mode decomposition to check if the performance of the scheme would be improved.

Focal slow EEG activity from temporal region in intermittent, localized fashion or temporal intermittent rhythmic delta activity(TIRDA) have close association with temporal epilepsy and extra temporal epilepsy [1][2][3]. Focal slow EEG activity also indicates tumor or a type of lesion related to epilepsy case with good confidence. In the current study, this fact has been utilized to design a classification system of focal and non-foal signals for localization of the epileptic focus. S-transform has good resolution in depicting low frequency section of non-stationery signals compared to existing time-frequency transforms. The methodology used for the localization problem is the same as detection except that the feature extraction process is based on characterizing lower sub-plane of the S-transform (delta and theta rhythms). Figure 4.1 illustrates an overview of the proposed scheme and details on the steps utilized have been discussed in the subsequent sections.

### 4.2 Preprocessing of EEG Segments

The frequency range which contains most of the information content related to seizure events is from 0.5 -35 Hz. In addition, most recordings have a 50-Hz frequency power line interference contamination. Therefore, the signals need to be lowpass filtered to eliminate the power line interference and other high-frequency components generally produced by muscular activity. A Butterworth filter of order 10 with a cutoff frequency of 45 Hz is used in this study to deal with this type of interference. Forward and backward filtering was used in order to minimize phase distortions.

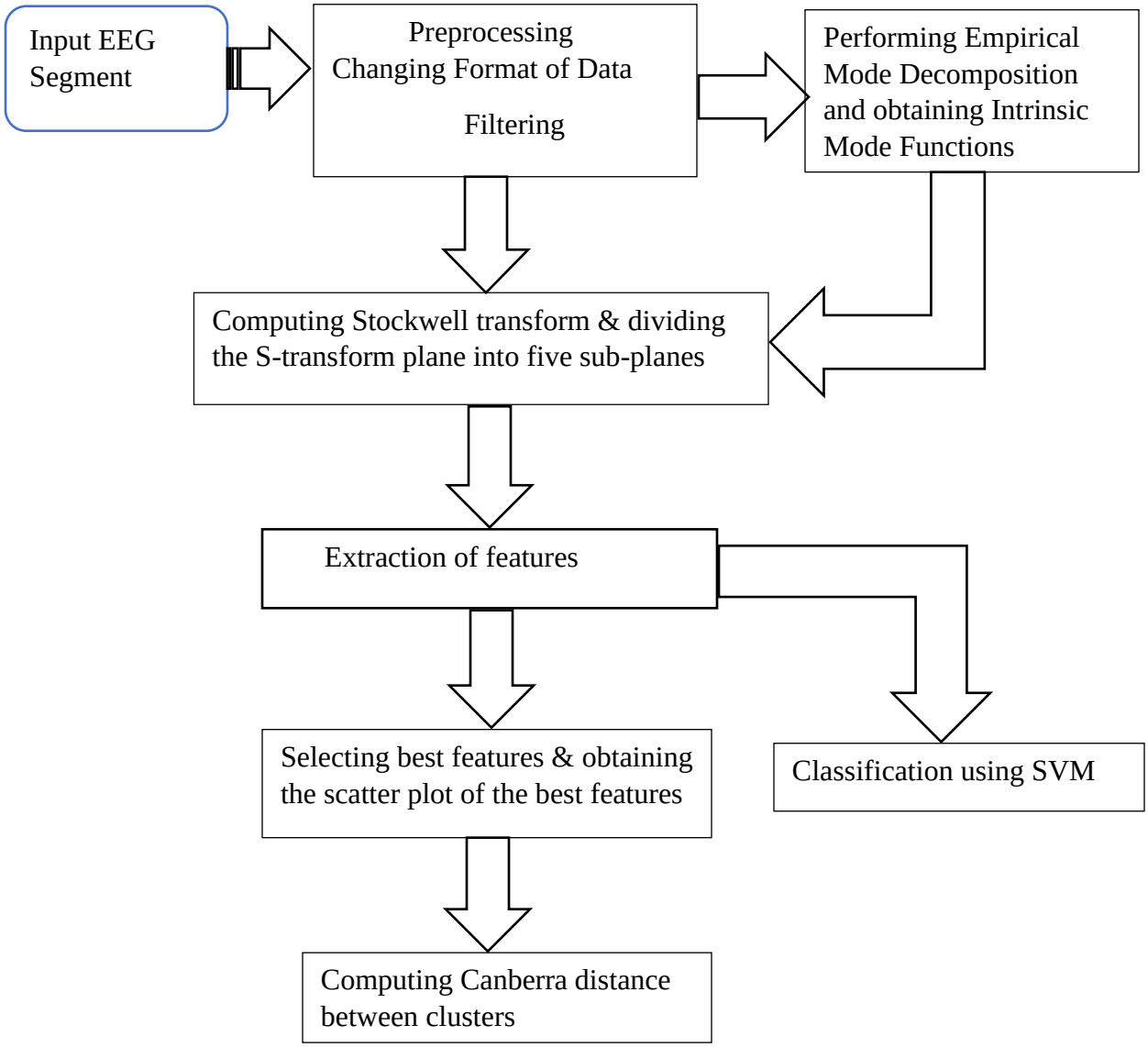


*Figure **4.1 Overview of the proposed seizure detection and localization scheme***

### 4.3 Stockwell Transform

The Stockwell (S) transform is first proposed by R.G. Stockwell et al. in 1996 [4]. The S-transform suitably combines the strengths of the STFT and wavelet transforms. It can be conceptually viewed as the hybrid of short-time Fourier and wavelet analyses. The low resolution of the STFT and the absence of local phase information in the Wavelet transform led to the development of the S- transform. It is modified STFT that uses moving and scalable localizing Gaussian window. The factor that controls the width of the Gaussian localizing window is defined in a way to have a better self-adaptability to different frequency components. Compared to the CWT, the S-transform has the property of retaining absolutely referenced phase information by using a non-translating Fourier kernel during signal decomposition, while preserving a good time-frequency resolution. In general, the S-transform can be viewed either as a variable sliding window STFT or as a phase-corrected CWT. The S-transform has a very good time-frequency resolution with good performance of noise reduction compared to STFT, CWT and Chon class quadratic time frequency transforms.

#### 4.3.1 Definition and Relation of the S-transform with STFT and CWT

As stated above, the S-transform can be considered as a STFT with moving and scalable localizing Gaussian window. The Equations of the STFT and a normalized Gaussian window are shown in Eqn. (4.1) where *w* is the localizing window function.

$$\boldsymbol{STFT(\tau, f) = \int_{-\infty}^{\infty} x(t) w(t-\tau) e^{-j2\pi ft}\ dt} \quad \text{and} \quad \boldsymbol{g(t) = \frac{1}{\delta\sqrt{2\pi}} e^{\frac{-t^2}{2\delta^2}}} \tag{4.1}$$

According to the nature of the Gaussian window, δ is the scale factor to change the width of the Gaussian window. In order to make the width of the Gaussian window have a better self-adaptability to different frequency components, δ is defined to be a function of the frequency as $\delta(f) = \frac{1}{|f|}$. Then the Gaussian window would be:

$$\mathbf{g(t) = \frac{|f|}{\sqrt{2\pi}} e^{\frac{-t^2 f^2}{2}}} \tag{4.2}$$

The S-transform is then defined as a modified STFT with a Gaussian localizing window with this scaling factor and can be written as:

$$\boldsymbol{ST(\tau, f) = \int_{-\infty}^{\infty} x(t)\ \frac{|f|}{\sqrt{2\pi}} e^{\frac{-(\tau-t)^2 f^2}{2}}\ e^{-j2\pi ft}\ dt} \tag{4.3}$$

The average of the window needs to be 1, that means $\int_{-\infty}^{\infty} g(t,f)dt = 1$. From Eqn. (4.3), one can deduce that the S- transform provides frequency dependent resolution while maintaining a direct relationship with the natural Fourier transform. The factor that controls the width of the window, δ, is defended as the reciprocal of the absolute value of frequency, is wider in the time domain at lower frequencies, and narrower at higher frequencies. In other words, the S-transform provides good localization in the frequency domain for low frequencies while providing good localization in time domain for higher frequencies. Alternatively, the S-transform can be viewed as a continuous wavelet transform with a special mother wavelet multiplied by the phase factor. The CWT, W (τ, d), of a function h(t) is defined by:

$$\boldsymbol{W(\tau, d) = \int_{-\infty}^{\infty} x(t) w(t-\tau, d) dt} \tag{4.4}$$

In Eqn. (4.4), *w (t-τ, d)* is defined as the mother wavelet function. The dilation factor *d* controls the width of the wavelet basis. So it controls the frequency resolution. But the mother wavelet function has to satisfy the admissibility condition [5]. Thus S-transform can be defined as a phase corrected CWT as follows:

$$\boldsymbol{S(\tau, f) = e^{-j2\pi f\tau}\, W(\tau, d)} \tag{4.5}$$

The mother wavelet of the S-transform, *w (t, f)*, is defined as:

$$\boldsymbol{w(t, f) = \frac{|f|}{\sqrt{2\pi}} e^{\frac{-(\tau-t)^2 f^2}{2}} e^{-j2\pi ft}} \tag{4.6}$$

and in Eqn. (4.5) the factor *d* is defined as the inverse of the frequency, *f*. The mother wavelet of the S-transform as strict CWT does not satisfy the zero mean condition. An interesting fact here is that the time localizing Gaussian parameter ($e^{\frac{-(\tau-t)^2 f^2}{2}}$) translates while the oscillatory exponential kernel ($e^{-j2\pi ft}$) remains stationary. Inserting the equation of the mother wavelet equation in Eqn. (4.5), the final expression of the S-transform becomes:

$$\boldsymbol{S(\tau, f) = \int_{-\infty}^{\infty} x(t) \frac{|f|}{\sqrt{2\pi}} e^{\frac{-(\tau-t)^2 f^2}{2}} e^{-j2\pi ft} dt} \tag{4.7}$$

Since the oscillatory exponential kernel does not translate, the S-transform localizes the real and the imaginary components of the spectrum independently. Automatically, the S-transform localizes the phase spectrum as well as the amplitude spectrum. Thus, the S-transform retains

absolutely referenced phase information. In addition, unlike the CWT, the S-transform produces a time-frequency representation instead of a time-scale representation. The connection of the S-transform and the natural Fourier transform is simple, operation of averaging the local spectra of the S-transform over time simply gives the Fourier spectrum [6].

$$\boldsymbol{X(f) = \int_{-\infty}^{\infty} S(\tau, f) d\tau} \tag{4.8}$$

Comparing the equation of the Fourier transform and Eqn. (4.8), the signal *x(t)* could exactly be recoverable from the S-transform as follows:

$$\boldsymbol{X(t) = \int_{=-\infty}^{\infty} \{ \int_{-\infty}^{\infty} S(\tau, f) d\tau \} e^{j2\pi f t}\, df} \tag{4.9}$$

This direct relation to the S-transform to the Fourier transform and the linearity property of the S-transform makes both the inversion to time domain and the filtering process in the time-frequency domain possible. These greatly benefit signal filtering and de-noising researches [7]. The direct link between the S-transform and the Fourier transform can be found by rewriting the S-transform using convolution as follow.

Taking p(τ ,f)= $x(\tau)e^{-j2\pi f\tau}$ and g(τ, f)= $\frac{|f|}{\sqrt{2\pi}} e^{\frac{-\tau^2 f^2}{2}}$ , then the S-transform can be rewritten as:

$$\boldsymbol{S(\tau, f) = \int_{-\infty}^{\infty} p(t, f) g(\tau - t, f) dt = p(\tau, f) * g(\tau, f)} \tag{4.10}$$

The operator '*' in Eqn. (4.10) represent the convolution operation. By calculating the Fourier transform of S (τ, f), the convolution becomes a multiplication in the frequency domain.

$$\boldsymbol{F\{S(\tau,f)\} = P(\alpha, f) * G(\alpha, f) = X(\alpha + f) e^{\frac{-2\pi^2\alpha^2}{f^2}}} \tag{4.11}$$

In Eqn. (4.11), $\alpha$ is the frequency Fourier variable related to τ. Hence, the S-transform can be recovered by applying the inverse Fourier transform to the last equation.

$$\mathbf{S(\tau, f) = \int_{-\infty}^{\infty} X(\alpha + f) e^{\frac{-2\pi^2\alpha^2}{f^2}} e^{-j2\pi\alpha\tau} d\alpha} \tag{4.12}$$

Implementation of the discrete S-transform can be deduced from Eqn. (4.12) by using the advantages of the FFT (Fast Fourier Transform) and convolution algorithms. More about the implementation of the discrete S-transform can be found in [8][9].

### 4.3.2 Comparison of the S-transform, CWT, and Cohen's Class Quadratic Time-Frequency Distributions

The S-transform gives linear distribution with progressive time and frequency resolution. CWT and STFT are also linear. Linear distributions are free from cross terms. The major disadvantage of quadratic time-frequency distributions (QTFD) is byproduct or cross terms. The quadratic nature of the distributions makes the performance of QTFD on noisy signals very bad. If a signal is modeled as data(t) = signal(t) + noise(t), then the S- transform gives S{data} = S{signal} + S{noise}. Applying quadratic time-frequency distribution(QTFD) on the modeled data, it gives us QTFR{data} = QTFR{signal} + QTFR{noise} +2 ∗QTFR{signal}∗ QTFR{noise}. The additional terms or the cross terms makes QTFD to propagated noise due to the quadratic nature of the distribution.

The discrete Fourier transform (DFT) has a very well defined sampling of the frequencies, in order to be both complete and orthonormal. The S-transform in its discrete form has the identical sampling of the frequency space and retains the sampling of the signal in the time domain as DFT. Cohen's class distribution also share this property. On the other hand, CWT has a loosely defined scaling. It normally employs an octave scaling for frequencies, which results in an oversampled representation at the low frequencies and an under sampled representation at the higher frequencies.

The S-transform relative to the others has direct connection between the original signal, the amplitude, frequency and phase of the signal which can be obtained directly from the S-transform coefficients. As the S-transform output is generally complex, we can read the amplitude A(t) = absolute value of (S-transform (t, f)), the frequency *f*, and the phase information $\phi(t)$ is arctan of the ratio of the imaginary and real components for each time step from the S-transform. Accordingly, a signal(t), in time domain can be expressed as follow:

$$\text{Signal}(t) = A(t)\cos(2*pi*f(t)*t + \varphi(t)) \tag{4.13}$$

where in Eqn. (12), $A(t)$, $f(t)$ and $\phi(t)$ are the amplitude, frequency and phase at any time instant *t* respectively. This direct extraction of a signal is due to the combination of absolutely referenced phase information and frequency invariant amplitude of the S-transform, and such direct extraction cannot be done with CWT. The unit area localizing function (the Gaussian envelope)

preserves the amplitude response of the S-transform since it is normalized by the factor $|f|/2\pi$ to the unit area as shown in Eqn. (4.6). Thus, the S-transform returns an amplitude A regardless of the frequency f in a similar concept as the amplitude of the Fourier transform. In contrast the amplitude of the CWT is large for the lower frequencies and diminishes at the higher frequency components.

As explained in Chapter 3, QTFDs show how the signal energy is distributed in time and frequency, not the signal amplitude. Hence, the interpretation is different.

When we come to phase information, the S-transform retains the absolute phase information, whereas the phase information is lost in the CWT. In CWT the phase is relative to the center (in time) of the analyzing wavelet, and as the wavelet translates, the reference point of the phase translates and hence the relative phase becomes meaningless. With the S-transform, the sinusoidal component of the basis function remains stationary, while the Gaussian envelope translates in time. Thus, the reference point for the phase remains stationary and the phase has the same meaning as in the Fourier domain [6].

### 4.3.3 Comparison of Time-Frequency Distributions Through Simulated Signal

The time-frequency distributions stated above are compared with respect to their performance under noise and the ability to distinguish different signals. Short time Fourier transform, Wigner-Ville, continuous wavelet transform and S-transform of a synthetic signal consisting of a low frequency signal for the first half, a middle frequency signal for the second half, and a short lived high frequency burst with Gaussian white noise is shown in Fig.4.2. The Gaussian white noise is added to the signal with signal to noise ratio of 10 decibels.

As one can see from Fig 4.2., STFT has poor resolution in low frequency signal and low stability in noise conditions. The high frequency burst is smoothed out because of the poor time resolution of the STFT. The main problem of Wigner-Ville is cross term as it can be observed from the Fig.4.2. The cross term causes the high frequency bursts to be misrepresented and non-distinguishable. The S-transform has better anti-noise property of the three-time frequency transforms. From Fig.4.2, we can observe the time resolution of S-transform is better than CWT. The S transform can detect the occurred time and its energy variance of the high-frequency burst. In additions, the S transform shows better frequency resolution for the low frequency signal.

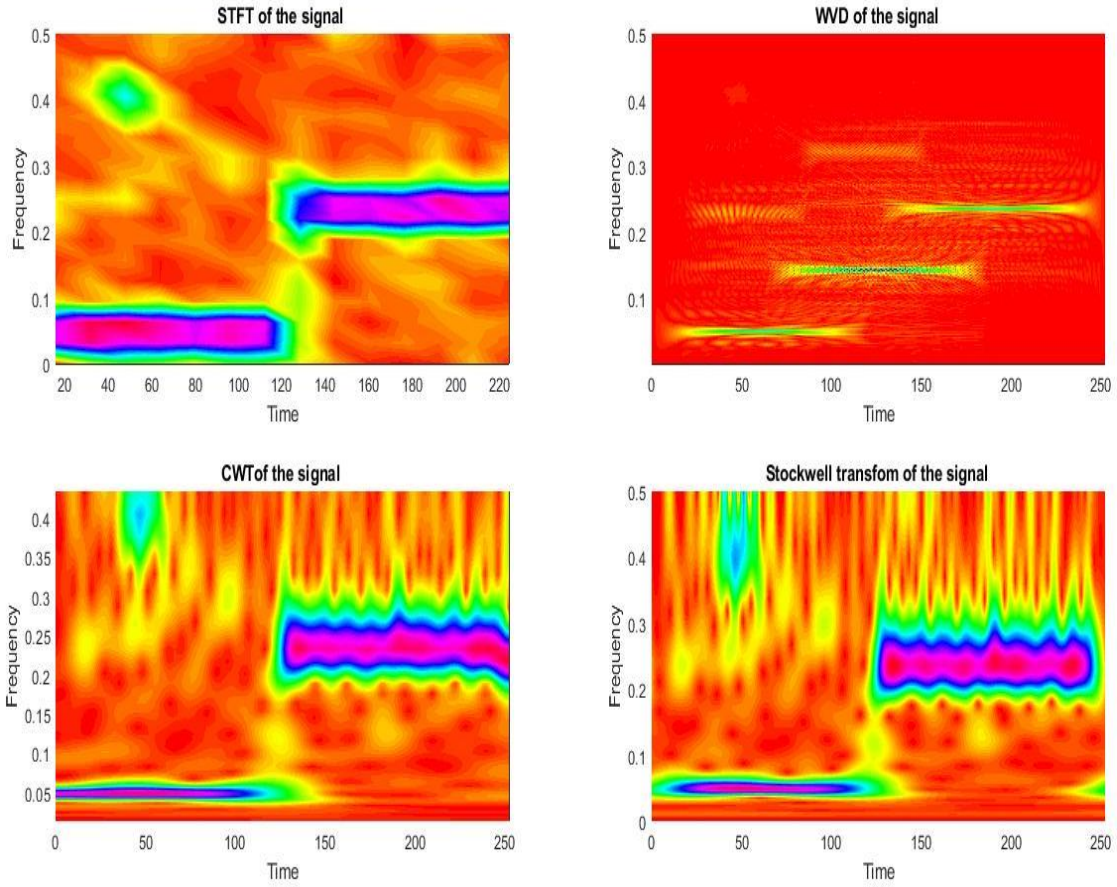


*Figure **4.2 Performance of different time–frequency under noisy signal***

## 4.4 Empirical Mode Decomposition (EMD)

The EMD decomposes the EEG signals into symmetric,oscillatory and band-limited IMFs through a method called sifting process [10]. A brief about EMD is stated in Chapter 3. A short summary of the sifting process is presented for completness of the current chapter. Let $X(t)$ be a signal decomposed into $k$ number of intrinsic mode functions (IMFs), and residual $r_k(t)$ using the sifting process. Each IMF(t) should fulfill the following two conditions. The first condition is the number of extrema and the number of zero-crossings should be either equal or differ at most by one, in the whole dataset. The second one is the mean value of two envelopes, one defined by connecting local maxima and the other defined by connecting local minima, at any point should be zero. The steps of the sifting process are listed as follows:

1. Find local maxima and minima for the signal $X(t)$ and construct two envelope signals, an upper envelope $E_{max}(t)$ using local maxima, and a lower envelope $E_{min}(t)$ using local minima.

2. Compute mean of the envelope for $i_{th}$ iteration, $m_{k,i(t)}$ where $m_{k,i(t)}=1/2|E_{max(t)}+E_{min(t)}|$.

3. With $C_k(t) = X(t)$ for the first iteration, subtract mean envelope from residual signal, $C_k(t)=X(t)-m_{k,i}(t)$. If $C_k(t)$ satisfy the following two conditions of IMF, it will be taken as the firtst IMF. If $C_k(t)$ does not match the criteria of an IMF, steps 4 and 5 are skipped. The procedure will be iterated again at step 1 with the new value of $C_k(t)$ as $X(t)$ until it matches the condition of IMF.

4. If $C_k(t)$ matches the criteria of an IMF, a new residual is computed. To update the residual signal, subtract the $k_{th}$ IMF from the previous residual signal,

$$\boldsymbol{r_k(t)=r_{k-1}(t)-C_k(t)} \tag{4.14}$$

5.Then begin from step 1, using the residual obtained as a new signal $r_k(t)$, and store $C_k(t)$ as an intrinsic mode function. For N intrinsic mode functions, the original signal is represented as,

$$\boldsymbol{X(t) = \sum_{i=1}^{N} IMFi(t) + rN(t)} \tag{4.15}$$

The common stopping criterion used to terminate the sifting process is a Cauchy type stop criterion proposed in [9]. According to Cauchy stoping criterion, first the sum of difference (SD) is defined as follow:

$$\boldsymbol{SD = \frac{|IMF\ previous - IMF\ current|}{|IMFcurrent|2}} \tag{4.16}$$

The sifting process stops when current SD is less than a threshold value. The interesting point of EMD is that the IMFs are derived directly from the signal itself and does not require any a priori known basis. Hence the analysis is adaptive, in contrast to Fourier or Wavelet analysis, where the signal is decomposed in a linear combination of predefined basis functions.

### 4.5 Feature Extraction

All of the features used in the current study are extracted from the S-transform time-frequency plane. The S-transform plane is used in different ways to get relevant features. To characterize seizure EEGs from non-seizure ones, the PSD of the signal over the S-transform, which

represents the distribution of the energy of the signal over the time-frequency plan, is extracted as a feature. It can be calculated simply by squaring the absolute value of the coefficient of the S-transform. Generally, EEG signature of (seizure) ictal segment is full of high amplitude polymorphic waveforms and inter-ictal one is characterized by occasional transient waveforms. In addition, seizure EEG segments are expected to be energetic, have higher amplitude, compared to inter-ictal and healthy EEG's. Those facts are depicted by defining a function that shows average PSD distribution over the time axis from the S-transform. Instead of considering joint distribution of PSD over time-frequency axis as a whole, the PSD distribution over time axis or frequency is taken separately. That means average distribution of PSD over time or frequency axis can be derived from the S-transform plan directly. If the coefficient of the PSD is summed over the frequency axis, average PSD distribution over time can be derived. If the coefficient of the PSD is summed over the time axis, then average PSD distribution over the frequency axis would be obtained. The average PSD distribution over the time axis offers insight about EEG signatures of ictal and inter-ictal segments clearly. Figure 4.3 presents the average PSD over the time and frequency axes for an arbitrary EEG signal as well as the average PSD over the time axis for the three types of EEG segments, i.e. ictal, inter-ictal and healthy.

Statistical features such as standard deviation, skewness, line length and median absolute deviation (MAD) are extracted from the average PSD distribution over time vector. The MAD is a measure of statistical dispersion. The absolute deviation of an element of a data set is the absolute difference between that element and a given point. Common measures of statistical dispersion are the variance and standard deviation. The MAD is considered as a simpler way to quantify variation than using variance or standard deviation. For a signal *S= (s (1), s (2), …, s(n))*, the MAD is defined as the median of the absolute deviations from the data's median as follow:

$$MAD = median(|S - median(S)|) \tag{4.17}$$

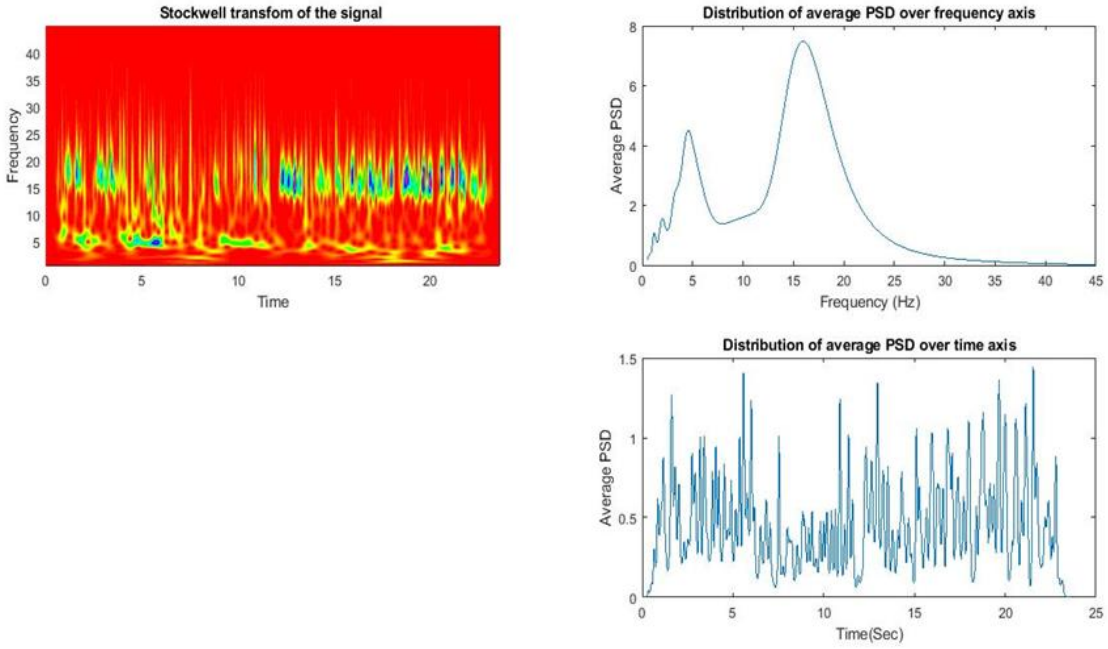


*Figure 4.3 (a) The S-transform of an EEG signal and average PSDs over the time and frequency axes.*

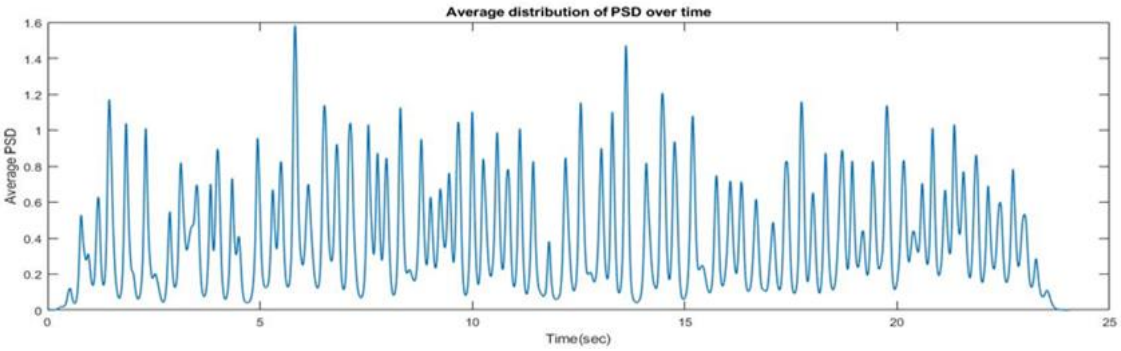


*b) Seizure(ictal) EEG segment*

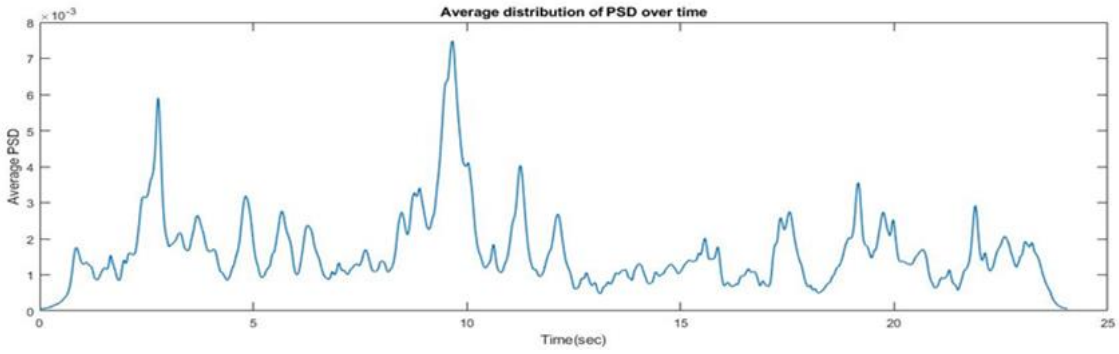


*c) Inter-ictal EEG segment*

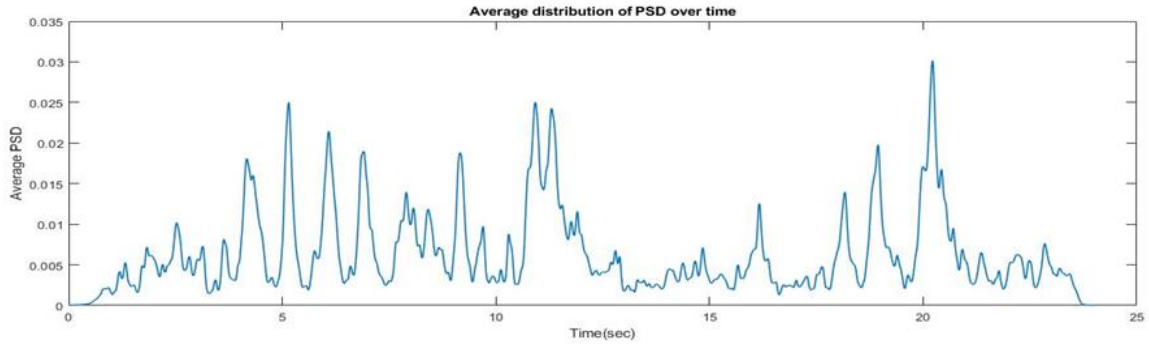


*d) Healthy EEG segment*

***Figure 4.3 (b-d) Average distribution of PSD over time axis for the three class of EEG.***

MAD is more flexible with outliers existing in the data. Since large deviations are possible with seizure signals, a median based measure of dispersion should be a good choice for detection [11]. Line length is another statistical feature used to quantify average distribution of PSD over the time axis. The line length of a signal, $L$, is defined as sum of the absolute vertical distance between successive samples of the signal, defined as:

$$L = \frac{1}{N-1}\sum_{i=1}^{N-1} abs(S_{i+1} - S_i) \qquad (4.18)$$

where $S$ stands for the signal considered and $N$ is the total number of samples. The line length feature well demonstrates the amplitude–frequency characteristics of the EEGs [12]. Those statistical features could be more informative if they are extracted from each sub-band of EEGs independently. This can be done by dividing the frequency line and following the same procedure of feature extraction as described above. This is to amplify the information which is not obvious when the full time-frequency plane is considered.

Temporal epilepsy has association with focal slow EEG activity from temporal region in intermittent, localized fashion (also called temporal intermittent rhythmic delta activity, TIRDA). This fact can be utilized to extract features that can classify healthy and inter-ictal EEG segments effectively. The frequency axis is divided into five broad spectral sub-bands of the EEG signal which are generally of clinical interest: delta (0 - 4 Hz), theta (4 - 8 Hz), alpha (8 - 16 Hz), beta (16 - 32 Hz) and gamma rhythm (32-45Hz). Energy of each sub-band can be calculated by integrating or summing over the time and frequency axis. Each feature represents the fractional energy of the signal in a specific frequency band or rhythm. The ratio of energy in delta sub

band to the energy of the higher frequency sub-bands (alpha and beta rhythms) is taken as classifying feature between healthy and inter-ictal EEG segments.

EEG of a healthy adult is dominated by alpha rhythms. Considering non-focal EEGs are considered healthy EEGs, a feature that can discriminate non- focal EEGs from the focal ones from the alpha sub-band could be derived. Now the S-transform alpha sub–plane can be considered as intensity image. By dividing each of the S-transform coefficients by the maximum of the coefficients, the coefficients would take values between 0 and 1. The histogram of each sub-band image is adjusted into 256 bins and let's assume, *m* is the histogram count. The count *m* is normalized by the size of the sub-image to get probability density. Let the size of the sub-image be H by W. Then the normalized count would be $m = \frac{m}{H*W}$ .The normalized count is then used to calculate the entropy of the sub-image. The entropy is calculated as:

$$H = \sum_m(-m * log(m)) \tag{4.19}$$

**4.6 Classification Using SVM**

When a problem lacks definite or explicit mathematical model or when the mathematical model of the problem is very complex, the idea of a learning system comes to picture. Generally, a learning system is training a computer to perform certain task, classification in our case. It uses existing examples or known set of data to find patterns and building classification models for problem solving. Several classification methods have been proposed in the literature. Artificial Neural Network (ANN) and Support Vector Machines (SVM) are two most common supervised learning algorithms in EEG analysis. While the performance of SVM and ANN with respect to linear data is quite similar, the difference is observed in non-linear data [13]. Due to simplicity and high performance for linear data, SVM is adopted in this thesis work. SVM uses the kernel function as margin between classes and constructs an optimal hyperplane to classify a data into different classes. SVM provides a simple geometric interpretation and reduced classification errors compared to ANN. SVM algorithm takes the input data and projects it to higher dimensional space where a maximal separating hyper plane is constructed. The kernel function defines the characteristics of the input data in this high dimensional space. Different kernel functions such as linear kernel, polynomial kernel, radial basis function (RBF) kernel and

sigmoid kernel are used according to the problem. The hyperplane for a linear classification can be stated as:

$$h_{w,b}(x) = y\,(w^T x + b) \tag{4.20}$$

where $y \epsilon \{-1,1\}$, $w \epsilon R^n$, $x \epsilon R^n$ , $b$ is a real number, $w$ determines direction, $b$ determines position and then the input vector $x$ is classified into two classes. Since, the optimal hyperplane is the one that separates the high probability density areas of two classes with maximum possible margin between them, the goal is to determine the direction that provides the maximum margin. SVM attempts to find a model that best explains relationship between data input and class output.

### 4.7 Performance Evaluation

The performance of the proposed SVM classifier is evaluated using sensitivity (SEN), specificity (SPF) and accuracy (ACC) parameters. Sensitivity, specificity and accuracy are three ideal criteria for assessing the classification performance of the proposed algorithm. Even though other parameters are found in the literature, those measures have been commonly used as performance indicators and provide higher reliability when used together. Hence no single measure among the three is enough for a complete assessment of the classification performance, because of which, the proposed method makes use of all of them.

Considering seizure as a positive event and non-seizure as a negative event, then for seizure detection work there could be four possible scenarios about the detection result. The first one is TP (true positive), the number of seizure EEG segments identified as seizure EEG segment. The second one is TN (true negative), the number of non-seizure EEG segments classified as non-seizure EEG segment. The third one is FP (false positive) is the number of non-seizure EEG segments recognized as seizure segments EEG signals and finally FN (false negative) is the number of seizure EEG segments distinguished as non-seizure EEG segment. From these values, various measures like sensitivity, specificity and accuracy can be calculated as follow.

$$SEN = \frac{TP}{TP+FN} \times 100(\%) \tag{4.21}$$

$$SPF = \frac{TN}{TN+FP} \times 100(\%) \tag{4.22}$$

$$ACU = \frac{TP+TN}{TP+TN+FP+FN} \times 100(\%) \tag{4.23}$$

## Reference


1. M. Javidan, ''Electroencephalography in Mesial Temporal Lobe Epilepsy: A Review,” Epilepsy Research and Treatment, Vol. 2012, Article ID 637430, pp.17, 2012.

2. J. C. Baayen, A. de Jongh , C. J. Stam et al. ''Localization of Slow Wave Activity in Patients with Tumor-Associated Epilepsy'', Brain Topography, Vol. 16, No. 2, 2003.

3. Commission on Classification, International League Against Epilepsy proposed provisions of Clinical and electroencephalographical classification of epileptic seizures. Epilepsia, Vol. 22, PP. 489-501, 1981.

4. R. G. Stockwell, L. Mansinha and R. P. Lowe, ''Localization of the complex spectrum: The S-transform,'' IEEE Transactions on Signal Processing, Vol. 44, No. 4, 1996.

5. G. Strang and T. Nguyen, Wavelet and filter banks, (Second Edition), Wellesley-Cambridge Press, Chapter-7, 1997.

6. A. Moukadem, Z. Boubuila, D. O. Abdeslam et al. ''A new optimized Stockwell transform applied on synthetic and real non-stationary signals,'' Digital Signal Process, Vol. 46, 2015.

Available online: http://dx.doi.org/10.1016/j.dsp.2015.07.003.

7. K. Senapati, A. routray, ''Comparison of ICA and WT with S-transform based method for removal of ocular artifact from EEG signals”, J. Biomedical Science and Engineering, Vol. 4, May 2011.

8. L. Yun, X. Xiaochun et al. ''Time-frequency Based on the S-transform'', International Journal of Signal Processing, Image Processing and Pattern Recognition, Vol. 6, No. 5, pp. 245-254, 2013.

9. S. Assous and B. Boashaah, ''Evaluation of the modified S-transform for time frequency synchrony analysis and source localization'' EURASIP Journal on Advances in Signal Processing, Vol. 49, No. 1, 2012.

10. W. Gang, W. Zhaohua, H. Norden, "On Intrinsic Mode Function." Advances in Adaptive Data Analysis Vol. 2, pp. 277-293, 2010.

11. P. J. Rouss and C. Croux, “Alternatives to the median absolute deviation,” Journal of the American Statistical Association, Vol. 88, pp. 1273–1283, 1993.

12. R. Esteller, J. Echauz, T. Tcheng , “Comparison of line length feature before and after brain electrical stimulation in epileptic patients, ” In: Engineering in Medicine and Biology Society. IEMBS’04. 26th Annual International Conference of the IEEE, vol.2, pp. 4710–13,2004.

13. J. Ren, ‘’ANN vs. SVM: Which one performs better in classification of MCCs in mammogram Imaging,'' Knowledge-Based System, Vol. 26, pp. 144–153, 2012.

# CHAPTER FIVE

# 5. RESULTS AND DISCUSSION

The major limitation of the current work is that only long time recorded EEG data from databases are used. Recording from EEG machines is not used. But the ultimate aim of the study is to test the performance of the system on recorded time series data and finally to check online performance of the system. To fill this gap EEG data from different database are used. For seizure detection, data from the epilepsy center at the University of Bonn were used while for epilepsy focus localization Bern-Barcelona EEG database was used [1][2].Review of EEG segments by experienced neurologist and their annotations is taken as ground truth or gold standard information. The experimental tests presented in this study were performed on a core i7, CPU: 3.40 GHZ and 4GB RAM computer and implemented in MatLab (MatLab 2017a).

## 5.1 Dataset

For seizure detection work, five sets each containing 100 single channel EEG segments (denoted as Z, O, N, F and S) of 23.6-seccond duration with a sampling rate of 173.6 HZ were obtained from publicly available Bonn University database. Set Z and O were taken from the surface EEG recordings of five healthy volunteers using the standardized electrode placement technique. The volunteers were recorded in relaxed and awake state with eyes open (set Z) and eyes closed (set O), respectively. Set N, F and S were obtained from five different epileptic patients recorded during presurgical diagnosis using intracranial electrodes. The patients were diagnosed for temporal epilepsy with epileptogenic zone being the hippocampal formation. Set N and F contained only activity measured during seizure free intervals. Set N were recorded from within the epileptogenic zone while set F were recorded from the hippocampal formation of the opposite hemisphere of the brain. Set S contains seizure activity, selected from all recording sites exhibiting ictal activity.

The EEG dataset used for epileptogenic zone localization were acquired from the Bern-Barcelona EEG database. The dataset contains intracranial EEG recordings from five patients suffered from long standing drug-resistant temporal lobe epilepsy. The five patients were candidates for surgery. Multichannel EEG signals were recorded with intracranial strip. The recordings were done to investigate the brain areas from which seizures originated or focal areas.

The recording channels were classified as focal and non-focal by at least two neurologists, who are board-certified electroencephalographers, based on EEG signal changes as judged by visual inspection. The EEG signals were sampled at a 512-Hz sampling frequency. The recordings contain pairs of EEG signals, denoted by “x” and “y”. The dataset consists of 3750 pairs of focal EEG signals and 3750 pairs of non-focal EEG signals, with each EEG segment having 10,240 samples. In this thesis work, the first 100 focal and 100 non-focal pairs of EEG segments have been used. Exemplary EEGs are shown in Fig.5.1.

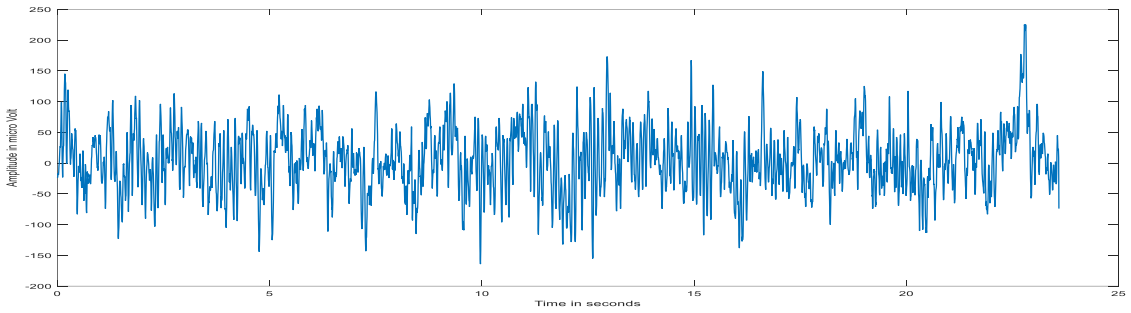


(a)

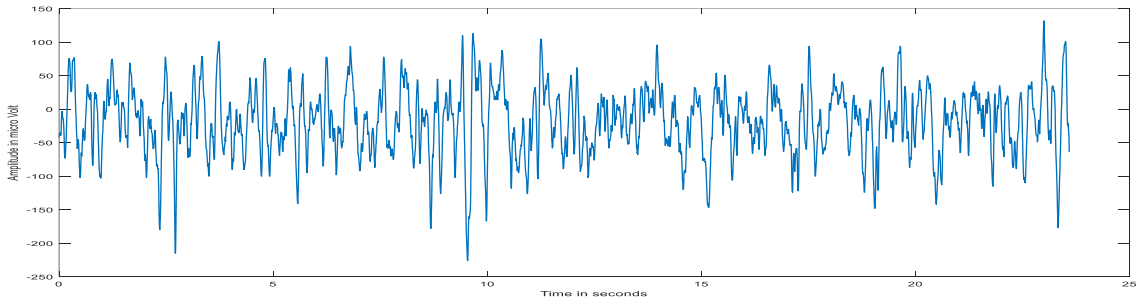


(b)

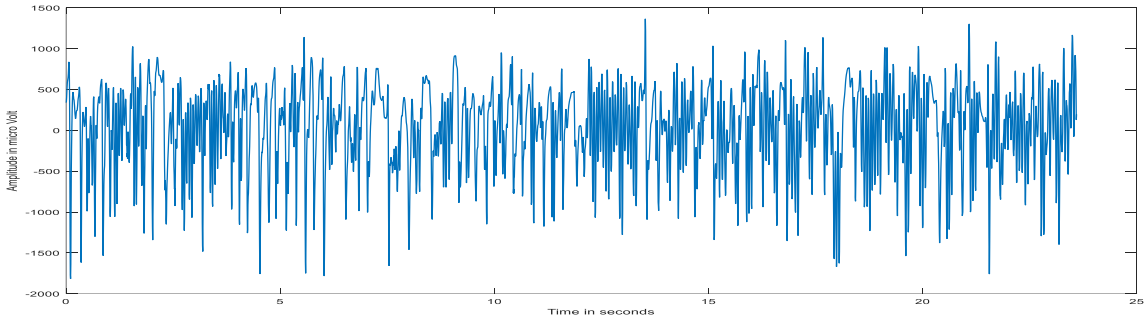


(c)

*Figure 5.1 Segments of EEG data for seizure detection (a) Normal, (b) Inter-ictal (c) Ictal.*

## 5.2 Results on Seizure Detection

As stated in the methodology section, the S-transform is applied on a pre-processed EEG segment. Then, the S- transform plane is generated by taking the absolute value of each coefficient since the coefficients are complex. Finally, PSD distribution in time-frequency is calculated by squaring the S-transform coefficients. The PSD distribution in time-frequency plane of healthy, interictal, seizure EEG segments is shown in Fig. 5.2. The PSD distribution plane is very informative. Seizure EEG segments are expected to be energetic compared to interictal and healthy EEG's. It is also expected to have distorted look, have activities in lower and higher frequency regions. On the other hand, EEG segments from healthy persons are expected to be dominated by activities in alpha and beta rhythms (from 7Hz-30Hz). Those facts are clearly shown in the PSD plane. To make facts more visible, two function are defined, average distribution of PSD in frequency axis and in time axis, from the S-transform plane. The average distribution of PSD over frequency axis is derived by summing coefficients in time direction. If the coefficients are summed in the frequency direction, the average distribution of PSD over time axis can be obtained. Average distribution of PSD in time and frequency axis is graphed separately. The graphs are showed side by side with the S-transform plane in Fig. 5.2. Those graph clearly depict the characteristics of EEG segments. EEG of a healthy adult subject recorded in closed eye condition is dominated by alpha rhythms with a bell-shaped frequency distribution curve, centering around 10.0 hertz as stated in Chapter 2. The average distribution of PSD over the frequency axis prove this fact clearly. High energetic and distorted look of the seizure EEG segments is summarized in average PSD over time and frequency graphs. Interictal EEG segments are dominated by delta and beta rhythms, low frequency activities. This is true especially for EEG segments that are taken from temporal lobe epilepsy cases. As shown in average PSD distribution over frequency axis or the S-transform plane, much of the EEG activities are concentrated in the lower frequency section. Besides, the average PSD distribution over the time axis depicts the interictal discharge or spike character of the EEG segments.

Our seizure detection scheme tries to address two different classification problems at once. Classification of seizures and non-seizures is examined as the first problem. The non-seizure class includes Z, O, N and F datasets while the seizure class includes the S dataset. The second classification problem includes three classes: healthy (Z and O data set), seizure-free or interictal (N and F data set) and seizure (S).

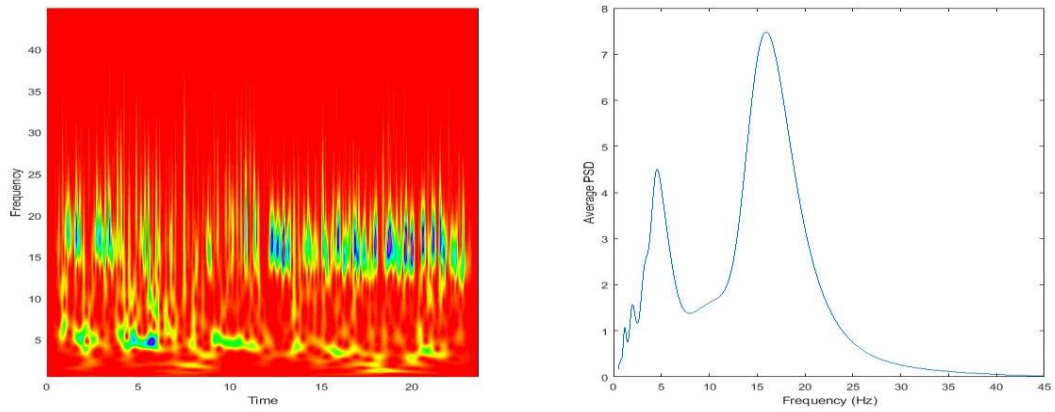


**(a) Ictal EEG segment**

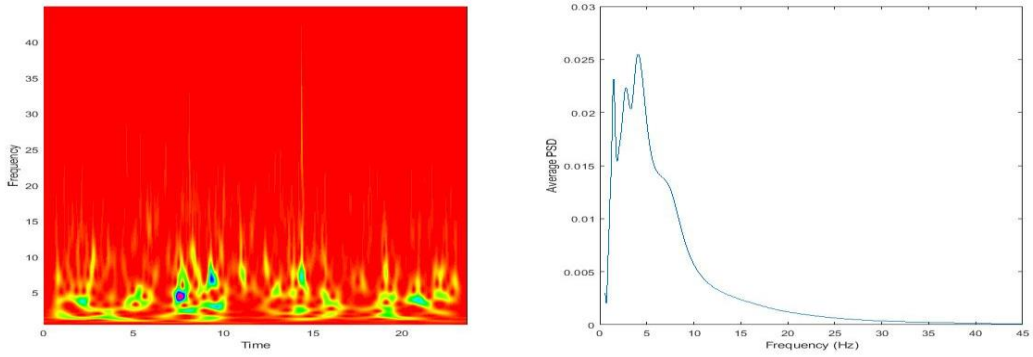


**(b) Inter –ictal segment**

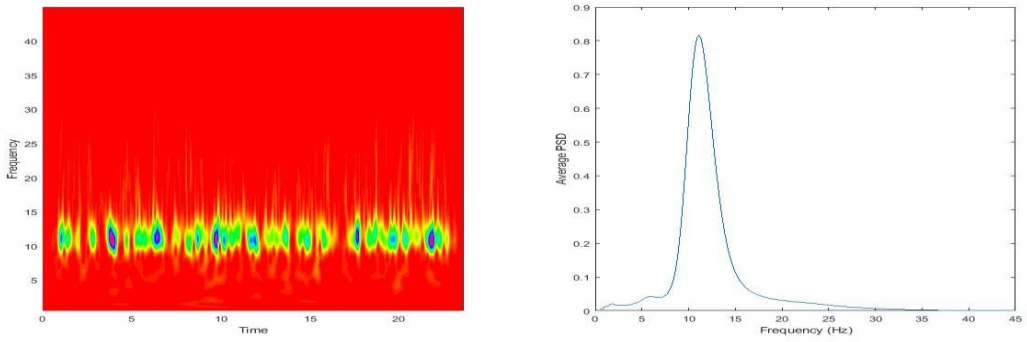


**(c) Healthy EEG segment**

*Figure 5.2 PSD of the S-transform plane and average distribution of PSD over the frequency axis.*

The data sets are combined in different order to create 4 possible problems. The first one is S, F, O while S, F, Z is second combination. Third one is S, N, O and finally S, N, Z is fourth one.

From those four possible problems, best classification accuracy is expected from the S, N, O group. The N dataset represents interictal phase in best since it is recorded from within the epileptogenic zone. The set O was recorded when the volunteers are eyes closed, awake and relaxed condition. Set O is expected to depict normal EEG in best since it would not be distorted by opening of eyes. Inferior results are expected from the S, F and Z combination. The Z datasets were recorded in open eye conditions while the F datasets were from the hippocampal formation of the opposite hemisphere of the brain. Therefore, the Z datasets would be affected due to eye opening and the F datasets were picked not from exact area affected by epilepsy. Accordingly, the result is expected to be poor compared to the other combinations of datasets.

Considering the facts described above into account, different features are extracted. Energy over sub-bands that are clinically important: delta (0 - 4 Hz), theta (4 - 8 Hz), alpha (8 - 16 Hz), beta (16 - 32 Hz) and gamma rhythm (32-45Hz), is the first feature to be extracted from the S-transform plane. The EEG activities of inter-ictal segments are concentrated in the lower frequency sub-bands (delta and theta). On the contrary, much of the EEG activities in normal segments are concentrated in higher frequency sub-band alpha and beta rhythms. As a result, the ratio of energy in delta sub-band to the energy of the higher frequency sub-bands (alpha and beta rhythms) is used as a feature to discriminate between normal and interictal EEG segments. Another feature extracted to discriminate between normal and interictal EEG segments is entropy of the S-transform sub–plane taking each sub-plane as intensity image. Especially, entropy of alpha sub-band taking it as intensity image is very relevant feature.

Seizure segments are expected to be energetic and in general have distorted look. This is due to the fact that seizure segments are recorded when the system or brain inters into a chaos phase. But energy as a feature is not enough to classify seizure and non-seizure segments. The average distribution of PSD over time is divided into epochs of a predetermined length of one second duration. Three statistical features namely standard deviation, line length and median absolute deviation (MAD) are extracted from the average distribution of PSD over time graph. From those statistical features, MAD performed better. 100 EEG segments from each dataset were used to generate a feature vector. Scatter plot of ratio of delta sub-band energy to higher frequency sub-bands as one feature and MAD as another feature were generated to check performance of the classification scheme in pictorial form. The scatter plots of S, N, O and S, F,

Z dataset using logarithmic scale is shown Fig. 5.3 below. Best result is obtained in the S, N and O combination case and the worst result is obtained in the case of S, F and Z combination as expected.

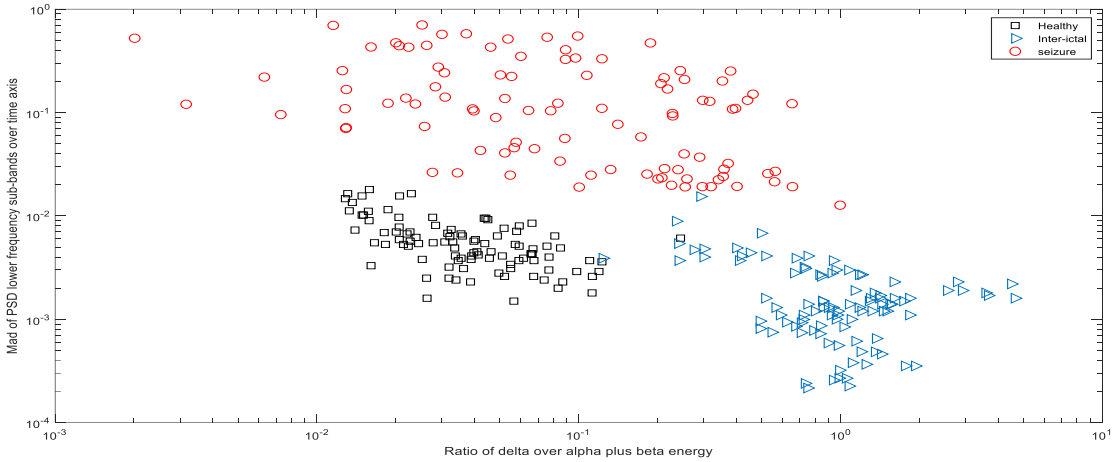


*Figure 5.3 (a) Scatter plot of S, N and O dataset.*

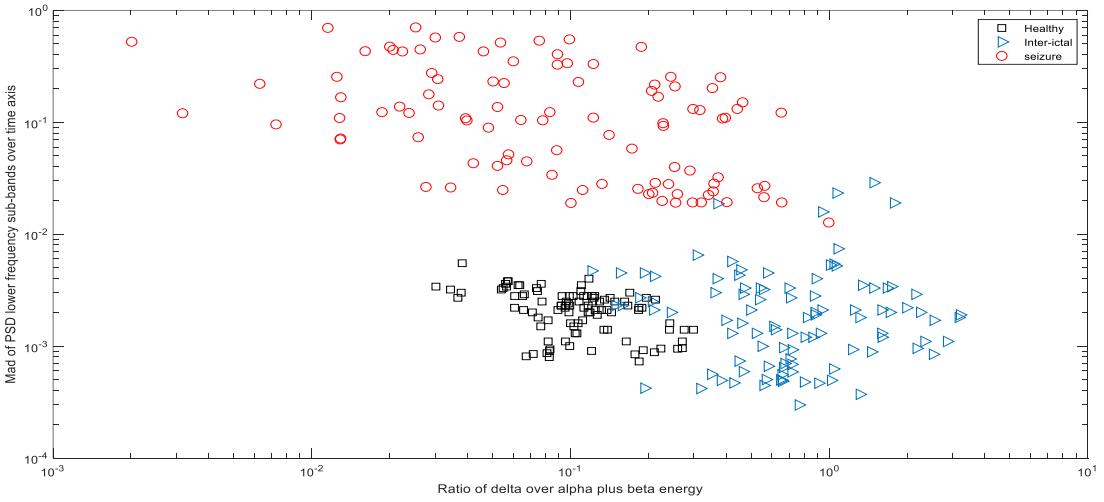


*Figure 5.3 (b) Scatter plot of S, F and Z data sets.*

The distance between seizure and non-seizure cluster in the scatter plot can be further improved by using sub-plane of the S-transform plane instead of using the whole S-transform plane to extract features. Using sub-plane (portion) of the S-transform plane amplify the difference between seizure and non-seizure EEG's, especially between healthy and seizure EEG's. The sub-plane used here ranges between 0.5 to 7 Hz in frequency and the entire time axis which can be

considered as a sub-plane of the delta and theta rhythms. The features are extracted in the same way as in previous section. Also, the average distribution of PSD over time axis is defined as the same way as in previous section. The three statistical features namely standard deviation, line length and median absolute deviation (MAD) are extracted from the average distribution of the PSD over time. Scatter plot of the MAD as main feature to differentiate between seizure and non-seizure data set and ratio of delta sub-band energy to higher frequency sub-bands as the second feature is generated. The distance between seizure and non-seizure clusters in the scatter plots shown in Fig.5.4 (in log scale) increased compared to the distance in the scatter plot of Fig. 5.3.

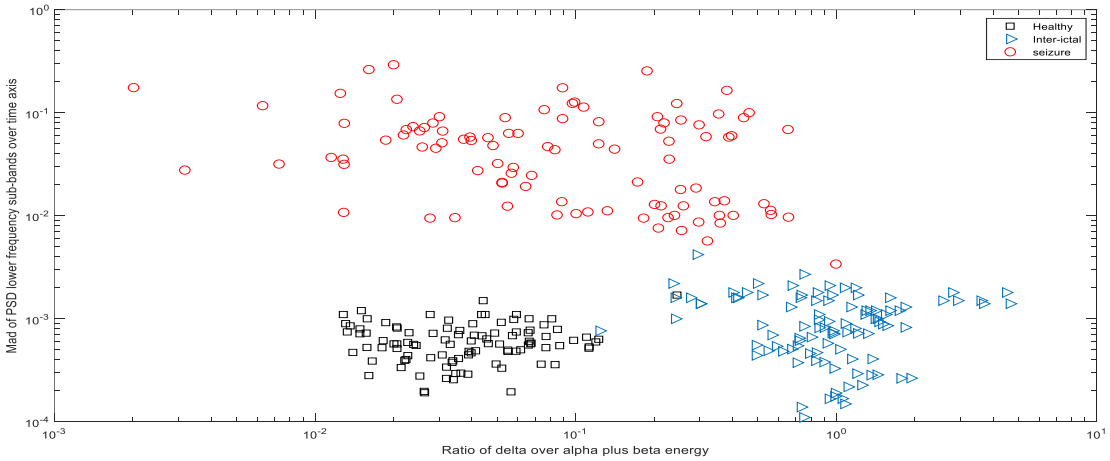


*Figure 5.4 (a) Scatter plot of S, N and O dataset of sub-plane of delta and theta rhythm.*

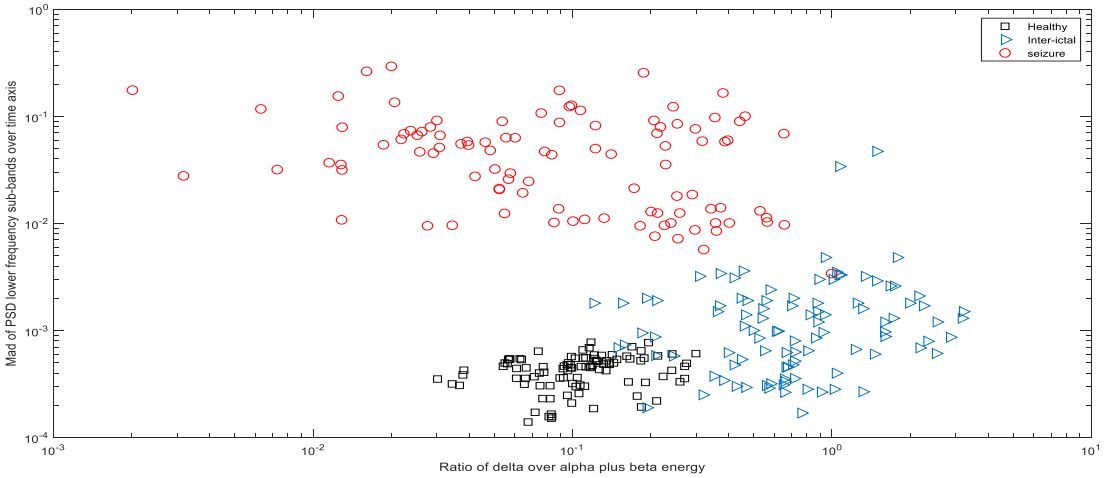


*Figure 5.4 (b) Scatter plot of S, F and Z data sets using sub-plane of delta and theta rhythm.*

Canberra distance [1][2] between the clusters is used to quantify the classification performance of the scheme. Table 5.1 shows the Canberra distance between each cluster in each possible dataset combination.

| | Using the whole PSD plane | Using a PSD sub-plane of lower frequency sub-bands |
|---|---|---|
| S-Z | 96.2624 | 98.1484 |
| S-O | 90.5257 | 97.4299 |
| S-F | 96.7656 | 95.6555 |
| S-N | 95.3430 | 93.4820 |

Table ***5.1 Canberra distance between seizure and non-seizure data sets.***

Both the scatter plot and the computed canberra distances proved that features extracted from sub-plane of lower frequency rhythms improves the distance between seizure and non-seizure clusters. The canberra distance between seizure (S) and normal (Z and O) datasets increases when the average PSD distribution over time axis is defined from sub-plane of lower frequencies from which the statistical features are extracted. But the distance between seizure and interictal (N and F) dataset decreases a little. This is due to most of interictal EEG segments activities are concentrated in the lower frequency region.

The major contributions of this thesis work are characterization of different class of the EEG segments and simple, two features based, pictorial classification with high accuracy. Most previously published papers use numerous and complex features to build their classification system. The characterization results of normal and interictal EEG segments of temporal epilepsy in the current work are in perfect match with the medically known facts. In order to compare the outcomes of the proposed system with that of schemes previously proposed in the literature, SVM is used to build a classification scheme using standard deviation, line length and median absolute deviation (MAD) as feature sets. Classification of seizure and non-seizure EEG segments is performed using SVM with linear kernel. Since three features are extracted from each EEG segment, the size of the input feature matrix would have a size of 3 by 100 for each dataset. The feature matrix is not too big and complex. Therefore, there is no need for reduction of the size of the feature space. From the 100 EEG segments, the first 50 segments are used for training and the rest 50 for testing. The performance of the proposed scheme for the different combinations is presented in table 5.2.

| Problems of different class combination | **Sensitivity** | Specificity | Accuracy |
|---|---|---|---|
| **Z-S (**Heathy with open eye and Seizure) | 100% | 100% | 100% |
| **O-S** (Heathy with closed eye and Seizure) | 100% | 100% | 100% |
| **N-S** (Inter-ictal from the epileptogenic zone and Seizure) | 99% | 99% | 99% |
| **F-S** (Inter –ictal from none the epileptogenic zone and Seizure) | 99% | 98% | 98.5% |
| **N-O** (Inter-ictal from the epileptogenic zone and Heathy with closed eye) | 99% | 99% | 99% |
| **N-Z** (Inter-ictal from the epileptogenic zone and Heathy with closed eye) | 92% | 99% | 96% |
| (**N and O) –S (**Non-seizure and seizure) | 99% | 99% | 99% |
| (**Z, O, N, F) – S** Non-seizure and seizure | 99% | 99.25% | 99.25% |

*Table 5.2 Performance of proposed seizure detection scheme*

## 5.3 Results on Seizure Detection Using EMD

The seizure detection scheme is assessed after EEG segments pass through EMD to check whether the performance of the classification between different dataset will be improved. The IMFs of the signals are arranged from higher to lower frequency components accordingly. Even though the frequency ranges are not exact, the IMFs have resemblance with rhythms of EEG signals. After EMD, the S-transform is applied on each IMF and just as in the previous section, features were extracted from average PSD distribution over time axis vector. The features extracted are MAD, standard deviation (STD), line length and skewness. The distance between seizure and non-seizure clusters will be improved using EMD. The range (mean ± STD) of the features extracted from the first four IMFs of each dataset is shown in Table 5.2.

| IMF | Features | S | F | N | O | Z |
|---|---|---|---|---|---|---|
| IMF1 | MAD | 45.2915± 74.8662 | 0.1757± 0.3035 | 0.1234± 0.2254 | 1.7484 ± 1.5678 | 0.4008±0.2139 |
| | STD | 0.1036 ± 0.1365 | 0.0026 ± 0.0074 | 4.8996e-04± 0.0011 | 0.0048 ± 0.0036 | 0.0011± 5.7293e-04 |
| | Line Length | 8.2753e-04 | 8.8782e-06 | 3.5626e-06 | 3.9920e-05 | 1.3887e-05 |
| | Skewness | 1.7381 ± 0.7928 | 1.0680 ± 0.7132 | 0.8090 ± 0.5495 | 2.3543 ± 0.7705 | 1.1813 ± 0.4895 |
| IMF2 | MAD | 14.5853 ± 15.3230 | 0.1408 ± 0.2797 | 0.1169 ± 0.2006 | 0.8512 ± 0.4859 | 0.2552 ± 0.1371 |
| | STD | 0.0456 ± 0.0455 | 0.0014 ± 0.0047 | 0.0011±3.9905e-04 | 0.0027 ± 0.0015 | 0.0023±8.0431e-04 |
| | Line Length | 2.9112e04 ± 4.6466e-04 | 3.1006e-06 ± 5.6568e-06 | 2.9962e-06 ± 6.7360e-06 | 1.5812e-05 ± 1.9950e-05 | 6.5796e-06 ± 9.8056e-06 |
| | Skewness | 2.4879 ± 0.8913 | 1.3696 ± 0.7153 | 1.1633 ± 0.4606 | 2.5620 ± 0.5183 | 1.5952 ± 0.5245 |
| IMF3 | MAD | 6.1917 ± 6.4476 | 0.2113 ± 0.3147 | 0.1371 ± 0.1548 | 0.1984 ± 0.1384 | 0.1422 ± 0.0656 |
| | STD | 0.0218 ± 0.0197 | 9.6937e-04 ± 0.0019 | 4.6967e-04 ±0.002 | 6.8674e-04 ±0.003 | 4.1215e-04 ±0.0007 |
| | Line Length | 1.2174e-04 ± 1.8661e-04 | 3.6969e-06 ± 7.6392e-06 | 3.1673e-06 ± 5.1822e-06 | 4.6522e-06 ± 1.0082e-05 | 3.4908e-06 ± 3.7655e-06 |
| | Skewness | 3.5200± 0.8205 | 2.5125 ± 0.5315 | 2.2895 ± 0.4300 | 2.4209 ± 0.3685 | 2.1815 ± 0.2806 |
| IMF4 | MAD | 2.0833 ± 2.7233 | 0.1884 ± 0.4918 | 0.0993 ± 0.1165 | 0.0570 ± 0.0469 | 0.0519 ± 0.0233 |
| | STD | 0.0101 ± 0.0107 | 7.9187e-04 ± 0.0018 | 3.8068e-04± 3.4341e-04 | 2.1701e-04 ± 1.4299e-04 | 1.7770e-04 ± 7.8705e-05 |
| | Line Length | 6.9385e-05 ± 1.1825e-04 | 3.0002e-06 ± 4.8680e-06 | 2.2569e-06 ± 3.4230e-06 | 1.4529e-06 ± 2.3886e-06 | 1.1844e-06 ± 1.2705e-06 |
| | Skewness | 4.3816 ± 0.9274 | 3.3738 ± 0.6051 | 3.1623 ± 0.4293 | 3.4113 ± 0.4395 | 3.1005 ± 0.4869 |

*Table 5.3 Ranges (mean ± standard deviation) of the features extracted from different IMFs of different data sets.*

## 5.4 Comparative Study on the Performance of the Proposed Seizure Detection Scheme and Other Methods Proposed Previously

Table 5.4 presents the performance of the proposed method versus others suggested in previous literatures. From publications listed on Table 5.4, works by S. Chatterjee et al. [3] and A.Yan et al. [9] are more related to the proposed method. The work of S. Chatterjee et al. used Stockwell transform as main methodology and tested on publicly available database of Bonn University. Standard deviation and energy of the S-transform coefficients were extracted as classifying feature. But a feature vectors space of 8 by 800 was needed to do classification task. Such a big

| | Year of publication | Method | Performance Measures (Accuracy, Sensitivity and Specificity respectively) |
|---|---|---|---|
| Healthy and seizure | 2017 | Stockwell transform, Power spectral density, SVM classifier [3] | 98.84%, 98.43% and 96.24% |
| | | Stockwell transform, Power spectral density, kNN classifier [3] | 100%, 100% and 100% |
| | 2014 | Wavelet transform, chaos analysis (phase-space reconstruction), and Euclidean distance [4] | 98.17%, 95% and 96.33% |
| | 2010 | Wavelet transform, Line length , artificial neural networks [5] | 99.6%,100% and 99.4% |
| | 2008 | Different Cohne's class time-frequency Analysis, artificial neural networks [6] | 100%, 99.8% and 99.8% |
| | 2019 | Approximate Entropy, Root mean square, power spectral density, Quadratic SVM [7] | 100%, 94%, and 98.75% |
| | 2016 | EMD & Renyi entropy K-nearest neighbor classifier [8] | 99.95 %,100% and 99.90 % |
| | | **Proposed method** | 100% ,100% and 100% |
| Inter-ictal and seizure | 2017 | Stockwell transform, Power spectral density, SVM classifier [3] | 98.45%, 98.21%, and 97.41% |
| | | Stockwell transform, Power spectral density, kNN classifier [3] | 99.25%, 100% and 98.85% |
| | 2015 | Stockwell transform, power spectral density, gradient boosting algorithm classifier [9] (Tested on University Hospital of Freiburg Data base) | 98.3%, 94.26% and 96.34% |
| | 2014 | Wavelet transform, chaos analysis (phase-space reconstruction), and Euclidean distance[4] | 98.17%, 95% and 96.33% |
| | | **Proposed method** | 99% 99% and 99% |
| Seizure and Non-Seizure (**S-ZONE**) | 2010 | Wavelet transform, Line length , artificial neural networks [5] | 97.75% , 98.61 % 94.6 % |
| | 2008 | Different Cohne's class time-frequency Analysis, artificial neural networks [6] | 97.73%, 93.2% and 94.6% |
| | | **Proposed method** | 99%,99.25% and 99.25% |

*Table 5.4 Comparative study on the performance of the proposed scheme seizure detection scheme.*

feature space limits the robustness of the algorithm if it has to be applied on different datasets. Also the effectiveness of the feature should be shown in figurative way like a scatter plot. Furthermore, not all five Bonn University datasets were considered. Besides, the authors ignored to do classification between healthy and inter-ictal EEG. Characterization the of the three class of EEGs is also ignored. While the performance of the scheme is generally comparable to the performance of the scheme proposed in this thesis. Unfortunately, the authors presented neither distance between classes using a distance matrix (like the Canberra distance used in this thesis) nor scatter plots, which made the comparison difficult. The work of A.Yan et al. also has similar issues. In this work, a 13 x the number of EEG segment (if 100 EEG segments are considered, it

would be 13 x 100) feature vector space was used. The work considered only inter-ictal and seizure classification. Even after applying post–processing of the classification stage, the results obtained were inferior to the results obtained using the method proposed in this thesis. Their scheme has been tested on University Hospital of Freiburg Data base while the proposed scheme in this tested has been tested on Bonn University database, often used to test effectiveness of an EEG signal processing tool.

### 5.5 Results on Focus Localization

The purpose of epileptogenic focus localization is delineation of epilepsy affected brain area in focal epilepsy. EEG signals from channels of epilepsy affected brain area, focal EEG, have different characteristics compared to EEG from channels of normal brain area, non-focal EEG. In simple terms, the current work focuses on classification of multichannel EEG signals into focal and non-focal EEG for focus localization. The inspiration came from the results in the previous section, i.e. classification of normal or healthy (Z and O dataset) and interictal or abnormal (F and N dataset) EEG segments. But in localization tasks, the normal and abnormal EEGs come from one system whereas O and N datasets come from different subjects/persons or systems. Focal slow EEG activity from temporal region in intermittent, localized fashion (or Temporal Intermittent Rhythmic Delta Activity, TIRDA) has close association with temporal epilepsy. This fact is used to extract the first feature, ratio of energy in delta sub-band to the energy of the higher frequency sub-bands (alpha and beta rhythms). When the signal gets slow, much of the energy is concentrated in the lower frequency sub-band (delta and theta). Normal EEGs, as characterized in the detection section, are more dominated by alpha sub-band. In this work, non-focal EEGs are considered normal EEGs. Therefore, non-focal EEGs can be discriminated from focal ones by extracting features from the alpha sub-band. Considering the alpha sub-plane from the S-transform as intensity image, the entropy of the intensity of the image is taken as the second feature. The third feature comes from empirical mode decomposition of EEG signals. As the IMFs of the signal are arranged from higher frequency components to lower frequency components, focal EEGs are more characterized by lower frequency IMFs than the non-focal EEGs. The EEG signals are decomposed into IMF and the sum of the third up to the sixth IMF were taken as input to the S transform. Skewness of the average distribution of PSD

over the frequency axis of the summed signal is taken as third feature. The reasoning of the third feature again comes from slowing focal EEGs.

The scatter plot of the first feature (the ratio of delta to sum of alpha and beta sub-bands) and the second feature (the entropy of alpha sub-band) is shown in Fig. 5.5 (a). As stated above, much of the energy of focal EEGs is concentrated in the lower frequency sub-bands. As a result, the ratio of delta to sum of alpha and beta sub-band (the first feature) of most of focal EEGs is greater than the non-focal EEGs. The first feature value of most focal EEGs is above 0.4 and on the contrary most of the non-focal EEGs assume values less than 0.4. But the first feature does not discriminate focal and non-focal signals as in case of interictal and normal EEGs. This is due to the fact that focal and non-focal signals were recorded from the same system or person. That means interference may occur between the focal and non-focal EEGs, especially on the boundary regions. But the interictal and normal EEGs were recorded from two different subjects or systems. This is major reason for drop in performance of the first feature. The second feature, entropy of alpha sub-band plane, performs better than the first feature. Using simple thresholding at 3.5, the second feature could classify focal and non-focal EEGs with 82 % sensitivity, 85% specificity and 84% accuracy.

Again the scatter plot of the second feature to the third feature is shown in Fig. 5.5 (b). Since focal EEG gets slow in localized fashion, focal EEGs are more characterized by lower frequency IMFs than the non-focal EEGs. After the signal is decomposed into IMFs, using EMD technique, focal EEG can be approximated by the sum of the third up to the sixth IMFs. The sum of the IMFs is taken as input to the S transform. Skewness of the average distribution of PSD over the frequency axis of the summed signal is taken as third feature. Using simple thresholding at 2.5, the third feature could classify focal and non-focal EEG with 84 % sensitivity, 90.2% specificity and 88% accuracy.

Given this outcome by the proposed seizure localization scheme, a comparable result was found in [9]. The authors in [9] used EMD to compute IMFs of focal and non- focal EEG signals. Six different entropy measures were computed from the first eight IMFs of focal and non-focal EEG signals. A size of 60 by 100 input feature space was formed to be classified by Least squares support vector machine (LS-SVM). This work is tested on publicly available Bern-Barcelona EEG database and maximum classification accuracy of 87%, sensitivity of 84%, specificity of

90% was obtained using the LS-SVM classifier using the Morlet wavelet kernel. Again, one drawback of this method is the big size of the feature space used for classification which limits its robustness. The authors tried to reduce the size of the feature space using the Student's t-test method which in turn reduced the complexity of the classifier. But even after that, the authors should have to use complex kernels, Morlet kernel to obtain better results. The result they obtained was low on simple kernels like RBF kernels. The proposed method in this thesis performed better and yet it is simple, robust and considers the fact that the EEG signals come specifically from temporal lobe cases.

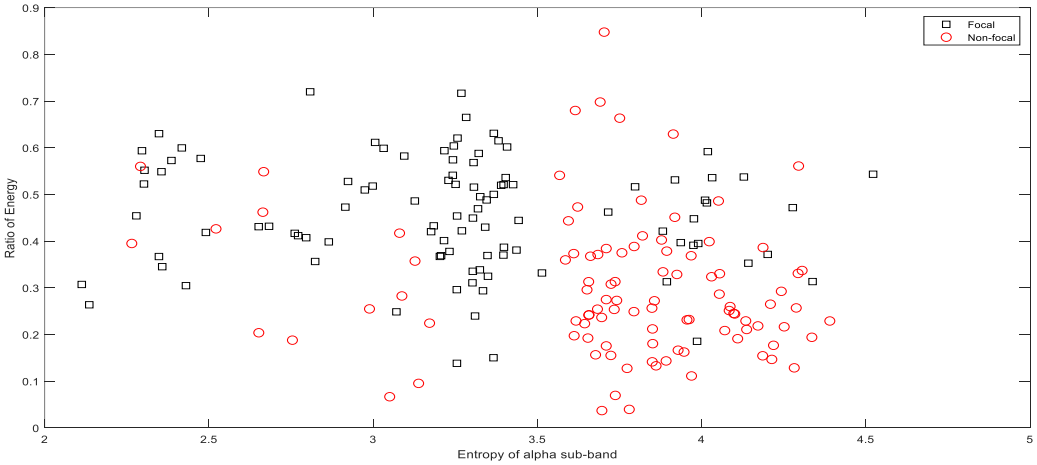


*Figure 5.5 (a) Scatter plot of feature 1 versus feature 2.*

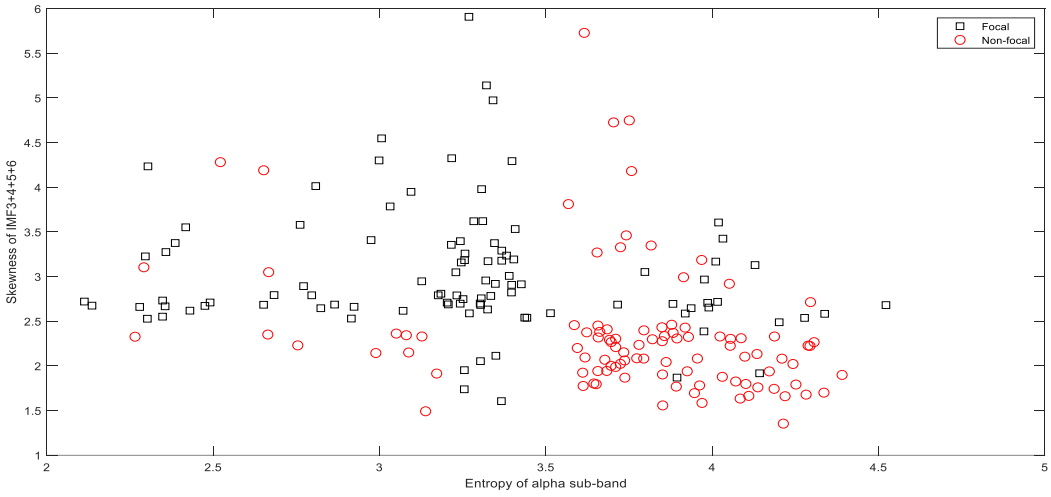


*Figure 5.5 (b) Scatter plot of feature 2 versus feature 3.*

**Reference**

1. V. Kumar, J.K. Chhabra, “Performance Evaluation of Distance Metrics in the Clustering INFOCOMP,’’ Vol. 13, No. 1, pp. 38-51, June 2014.

2. D. Napoleon, M. Praneesh , “Canberra Distance based Approach for Classifying Remote Sensing Images using Affinity Propagation,” International Journal of Advanced Research in Computer Science, Vol. 4, No. 10, Sep-Oct 2013.

3. S. Chatterjee, N.R. Choudhury and R. Bose, “Detection of epileptic seizure and seizure-free EEG signals employing generalized S-transform,” IET Science, Measurement & Technology, Vol. 11, Iss. 7, pp. 847-855,2017.

4. S.H. Lee, J.S. Lim, J.K .Kim, et al., “Classification of normal and epileptic seizure EEG signals using wavelet transform, phase-space reconstruction, and Euclidean distance, ” Comput. Methods Programs Biomed., 2014, Vol. 116, pp.10–25.

5. L. Guo, D. Rivero, J. Dorado et al., “Automatic epileptic seizure detection in EEGs based on line length feature and artificial neural networks,”' Journal of Neuroscience Methods Vol. 191,pp.101–109,2010.

6. A. T. Tzallas, M. G. Tsipouras, D. I. Fotiadis, “Epileptic seizure detection in EEGs using time-frequency analysis,” In Proceedings of the Twentieth IEEE International Symposium on Computer-Based Medical Systems, pp. 135–140, IEEE Computer Society Washington, DC, USA, 2007.

7. S. Zahan and Md. R. Islam, “Epileptic Seizure Detection and Classification using Support Vector Machine from Scalp EEG Signal,”1st International Conference on Advances in Science, Engineering and Robotics Technology 2019 (ICASERT 2019)

8. A. Feltane, “Time-Frequency Based Methods for Non-Stationary Signal Analysis with Application To EEG Signals,” Open Access Dissertations. Paper 445, 2016.

9. A. Yan, W. Zhou, Q. Yuan , “ Automatic seizure detection using Stockwell transform and boosting algorithm for long-term EEG, " Epilepsy & Behavior Vol.45,PP.8–14,2015.

10. R. Sharma, R. B. Pachori, U.R. Acharya, “Application of Entropy Measures on Intrinsic Mode Functions for the Automated Identification of Focal Electroencephalogram Signals”, Entropy, Vol. 17, pp. 669-691, 2015. doi:10.3390/e17020669

# CHAPTER SIX

# 6. CONCLUSION AND FUTURE WORKS

## 6.1 Conclusion

Various researches on epileptic EEG signals have been conducted almost for the last four decades to develop atomized scheme that can help the diagnosis and treatment process. Automatic seizure detection is such a system and it can be a solution to the time consuming, inefficient and subjective manual task. Automatized localization of the epileptogenic focus also helps both the treatment and diagnosis process of focal epilepsy. This thesis takes the following concepts as foundational arguments in developing automatized schemes. First, developing atomized epileptic EEG processing system considering all types of epilepsy at once is difficult and inefficient. Considering each type of epilepsy separately and finally developing holistic automatic scheme is the right approach to tackle the problem. Secondly, the signal analysis methodology should take the characteristic of EEG signals into account. In short, EEG is non-linear, non-stationary and multicomponent signal. Particularly, epileptic EEGs involve highly localized events such as bursts, spikes, and discontinuities. Therefore, the chore mathematical algorithm of such kind of a system should able be to handle a signal with those characteristics.

The proposed automatized scheme in this thesis focused mainly on temporal lobe epilepsy and used the S-transform as core of the method. The S-transform is a time-frequency-based technique which has great potentials to effectively analyze non-stationary signals like EEGs. Relevant features are extracted from power spectral density of the S-transform time-frequency plane and sub-planes to classify EEG segments for seizure detection. EEG segments are classified into seizure, inter-ictal and non-seizure using SVM. The seizure focus localization problem is also addressed with the same way. Features, relevant enough to classify EEGs into focal and non-focal segment, are extracted from power spectral density of the S-transform time-frequency plane and sub-planes. EMD (adaptive, data-dependent signal decomposition method) was also employed with the S-transform. EMD is suitable for the analysis of nonlinear and non-stationary signals and decomposes signals into intrinsic mode functions. After the S-transform is implemented on IMFs of EEG segments, features are extracted. Employing EMD improves the classification efficiency of the EEG segments, especially seizure and normal signals. The performance of the current work is much superior compared to previous results reported in

literatures. Beside developing efficient detection and location scheme, the major contribution of the thesis work can be summarized as:

- Previous works in seizure detection and focus localization used large number of complex features which will be burden of computation during classification. The proposed scheme uses few medically sound full features from the S-transform plane.
- In addition to seizure detection, seizure, interictal and normal EEGs are characterized very well which can be very helpful for the diagnosis of epilepsy. Scatter plot is generated with two best performing features. The scatter plot classifies the three classes of EEGs at once in simple and figurative way. Since the distance between the clusters is good enough, the scatter plot clearly discriminates the three classes of EEGs.

### 6.2 Recommendations and Future Works

Following the introduction of computerized digital recording techniques, storage and transmission of EEG signals came into reality and as a result the clinical roles of EEG in diagnosis and monitoring of brain related cases increased dramatically. On this ground, computer aided EEG signal processing algorithms could play a lot in diagnosis and treatment of epilepsy. Even though the area of epileptic EEG signal processing analysis has been researched for last four decades, it is still a hot research area. The results of the current thesis study are promising but there are still further investigations required in some aspects. First of all, validation on large data in clinical scenarios should be carried out. In addition, the current work is devoted to temporal lobe epilepsies only. Other types of epilepsies should also be investigated independently and other than detecting seizure signals, seizure and inter-ictal EEGs should be characterized. In aspects of focus localization, EEGs from channels near and far to focus of epilepsy have different characteristics. In this regard, the distance dependent characteristics of non-focal EEGs should be investigated further.

# Appendix

The MATLAB code for the main functions to compute the S- transform and extract features.

Function to compute the S-transform

```
function [SH,nrml]=S1ta(h,kl,ku,m,q)
%{
S-transform of a 1-D series,h(), computed by convolution of
normalised gaussian in time (gaus) and h() modulated with a
specific voice(hwt)

INPUT
h(): input time series h(),
kl and ku: lower and upper frequencies of desired spectral band,
OUTPUT
SH(,): The S-transform of h()
nrml(:normalising vector formed by the sum(area) of gaus() at each voice.
Usage Note: nrml() may be used to highlight diferent frequencies.
Many high frequencies are low in amplitude. Use nrml() to 'distort' SH(,)
by dividing each column by nrml() (or some power nrml().^n).

Note: s1tb.m is fast but uses lots of memory (4(NxN)+7N)
s1ta.m is slightly slower but uses much less  memory ((NxN)+5N)
TimeTest: On a test with a 100 point h()  s1ta.m 0.61s; s1tb.m 0.50s, on a
P133 laptop.

The gaussian window is defined in time; the width is
 proportional to frequency.
 fq(N) defines the frequency vector
 fqa(N) is the range of fq() defined by input kl and ku
 wt(N) product of t(N) and fq(k)
 hwt(N) product of h(N) and a single freq cosinusoid.
 gaus(N) gaussian, in time, width depends on freq.
 nrml(N) represents the sum(area) of each gaus(N)
 SH(N,N) is a row by row convolution of hwt() and gaus()
%}
%START
%Check if input h() is a scalar(error) or row, column vector
if nargin==3;m=0;q=0;end;
    h = h';
    n = length(h);
    ind = [0:n-1]';
    rrr = polyfit(ind,h,2);
    fit = polyval(rrr,ind);
    h = h - fit;
    sh_len = floor(length(h)/10);
    wn = hanning(sh_len);
    if(sh_len==0)
       sh_len = length(h);
       wn = 1&[1:sh_len];
    end
    % make sure wn is a column vector, because timeseries is
    if size(wn,2) > size(wn,1)
```

```
      wn=wn';
    end
    h(1:floor(sh_len/2),1) = h(1:floor(sh_len/2),1).*wn(1:floor(sh_len/2),1);
    h(length(h)-floor(sh_len/2):n,1) = h(length(h)-
floor(sh_len/2):n,1).*wn(sh_len-floor(sh_len/2):sh_len,1);
    h = h';
    if (q~=m)
        h = h(q-m+1:n-q+m);
    end;

s=size(h);
if s(1)==1 & s(2)== 1;  error('??error s1lm: h is a scalar'); end
if s(1)>1 & s(2)>1; error('??error s1lm: h is not a 1-D array'); end
if s(1)>1 & s(2)==1; rc=0; ha=rot90(h); N=s(1); end%h() is a column and is
converted to a row
if s(1)==1 & s(2)>1;  ha=h; rc=1; N=s(2); end %h() is a row

nhaf=fix(N/2)+1;
nmid=fix(N/2);
if nargin==1;kl=0;ku=nmid;end%default kl and ku, if only h()given
if nargin==2;ku=nmid;end%default ku
odvn=1; %N odd
if fix(N/2)*2==N; odvn=0;end %N even
M=ku-kl+1;
topi=2*pi;
%%Preform arrays
gaus=zeros(1,N); hwt=zeros(1,N); nrml=zeros(1,M); SH=zeros(M,N);
```

Computing S-transform plane, sectioning the S-transform plane into five EEG rhythms and feature extraction

```
% loading the signal
% Healthy EEG with eyes open recorded extracranially
%                   sig= load('Z012.txt');
% Healthy EEG with eyes closed recorded extracranially
                  sig= load('O001.txt');
% seizure-free intervals EEG from epileptogenic zone recorded intracranially
%                   sig= load('N065.txt');
% seizure-free intervals EEG from the hippocampal formation of the opposite
hemisphere of the brain
%                  sig=load('F055.txt');
% seizure activity EEG recorded intracranially
%                sig= load('S096.txt');
% Plotting the EEG signal on time axis

N=length(sig);
fst=173.61;
ts=1/fst;
fs = 1/(N*ts);
tmax=(N-1)*ts;
T=0:ts:tmax;
% Stockwell transform
sig=sig';
N = length(sig);
s = sig(1:N)';
```

```
len = N;
N2 = 2./N;
nhaf = fix(N/2)+1;
fq = [0:nhaf-1 -nhaf+[2:nhaf-1]];
t = 0:N-1;
kl = 0;
ku = nhaf-1;
kl1 = kl+1;
ku1 = ku+1;
M = ku-kl+1;
profile on
frq = linspace(0,N/2,N/2+1);
data = s;
ddd = length(s);
dlen = length(data);
dfnew = floor(dlen/20);
u = log2(dlen);
if(mod(u,2)~=0) dlen = 2^ceil(u);end;
df = floor((dlen-ddd)/2);
rem = mod(dlen-ddd,2);
temp =df;
if (df<dfnew)
    df = dfnew;
    dfnew = temp;
end;
lennew = length(data);
kldata  = 0;
nhafdata= fix(dlen/2)+1;
kudata = nhafdata-1;
frqdata = linspace(0,dlen,dlen);
[st_matrix_data,nrml] = S1ta(s,kldata,kudata,0,0);
kk2 = st_matrix_data;
fst=173.61;
ts=1/fst;
tmax=(N-1)*ts;
T=0:ts:tmax;
xf=0:fs:fst-fs;
cf=0:fs:fst/2;
% pi-color
st_matrix_datay=(abs(st_matrix_data(1:(fix(ddd/2)+1),:))).^2;
ff_indg= find(cf >= 0.5& cf <=45);
dxdg = cf(1,ff_indg(1):(ff_indg(end)));
CTg=(st_matrix_datay(ff_indg(1):(ff_indg(end)),:));
figure, pcolor(T,dxdg,(st_matrix_datay(ff_indg(1):(ff_indg(end)),:)))
colormap hsv
brighten (0.1)
shading interp

% delta
ff_ind = find(cf >= 0.5& cf <= 5);
dxd = cf(1,ff_ind(1):(ff_ind(end)));
CT1=st_matrix_datay(ff_ind(1):(ff_ind(end)),:);
Tsig1=sum(CT1);
figure,plot(T,Tsig1);
```

```
% theta
ff_ind1= find(cf > 4 & cf <=7);
dxd1=cf(1,ff_ind1(1):(ff_ind1(end)));
CT2=st_matrix_datay(ff_ind1(1):(ff_ind1(end)),:);
Tsig2=sum(CT2);

% alpha
ff_ind2= find(cf>8 & cf <= 16);
dxd2=cf(1,ff_ind2(1):(ff_ind2(end)));
CT3=st_matrix_datay(ff_ind2(1):(ff_ind2(end)),:);
Tsig3=sum(CT3);
figure,plot(T,Tsig3)

% beta
ff_ind3= find(cf > 16 & cf <= 32);
dxd3=cf(1,ff_ind3(1):(ff_ind3(end)));
CT4=st_matrix_datay(ff_ind3(1):(ff_ind3(end)),:);
Tsig4=sum(CT4);

% gamma
ff_ind4= find(cf > 0.5 & cf <= 30);
dxd4=cf(1,ff_ind4(1):(ff_ind4(end)));
CT5=st_matrix_datay(ff_ind4(1):(ff_ind4(end)),:);
Tsig5=sum(CT5);
```

Sample function to extract feature

```
function [ Sk,Sk1] = HSE( CT)
UV=max(max((sig)));
sig=(sig)./UV;
[H,W]=size(sig);
[m,Binsx]=imhist(sig);
m=m/(H*W);
figure,plot(Binsx,m,'k')
Sk=skewness(m);
```